Titre: Title:	Low density polyethylene/thermoplastic starch blends
Auteur: Author:	Francisco Rodríguez Díaz
Date:	2002
Type:	Mémoire ou thèse / Dissertation or Thesis
Référence: Citation:	Rodríguez Díaz, F. (2002). Low density polyethylene/thermoplastic starch blends [Thèse de doctorat, École Polytechnique de Montréal]. PolyPublie. https://publications.polymtl.ca/7063/

INFORMATION TO USERS

This manuscript has been reproduced from the microfilm master. UMI films the text directly from the original or copy submitted. Thus, some thesis and dissertation copies are in typewriter face, while others may be from any type of computer printer.

The quality of this reproduction is dependent upon the quality of the copy submitted. Broken or indistinct print, colored or poor quality illustrations and photographs, print bleedthrough, substandard margins, and improper alignment can adversely affect reproduction.

In the unlikely event that the author did not send UMI a complete manuscript and there are missing pages, these will be noted. Also, if unauthorized copyright material had to be removed, a note will indicate the deletion.

Oversize materials (e.g., maps, drawings, charts) are reproduced by sectioning the original, beginning at the upper left-hand corner and continuing from left to right in equal sections with small overlaps.

ProQuest Information and Learning
300 North Zeeb Road, Ann Arbor, MI 48106-1346 USA
800-521-0600

UNIVERSITÉ DE MONTRÉAL

LOW DENSITY POLYETHYLENE/THERMOPLASTIC STARCH BLENDS

FRANCISCO RODRÍGUEZ
DÉPARTEMENT DE GÉNIE CHIMIQUE
ÉCOLE POLYTECHNIQUE DE MONTRÉAL

THÈSE PRÉSENTÉE EN VUE DE L'OBTENTION
DU DIPLÔME DE PHILOSOPHIAE DOCTOR (Ph.D.)
(GÉNIE CHIMIQUE)
AOÛT 2002

UNIVERSITÉ DE MONTRÉAL

ÉCOLE POLYTECHNIQUE DE MONTRÉAL

Cette thèse intitulée:

LOW DENSITY POLYETHYLENE/THERMOPLASTIC STARCH BLENDS

présentée par: RODRÍGUEZ Francisco

en vue de l'obtention du diplôme de: Philosophiae Doctor

a été dûment acceptée par le jury d'examen constitué de:

M. LEGROS Robert, Ph.D., président

M. FAVIS Basil D., Ph.D., membre et directeur de recherche

M. RAMSAY Bruce A., Ph.D., membre et codirecteur de recherche

M. BALKE Stephen, Ph.D., membre

M. LAFLEUR Pierre G., Ph.D., membre

ACKNOWLEGMENTS

This work has been carried out at the "Centre de Recherche Appliquée Sur les Polymères" of the École Polytechnique de Montréal. It was supported by the Natural Sciences and Engineering Research Council of Canada.

I would like to give a special acknowledgment to my Thesis directors Professor Basil D. Favis and Professor Bruce A. Ramsay by their passionate and enthusiastic interest to the progression of my work. I would also thank them for their patience during the numerous discussion that we had, which were helpful for my scientific formation.

I would like to thank all the staff of the Chemical Engineering Department of the 'Ecole Polytechnique de Montréal, especially to Jiamning, Stefania, Nick, Luc, Carol, Sebastien, Robert and Pei Lian. I would like to express my acknowledgment to Professor Suzanne Lacroix of the Engineering Physics Department for her helpful discussions in my first Paper.

I would to thank all my colleagues of the research group including the Mexican colleagues of other departments.

I would like to thank my wife Stella Maris for her support during the five years of studies in Montreal. I would like to thank my family: My Parents, my Brothers and Sisters and my Political Family.

Finally, I would like to thank God.

RÉSUMÉ

Ce travail présente une tentative pour la préparation d'un mélange de polyéthylène basse densité/amidon thermoplastique (TPS) avec des propriétés exceptionnelles. L'amidon thermoplastique est capable de couler et, pourtant, quand il est mélangé avec un polymère synthétique, il a un comportement semblable a celui observé dans les mélanges de polymères conventionnels. Dans cette étude, une extrudeuse mono-vis est combinée à une extrudeuse bi-vis pour le mélange à l'état fondu des composants. Le glycérol a été utilisé comme plastifiant pour l'amidon. Le contenu en glycérol dans le TPS a été varié de 29% à 40%.

La viscosité apparente du PE et du TPS a été mesurée directement dans l'extrudeuse bi-vis à l'aide d'une série des filières capillaires attachées à la tête de l'extrudeuse. La composition des mélanges PE/TPS a été mesurée par une analyse thermogravimétrie en considérant les différences entre les températures de décomposition thermique du TPS et du PE. Des échantillons ont été microtomés et leur microstructure a été observé en utilisant un microscope électronique à balayage (SEM). Des éprouvettes pour le test de traction ont été coupées longitudinalement à partir des rubans de PE/TPS récemment préparés. Ces éprouvettes ont été évaluées selon la norme ASTM D638. Pour déterminer les effets de l'orientation de la phase mineure et de l'humidité relative, des éprouvettes (type V) ont été coupées dans le sens transverse et longitudinal à la direction machine et conditionnées à 0% et 50% d'humidité relative. Le taux de continuité des mélanges PE/TPS a été déterminé par la dégradation hydrolytique des domaines d'amidon en utilisant une solution de HCl.

Dans les conditions de mise en forme particulière du procédé en une étape, il est possible de développer des rubans contenant des morphologies continues de TPS (hautement interconnectées) et co-continues (complètement interconnectées). Ces mélanges ont un allongement à la rupture, un module d'Young et une contrainte à la

rupture élevés dans la direction axiale. Les mélanges PE/TPS (55:45) préparés avec un contenu en glycérol de 36% maintiennent 94% de l'allongement à la rupture et 76% du module d'Young du polyéthylène. À des concentrations un peu plus basses de TPS (71:29, PE/TPS) avec le même contenu en glycérol, les mélanges retiennent 96% de l'allongement à la rupture et 100% du module d'Young par rapport au polyéthylène. Ces résultats exceptionnels sont obtenus en absence d'agent comptabilisant et sans prendre en considération les forts niveaux d'immiscibilité produits par la grande différence de polarité entre ces deux polymères. Même si l'allongement à la rupture dans la direction transverse est moins élevé que dans le sens longitudinal, il est encore suffisamment élevé pour montrer une fracture ductile à des hautes concentrations en TPS. L'extraction hydrolytique de l'amidon a montré que le mélange 55:45 possède une morphologie 100% continue, ce qui est important pour permettre la complète biodégradation de la phase amidon. Les mélanges préparés avec un TPS contenant 36% glycérol ont montré une très faible sensibilité à l'humidité. La similarité entre les index de réfraction du PE et du TPS et l'absence virtuelle de microvides à l'interface ont permis une très bonne transparence à tout niveau de composition.

La deuxième partie de ce travail est dédié à l'étude des propriétés thermiques et rhéologiques du TPS préparé dans l'extrudeuse bi-vis. Les propriétés rhéologiques du TPS sont comparées à celles du PE. L'analyse de la calorimétrie différentielle à balayage (DSC) montre la présence d'une température de transition vitreuse (Tg) au-dessous de la température ambiante. Cette transition indique la complète gélification des granules d'amidon. La Tg diminue de –45.6°C jusqu'à –56.2°C quand le contenu en glycérol augmente de 29% à 40%. Même si aucune transition est observée au-dessus de la température ambiante, la diffraction de rayons-X a détecté une structure cristalline qui est peut-être reliée à la présence des complexes amylose-lipides existant dans l'amidon de blé.

La viscosité en cisaillement et les propriétés rhéologiques dynamiques sont mesurées directement dans l'extrudeuse ou par l'utilisation de deux rhéomètres oscillatoires,

respectivement. Le balayage par rapport au temps montre que le TPS a une excellente stabilité thermique à 150°C, mais qu'il devient instable aux températures supérieures à 180°C. Ces résultats indiquent, cependant, que la stabilité du TPS peut être suffisant pour la mise en forme à des températures proches à 200°C, mais avec un temps de résidence court. La région de viscoélasticité linéaire du TPS atteint jusqu'à une déformation (γ) d'environ 0.02. Ceci est relié à la présence d'un réseau élastique. L'évaporation du glycérol conduit à l'augmentation graduelle des propriétés rhéologiques comme conséquence d'un accroissement en rigidité du TPS. De la même façon que les propriétés thermiques, les propriétés rhéologiques dépendent du contenu en glycérol. La viscosité en cisaillement du TPS (à ~ $130s^{-1}$) diminue 20% quand le contenu en glycérol augmente de 36 à 40%. Également, G' et G'' augmentent comme conséquence de la diminution de glycérol avec une réduction plus dramatique à environ 30%. Cela indique la limite de percolation des régions moues bien plastifiées et riches en glycérol.

La comparaison entre les viscosités en écoulement continu et en mode oscillant du TPS40 et du PE1 montre une différence importante sur le rapport de viscosité de ce système de polymères. Dans les conditions dynamiques, le TPS40 est plus visqueux que le PE1 alors que dans les conditions de cisaillement le TPS40 est moins visqueux que le PE1. La plus basse viscosité en cisaillement montrée par le TPS peut être attribuée à la haute déformation, au-delà de la région de viscoélasticité linéaire du TPS, expérimentée par ce matériau pendant le passage à travers la filière capillaire.

Dans la troisième partie de ce travail, la morphologie des mélanges PE/TPS préparée par le procédé de mise en forme à une étape est comparée à celle obtenue par la remise en forme du matériau original. L'influence de la composition et le taux de tirage en fondu est examiné. Une nouvelle méthodologie, basée sur le facteur de forme des particules dispersées, est utilisée pour la détermination d'une taille de particule sphérique équivalente du TPS dispersé. Cette approche permet la comparaison quantitative du diamètre moyen des particules de la phase dispersée indépendamment de ses formes.

Des mélanges préparés dans le procédé à une étape montrent un incrément dans les niveaux d'anisotropie comme conséquence d'une combinaison de la coalescence et la déformation des particules pendant le tirage en fondu. Les matériaux remise en forme exhibent des morphologies hautement stables. Les particules de TPS dans les mélanges remise en forme montrent une suppression de la coalescence et un très bas niveau de déformation. Ce phénomène s'explique par l'évaporation du plastifiant pendant la remise en forme. Le TPS se transforme d'une phase hautement déformable à une autre qui ressemble au comportement des matériaux partialement réticulés.

Dans la quatrième partie de ce travail, les mécanismes responsables de la ductilité des mélanges PE/TPS préparés par le procédé à une étape sont analysés. Les mélanges faites avec TPS contenant 36% et 40% glycérol, montrent une ductilité élevée. Les mélanges de PE1 et le TPS contenant 29% glycérol sont aussi ductiles et possèdent un module d'Young amélioré. Les mélanges de PE2 (basse viscosité) et le TPS (29% glycerol) présentent un comportement plutôt fragile aux différents concentrations de TPS évaluées. Les données de tests en traction sont comparées avec des modèles théoriques. Le module d'Young s'ajuste au modèle de Takayanagi pour une bonne adhésion. Contrairement, les propriétés à la rupture ne s'ajustent pas aux modèles simples parce que ces modèles ne considèrent pas les changements morphologiques reliés à la coalescence. L'évaluation *post mortem* des éprouvettes testées en traction montre comment la taille de particule et la distribution des tailles de particule influencent les mécanismes de fracture des mélanges PE/TPS. L'influence de l'humidité sur le mécanisme de dissipation de l'énergie est aussi démontrée. Les mélanges conditionnés à 0% humidité relative ont un mécanisme de dissipation de l'énergie basé sur la formation de craquelures, lequel est caractérisé par le blanchissement par contrainte dans l'entaille. Contrairement, les mélanges conditionnés à 50% humidité relative se maintiennent transparentes après les tests de traction car la formation des craquelures a été substituée par la déformation de la surface de la phase dispersée comme mécanisme de dissipation de l'énergie. De l'évaluation des microstructures *post mortem*, une série des mécanismes de fracture dépendant de la morphologie de mélange sont proposés. Les mécanismes se

divisent en trois étapes: le détachement, la croissance des vides et la défaillance. La complétion et l'extension des étapes dépendent principalement de la taille de particule et de la distribution des tailles de particule.

ABSTRACT

This work presents an approach to preparing polyethylene/thermoplastic starch blends with exceptional properties. Thermoplastic starch (TPS), as opposed to dry starch, is capable of flow and hence when mixed with other synthetic polymers can behave in a manner similar to conventional polymer-polymer blends. In this study, a one-step combined twin-screw/single screw extrusion setup was used to carry out the melt-melt mixing of the components. Glycerol was used as the starch plasticizer and its content in the TPS was varied from 29 to 40%.

The shear viscosity of raw PE and TPS was determined on-line from the twin-screw extruder using a series of capillary dies attached to the extruder head. PE/TPS blends prepared in a one-step process were evaluated from its composition, morphology, tensile properties and percent continuity. The composition of PE/TPS blends was determined by thermogravimetric analysis considering the differences in thermal decomposition between TPS (>300°C) and PE (≈ 400°). The morphology of cryogenically microtomed PE/TPS blends was qualitatively evaluated from SEM micrographs. Tensile specimens of type IV were cut longitudinally from the recently prepared PE/TPS ribbons and evaluated according to ASTM D-638. In order to evaluate the effect of minor phase orientation and humidity, samples (type V) were cut parallel and perpendicular to the machine direction and conditioned at 0% and 50% relative humidity. The percent of continuity of PE/TPS blends was determined by hydrolytic degradation of starch domains using a solution of HCl 6N at 60°C for 96 hours.

Under the particular one-step processing conditions used it is possible to develop continuous TPS (highly interconnected) and co-continuous polymer/TPS blend extruded sheet which possess a high elongation at break, modulus and strength in the machine direction. The PE/TPS 55:45 blend prepared with 36% glycerol content maintains 94%

of the elongation at break and 76% of the modulus of polyethylene. At a composition level of 71:29 PE/TPS for the same glycerol content, the blend retains 96% of the elongation at break and 100% of the modulus of polyethylene. These exceptional results are achieved in the absence of any interfacial modifier and despite the high levels of immiscibility in the polar-nonpolar TPS-PE system. The 55:45 blend possesses a 100% continuous or fully interconnected TPS morphology, as measured by hydrolytic extraction. This TPS configuration within the blend enhances its potential for environmental biodegradation which is an additional potential feature of the system. The elongation at break in the cross direction of these materials, although lower than the machine direction properties, also demonstrate ductility at high TPS concentrations. At a glycerol content of 36% in the TPS, the blends demonstrate only very low levels of sensitivity to moisture. A high degree of transparency is maintained over the entire concentration range due to the similar refractive indeces of PE and TPS and the virtual absence of interfacial microvoiding.

The second part of this work is devoted to the study of the thermal and rheological properties of TPS (glycerol content 29 to 40%) prepared in a TSE. Those properties are compared to those of LDPE. DSC analysis revealed the presence of a glass transition temperature (Tg) below ambient temperature, which indicated the complete gelatinization of starch granules. The Tg decreased from –45.6°C to –56.2°C as glycerol content increased from 29% to 40%. Even though no thermal transition was observed above room temperature, a crystalline structure, which can be related to the complexation of amylose with lipids present in wheat starch granules, was detected by X-ray diffraction.

Rheological properties in the shear and oscillation mode were determined on-line from the TSE and by using two oscillatory rheometers, respectively. Time sweep measurements demonstrated that TPS has excellent thermal stability at 150°C, but becomes unstable at temperatures above 180°C. The studies indicate however that TPS stability was maintained for short time periods at temperatures up to 200°C. These

results are important since they indicate that the potential exists to prepare stable TPS materialsat high temperatures by maintaining short residence times during processing. The linear viscoelastic domain of TPS extended to $\gamma \sim 0.02$ due to the restricted motion imposed by the presence of an elastic network. The evaporation of glycerol leads to a gradual increase in the rheological properties of TPS due to the stiffening of TPS. As was observed for the thermal properties, the rheological properties were also highly dependent on glycerol content. The shear viscosity of TPS (at ~ 130 s^{-1}) decreased 20% when the glycerol content was increased from 36 to 40%. Similarly, G' and G" decreased as glycerol content increased with a particularly dramatic reduction around 30% glycerol. This suggested the percolation threshold of the well-plasticized glycerol-rich soft regions.

Comparison of the shear and oscillation viscosity of TPS40 and PE1 show important differences in the viscosity ratio for this polymer pair. Under shear conditions, LDPE was more viscous than TPS while in the oscillation mode the trend is reversed. The lower shear viscosity displayed by TPS can be attributed to the very high deformation, out of the TPS linear viscoelastic domain, undergone by this material during the pass through the capillary die.

In the third part of this study, the morphology of LDPE/TPS blends prepared by a one-step extrusion/shaping process is compared to that obtained by reprocessing of the original blends. The influence of composition and melt drawing is examined. A novel methodology based on the form factor of the dispersed particle is used to estimate the equivalent spherical particle size of dispersed TPS. This approach allows for the quantitative comparison of average dispersed phase particles regardless of their shape. Blends prepared in the one-step extrusion process show increased levels of anisotropy as a consequence of a combination of coalescence and particle deformation during melt drawing. Re-processed materials demonstrate morphologies that are highly stable to a wide range of hot stretch ratio conditions. The TPS particles of re-processed blends show no-coalescence and a low degree of deformation. This phenomenon is explained

by plasticizer evaporation resulting from the second processing step. The TPS is transformed from a highly deformable phase to one resembling a partially crosslinked material. These data indicate that the one-step processing of LDPE/TPS blends can be used to generate a wide range of highly elongated morphological structures. A two-step approach, analogous to typical compounding and shaping operations and involving controlled glycerol removal in the second step can be used to prepare a wide range of highly stable, more isotropic, dispersed particle morphologies.

In the fourth part of this work, the tensile properties of LDPE/thermoplastic starch (TPS) blends prepared in a one-step process are studied more in detail as a function of TPS composition, glycerol content, morphology and relative humidity. Blends with TPS containing 36% and 40% glycerol, show an unusually high ductility. Blends prepared with TPS containing 29% glycerol and a high viscosity PE are also ductile and possess an improved modulus. Blends of a low viscosity PE and the same TPS result in a material with significantly reduced elongation at break. Data from the tensile testing of PE/TPS blends are compared with theoretical models. The Young's modulus fits the Takayanagi model for good interfacial adhesion. Conversely, properties at break did not fit simple models well because such models do not consider morphologies produced by particle coalescence during melt blending. The *post mortem* evaluation of tensile tested samples reveals how particle size and particle size distribution influence the fracture mechanisms of PE/TPS blends. The influence of humidity on the energy dissipation mechanism is also demonstrated. Blends conditioned at 0% RH have an energy dissipation mechanism based on craze formation which was characterized by stress whitening in the neck. Conversely, blends conditioned at 50% RH remain transparent after tensile testing because craze formation was replaced by the deformation of dispersed phase surface (shear yielding) as an energy dissipation mechanism. From the evaluation of the *post mortem* microstructure, a series of fracture mechanisms dependent on blend morphology are proposed. The mechanisms are composed of three stages: debonding, void growth and failure. The completion of generalized debonding is mainly dependent on particle size and particle size distribution effects. Smooth void growth can

be achieved when the stress is homogeneously distributed to all dispersed particles during debonding. This is achieved with a homogeneous distribution of small particles. The extent of void growth depends primarily on the thickness of matrix filaments which is related to the interparticle distance. Tensile failure depends on the completion of debonding or the extent of void growth.

The combination of the different structures observed in this work suggest the possibility of property tailoring via morphology control and glycerol content. Highly ductile materials can be obtained by a combination of fiber formation and unidirectional orientation during hot stretching. While a good balance of ductility and modulus can be attained with well-dispersed spherical particles.

CONDENSÉ EN FRANÇAIS

L'amidon est un polymère naturel, renouvelable et peu coûteux. L'amidon est un polysaccharide composé d'une fraction linéaire connue sous le nom d'amylose et une fraction branchée appelait amylopectine. Plusieurs auteurs ont publié sur le développement des matériaux à base d'amidon, mais ces matériaux présentent une basse ductilité et une sensibilité à l'humidité très élevée. Une bonne alternative pour l'utilisation de l'amidon est par son incorporation dans une matrice polymérique synthétique. Récemment, St.-Pierre et collaborateurs de ce laboratoire, ont développé un procédé dans une étape pour la mise en forme de mélanges polyéthylène basse densité (PE)/amidon thermoplastique (TPS). Ces mélanges ont présenté un allongement à la rupture très élevée à de basses concentrations de TPS, lequel tombe dramatiquement à des concentrations plus élevées, même s'ils restent ductiles.

En considérant ces résultats, les objectives de cette étude seront:

1. Le développement d'un système d'extrusion pour la mise en forme des mélanges PE/TPS avec une ductilité élevée dans un procédé en une étape.
2. L'étude des propriétés thermiques et rhéologiques du TPS.
3. L'analyse de l'influence des conditions de mise en forme sur la morphologie et la biodégradabilité de ces mélanges.
4. Une étude sur les mécanismes de fracture involucrés dans la haute ductilité des mélanges PE/TPS.

Les matériaux utilisés dans cette étude sont deux polyéthylènes basse densité avec différents indices de fluidité (PE1, 12g/10min et PE2, 20g/10min), de l'amidon de blé, du glycérol et de l'eau distillée. Des suspensions avec différentes concentrations d'amidon/glycérol/eau ont été préparées pour avoir des TPS avec différents rapports amidon/glycérol (40-29% massique).

Le système d'extrusion est composé d'une extrudeuse mono-vis connectée à la zone 5 d'une extrudeuse bi-vis. Contrairement au système utilisé par St.-Pierre, la suspension est alimentée dans la bi-vis pendant que le PE est alimenté dans la mono-vis. La gélification et plastification de l'amidon sont développées entre les zones 1-4 de la bi-vis. L'eau utilisée pour la gélification s'évapore dans la zone 4. Le PE fondu est alimenté dans l'extrudeuse bi-vis en zone 5 pour être mélangé avec le TPS dans la dernière partie de la bi-vis. Les mélanges sortent de l'extrudeuse par une filière rectangulaire pour être refroidis par une calandre à un taux de tirage en fondu (HSR) d'environs 2. Ce HSR est calculé par le rapport entre la vitesse linéaire du mélange fondu et cela des rouleaux.

Pour préparer du TPS pur, la configuration de l'extrudeuse bi-vis est modifiée en sortant les zones 5-7 pour en avoir une extrudeuse plus courte. Les conditions de mise en forme pour la préparation du TPS sont les mêmes que celles utilisées pour les mélanges. Une série de filières capillaires est utilisée à la place de la filière rectangulaire pour déterminer la viscosité en cisaillement du TPS et du PE.

Pour évaluer l'effet des conditions de mise en forme sur la morphologie de mélanges PE1/TPS (40% glycérol), des mélanges contenant 30% (fraction volume de TPS, ϕ_{TPS}=0.20) et 45% TPS (ϕ_{TPS}=0.32) ont été préparés et tirées à différent HSR. Une partie de ces mélanges est ajoutée avec plus du PE pour avoir des mélanges avec 1%, 10%, 30% et 45% TPS (ϕ_{TPS}: 0.006, 0.06, 0.20 et 0.32, respectivement). Ces mélanges sont re-mise en forme en utilisant seulement l'extrudeuse bi-vis avec la même configuration de vis et une température de mise en forme constante de 150 C. Ces mélanges sont tirés à différent rapport de tirage comme dans le cas précédent.

Les matières pures, PE et TPS avec différent contenu en glycérol, sont caractérisées de la façon suivante:

- La viscosité dynamique, le module élastique et le module de perte du TPS et du PE sont déterminés en utilisant deux rhéomètres oscillatoires à des températures entre 150 et 200 C à 1 Hz.
- Les propriétés thermiques du TPS sont évaluées par la calorimétrie différentielle à balayage.
- La structure cristalline du TPS est étudiée par la diffraction de rayons-X.
- L'indice de réfraction des films du TPS est déterminé en utilisant la technique standard ASTM D524-90
- L'évaporation du glycérol est déterminée par rapport à la perte de poids dans une balance thermogravimétrique (TGA).

Les mélanges PE/TPS sont caractérisés de la façon suivante:

- La composition des mélanges PE/TPS est déterminée par l'analyse thermogravimétrique en considérant les différentes températures de decomposition thermique entre le PE (environs 400 C) et le TPS (> 300 C).
- La morphologie des mélanges PE/TPS est évalué à partir des surfaces microtomées sur l'azote liquide. Un alliage or-palladium est déposé sur les surfaces par un appareil à électrodéposition pour permettre l'observation sous un microscope électronique à balayage (SEM). La morphologie de mélanges est quantifiée en utilisant une méthodologie qui permet la comparaison entre les diamètres de particules sphériques et celles de particules allongées.
- Les essais de traction sont déterminés d'accord à la norme ASTM D-638. Des échantillons plus petits sont coupés pour l'évaluation de propriétés en traction dans la direction transverse.
- Le percent de continuité et la biodégradabilité des mélanges PE/TPS sont déterminés en utilisant les dégradations hydrolytique et bactérienne, respectivement.
- Un analyse fractographique est effectué sur les éprouvettes cassées pendant les test de traction. Pour améliorer le contraste entre la phase TPS et la matrice du

PE, ces éprouvettes sont exposées au vapeur d'Iode avant d'être observées sous le microscope optique.

L'analyse des propriétés thermiques a montré, au dessous de la température ambiante, une transition qui dépende du contenu en glycérol. Aucune transition est observée en dessus de la température ambiante. Ça indique que la gélification de l'amidon est accomplie au 100%.

La viscosité en cisaillement du PE a été comparée à celle du TPS contenant 36% et 40% glycérol. Tous les matériaux présentent un comportement qui suivent la Loi de Puissance. Les deux PE sont plus visqueux que les TPS. Tout comme dans le cas des propriétés thermiques, la viscosité en cisaillement du TPS dépend du contenu en glycérol.

L'amidon, tout comme des autres polymères biologiques, présente un comportement viscoélastique semblable aux gels physiques. Contrairement, la plus part des polymères synthétiques, comme le PE, présentent le comportement typique d'un réseau enchevêtré. Un réseau enchevêtré se caractérise par un module élastique (G') plus bas que le module de perte (G") à des basses fréquences. De plus, les deux modules dépendent de la fréquence dans l'intervalle d'échelle typiquement mesurée. Par ailleurs, les gels physiques présentent un G' plus élevé que G". Dans ce dernier cas, les deux modules sont pratiquement indépendants de la fréquence.

Les valeurs de G' et G" du TPS dépendent du contenu en glycérol. Les deux modules diminuent quand le contenu en glycérol augmente. Cependant, ils ne montrent pas de changement dans le comportement viscoélastique aux différents contenus en glycérol. Il est important de souligner que le changement de glycérol entre 40% et 33% a produit des faibles accroissements de G', pendant que la diminution de glycérol de 33% à 29% résulte en une augmentation plus importante de G'. Ces résultats, combinés avec une

analyse détaillée de la structure du TPS, suggèrent la présence d'une limite de plastification pour le glycérol à environ 30%.

La comparaison entre les viscosités en cisaillement et dynamique du PE1 et TPS (40% glycérol) montre des aspects importants sur la rhéologie du TPS. PE, comme des autres polymères synthétiques, suive la règle de Cox-Merz. Cette règle suggère la coïncidence des viscosités dynamiques et en cisaillement à des hautes fréquences. Contrairement, TPS ne suive pas la règle de Cox-Merz. Cela se montre comme un changement important du rapport de viscosité dans le système PE/TPS. Dans de conditions dynamiques, le TPS est plus visqueux que le PE, pendant que dans les conditions en cisaillement le TPS est moins visqueux que le PE. Ça est important au moment de déterminer quelle viscosité doit être choisi pour l'utilisation dans des modèles pour la prédiction de la morphologie de ce système de polymères. L'évaluation de la viscosité dynamique aux déformations plus hautes que celles dans la région de viscoélasticité linéaire, montre que cette viscosité devient plus proche à celle mesurée en cisaillement. Ces résultats indiquent que la déformation produite dans les conditions de mise en forme est bien loin de la région de viscoélasticité linéaire.

L'effet du contenu en glycérol sur la morphologie des mélanges PE/TPS a été évalué de façon qualitative. Les mélanges du PE1 préparés avec TPS contenant 36% et 40% glycérol montrent des morphologies allongées. Par ailleurs, les mélanges du PE1 préparés avec du TPS contenant 29% présentent des morphologies plutôt sphériques et une taille de particule plus grande que celles ayant plus du glycérol. Ces dernières caractéristiques sont plus marquées par l'utilisation du moins visqueux PE2.

Pour évaluer l'effet du taux de tirage en fondu (HSR) sur la morphologie des mélanges PE/TPS, les mélanges préparés dans une étape et celles remise en forme ont été tirées à différent HSR. À bas HSR, il y a une large population des petites particules rondes dispersées autour de quelques particules allongées plus grosses. Quand le HSR augmente, la concentration de grosses particules elliptiques et des fibres augmente. Ce

phénomène est plus marqué dans le cas où la fraction volume de TPS augmente. La déformation est quantifiée en utilisant un facteur de forme (F) lequel dépend de l'aire et du périmètre de la particule dispersée. Les mélanges préparés avec une fraction volume de TPS de 0.20 montrent un faible réduction de F par rapport au HSR. Cette réduction est plus importante dans le cas des mélangés contenant une fraction volume de TPS de 0.32. La réduction de F est moins importante que ce qui a été prévu, probablement à cause de la présence d'une grosse quantité de petites particules. Pour isoler l'effet de la distribution des tailles de particules sur la déformation des particules dispersées, les particules sont séparées par intervalles de volume. L'analyse de ces intervalles de volume montrent qu'il n'y a pas d'effet de déformation sur les particules avec de volumes au dessous de 20 μm^3. En dessus de ce limite, les particules montrent une déformation qui augmente avec l'intervalle de volume. Ça suggère qu'il y a une limite de volume pour la déformation des particules de TPS (40% glycérol) quelque part entre les 20 et 30 μm^3.

La remise en forme a un importante effet sur la morphologie de mélanges PE1/TPS (40% glycérol). Les domaines de TPS sont plutôt sphériques même à des hautes fractions volume de TPS. Il n'y a pas de changement apparent à des HSR élevés. La comparaison du F avec HSR montre quantitativement l'absence de déformation dans les mélanges PE/TPS remise en forme. Il semble que une partie du glycérol a été volatilisée pendant le passage à travers la zone 4 de l'extrudeuse bi-vis à 150°C. Les particules de TPS deviennent plus rigides à cause de cette perte du glycérol. Une absence de déformation est observée dans les mélanges du PE produits avec le TPS contenant 29% glycérol.

L'influence du HSR sur la coalescence des mélanges PE/TPS a été analysée par rapport à l'évolution du diamètre équivalent des particules de TPS. L'augmentation du diamètre équivalent est une indication de la coalescence. Cependant cette coalescence est plus évidente dans le cas de Dv qui est influencé par les particules les plus grosses pendant que Dn est plutôt relié au nombre totale des particules. Dans le cas des mélanges remise

en forme il n'y a pas d'agrandissement de la taille de particule par rapport au HSR même à des hautes fractions volume de TPS. La suppression de la coalescence et l'absence de déformation ouvrent la possibilité pour le développement d'un ample spectre des morphologies hautement stables en utilisant la remise en forme des mélanges PE/TPS.

Les propriétés de traction des mélanges PE/TPS sont comparées avec des modèles théoriques. Le module d'Young relatif est comparé avec l'équation de Takayanagi pour une bonne et une faible adhésion. La dispersion du TPS contenant 29% glycérol, lequel est plus rigide, augmente le module du PE pur. Par contre, l'addition du TPS contenant 36% et 40% glycérol, qui sont plus mous, réduit légèrement le module du pur PE. Le module d'Young relatif montre un meilleur ajustement avec l'équation de Takayanagi pour une bonne adhésion que cela pour une faible adhésion. Ça peut être expliqué par le très bon contact à l'interface montre par les mélanges PE/TPS.

L'allongement à la rupture relatif des mélanges PE/TPS est comparé avec les modèles de Nielsen. Les deux modèles utilisés ne peuvent pas prédire l'effet de la fraction volume de TPS sur l'allongement à la rupture des mélanges PE/TPS. Les mélanges préparés avec les TPS contenant 36% et 40% glycérol, lesquels ont montrés une morphologie fibrillaire, maintiennent presque 100% de l'allongement à la rupture du pur PE même à une fraction volume de TPS d'environ 0.35. Par ailleurs, les mélanges PE1/TPS (29% glycérol), lesquels ont montré une morphologie sphérique, présentent une réduction graduelle de l'allongement à la rupture, mais elles demeurent ductiles même à des fractions volume en dessus de 0.40. Les mélanges préparés avec le moins visqueux PE2 et le TPS contenant 29% glycérol sont fragiles indépendamment de la fraction volume de TPS.

L'évaluation *post mortem* des éprouvettes testées en traction a permi d'étudier les mécanismes involucrés dans les fractures des mélanges PE/TPS. Des micrographies optiques ont été prises à différentes position au long des éprouvettes pour analyser les différent états de déformations expérimentées par les mélanges PE/TPS.

Les mélanges de PE1/TPS (29% glycérol), ceux qui ont montré une morphologie sphérique, sont analysés d'abord. À une fraction volume de 0.20, le détachement des particules de TPS commence par les plus grosses. Une distribution homogène de la contrainte appliquée permet le détachement des particules plus petites. Au début de la zone de constriction, la croissance de vides elliptiques peut être observée. Ces vides elliptiques se transforment à vides avec une forme pointue à cause de l'endurcissement par contrainte (stress hardening). Ces éprouvettes faillissent à cause de la formation de creux interne produit par la coalescence latérale des particules de TPS.

À une fraction volume de TPS de 0.29 il y a seulement des changement mineurs. Le détachement des particules de TPS est très semblable à celui montre pour les mélanges ayant une fraction volume de TPS de 0.20 avec le détachement des grosses particules suivit pas celui des plus petites. La croissance de vides est très semblable, cependant le nombre de creux internes est supérieur comme conséquence d'une taille de particule plus grosse et d'une distance entre les particules plus réduite.

Des changements majeurs sont observés dans les mélanges contenant une fraction volume de TPS de 0.38. Comme dans les cas précédents, le détachement commence à partir des grosses particules, mais dans ce cas, il ne se propage pas aux particules plus petites. Comme conséquence, la croissance de vides est limitée seulement aux grosses particules qui étaient déjà détachées. Des petites craquelures se forment au équateur des grosses particules. Ces craquelures se transfèrent aux particules voisines conduisant à la fracture de l'éprouvette.

Le cas le plus extrême de fragilité a été présenté par les mélanges faits avec PE2 et le TPS contenant 29% glycérol. Ces mélanges ne montrent pas une zone de constriction et résultent en une fracture fragile à toutes les concentrations de TPS testées. Elles montrent la présence de particules plus grosses que 150 μm. Au début des effets de tirage, il y a le détachement catastrophique des particules les plus grosses. Ça s'observe comme un détachement généralisé de la particule toute entière et pas seulement dans les

pôles comme dans les cas précédents. Le détachement complète de ces particules produit la formation prématurée de fissures qui se propagent rapidement vers les particules voisines résultant en une fracture fragile de l'éprouvette.

À partir de ces résultats, une série de modes de fracture en considérant les changements morphologiques produits par l'augmentation de la fraction volume de TPS a été proposée.

L'évolution de la fracture de mélanges préparés avec PE1 et TPS (36% glycérol) est analysée par rapport aux conditions d'humidité relative (0% et 50% HR). Ces mélanges présentent une morphologie allongée. Dans le cas de mélanges conditionnés à 0% RH, le détachement aux pôles des fibres de TPS est combiné avec la cassure même de la fibre. Proche à la zone de constriction, il y a la croissance de vides aux pôles des fibres et la séparation des segments de fibres cassées. Cela donne lieu à la formation de craquelures qui s'orientent perpendiculairement en direction de tirage. La croissance homogène de vides et la formation, bien distribuée, de plusieurs craquelures dissipent suffisamment contraint pour permettre la constriction stable de l'éprouvette. À un tirage plus prononcé, la réduction de la distance axiale entre les particules et la propagation des craquelures conduisent à la fracture de l'éprouvette.

L'histoire de la fracture observée dans le cas des mélanges conditionnés à 50% RH est très semblable sauf que dans l'étape de croissance de vides, il n'y a pas la formation de craquelures. Il semble que dans ce cas-là, il y a un mécanisme de dissipation de l'énergie différent au cas précédent. Il est bien connu que l'eau est un bon plastifiant pour l'amidon et que l'augmentation du contenu de plastifiant réduit le module élastique du TPS. Il semble que dans ce dernier cas le mécanisme de dissipation de l'énergie est relié à la déformation de la surface des particules de TPS plutôt qu'à la formation homogène de craquelures comme dans les mélanges conditionnés à 0% RH.

TABLE OF CONTENTS

LIST OF FIGURES

LIST OF TABLES

LIST OF ANNEX

CHAPTER 1. INTRODUCTION

The incorporation of materials obtained from agricultural sources into plastics can reduce our dependence on petroleum and increase the percent of biodegradable matter in plastic waste. Starch has been considered as an excellent candidate to partially substitute synthetic polymer in packaging, agricultural and other low-cost applications due to its abundance, biodegradability and low cost (Doane et al., 1992). Moisture sensitivity (Loomis et al., 1993, Shogren, 1993, Stenhouse et al., 1993, Van Soest et Borger, 1997) and brittleness (Stenhouse et al., 1993, Lawton et Fanta, 1994, Prinos et al., 1998, Averous et al., 2001b) are the main drawbacks of starch-based materials. Melt blending of starch with ductile hydrophobic synthetic polymers may overcome such drawbacks. Starch can be blended with synthetic polymer in its native granular form or destructured (gelatinized) and plasticized. Mechanical properties of starch-based materials depend on the starch content, interfacial adhesion with the polymeric matrix and the morphology and nature of starch domains. For instance, the incorporation of granular starch or gelatinized starch, with low plasticizer content (> 5 wt%), to a synthetic polymeric matrix can increase the elastic (Young's) modulus due to the stiffening effect of the rigid starch particles (Fanta et al., 1992, Willett, 1994, Prinos et al., 1998). On the other hand, the addition of soft starch with high plasticizer content can result in a reduction of such properties. However, the addition of starch to ductile synthetic polymers has generally resulted in brittle materials (Lawton and Fanta, 1994, Bikiaris et al., 1997b, Averous et al., 2000a). Ductility is critical for the preparation of blown films. In some cases fragile materials are unable to form stable blown film bubbles and produce paper-like films (Otey, et al., 1980, Bikiaris et al., 1997b).

Mechanical properties of immiscible polymer blends have been related to their morphological characteristics (Lovinger and Williams, 1980, Rizzo and Spadaro, 1984, Arends, 1992). The morphology of immiscible polymer blends is controlled by droplet

breakup and coalescence mechanisms. These mechanisms depend on a series of parameters including the shear rate (stress) during mixing, interfacial tension and the viscosity and elasticity ratios (Favis, 1991, Willis et al., 1991). In the polyethylene (PE)/thermoplastic starch (TPS) immiscible system, the rheological properties of PE are well-known while the level of understanding of TPS rheological properties is not high enough. Apparent viscosity of TPS has been studied directly from the extrusion through capillary and slit dies and shows a power-law behavior (Senouci and Smith, 1988, Della Valle et al., 1992, Willett et al., 1995, 1998, Aichholzer and Fritz, 1998). However, the effect of processing parameters and plasticizer content on power law constants (K and m) differ from one work to the other (Willett et al., 1998). The dynamic rheological properties of TPS has been evaluated using oscillatory rheometers displaying a gel-like viscoelastic behavior (Della Valle, et al., 1998, Ruch et Fritz, 2000). This behavior is caused by the presence of an elastic network which has been related to amylose-complex crystalline regions (Della Valle, et al., 1998, Conde-Petit and Escher, 1995) and to the very high molecular weight of starch (Della Valle, et al., 1998, Ruch et Fritz, 2000).

Starch biodegradability is another attractive feature of starch-based materials. In the case of starch-based materials prepared with non biodegradable synthetic polymer only the starch fraction is biodegradable. In such a case, the biodegradation extent depends directly on starch concentration (Chandra and Rustgi, 1997, Bikiaris et al., 1997b, 1998, Prinos et al., 1998). At starch concentrations below 30 wt%, the starch fraction can be considered as completely encapsulated in the bulk by the nonbiodegradable matrix, with only the surface starch being available for biological attack (Bikiaris et al., 1998, Prinos et al., 1998).

St.-Pierre et al. (1995) have reported the production of ductile LDPE/TPS blends in a one-step process. However, the starch concentrations used were below 30 wt%. The ultimate objective of the present work was to develop an extrusion system for the preparation PE/TPS blends close to the dual-phase continuous region in a one-step process allowing full control of TPS moisture content. In order to improve the

understanding of the parameters that influence the morphology of such blends, the physical properties (thermal and rheological) were analyzed. Different morphologies were produced and the influence of blend morphology on both tensile properties and extent of biodegradation were studied. Considering the capital importance of the ductility of PE/TPS blends, an in-depth study of the fracture mechanism that permits high elongation at break of such blends was conducted and will be discussed in detail in this thesis.

CHAPTER 2. LITERATURE REVIEW

2.1 Starch.

2.1.1 Generalities.

Starch is a carbohydrate stored by plants as an energy reserve. It can be found in the form of granules in roots, tubers, stem-pith, leaves, seeds, fruits and pollen. Starch granules have a great variety of forms, i.e., spheres, ellipsoids, polygons, platelets and irregular tubules which range in size from 0.5 to 175 μm (Zobel, 1988). Starch is a polysaccharide composed of a linear molecule fraction called amylose and a branched counterpart known as amylopectin (Figure 2.1). Glucose is the polymeric repetitive unit in both molecules, Linear amylose molecules contain α-1,4 linkages with a degree of polymerization between 1500 and 6000, while amylopectin is formed by α-1,4 and α-1,6 linkages and a larger degree of polymerization (3×10^5-3×10^6) (Zobel, 1988). Starch properties are dependent on the amylose-amylopectin ratio and their structural characteristics.

2.1.2 Starch gelatinization and plasticization.

The gelatinization of starch is a process that permits the release of starch macromolecules from the granules. It can be carried out by exposing starch granules to heat and shear in the presence of moisture. As in the case of synthetic polymer, such as polyethylene and polypropylene (Suwanda et al., 1988a, 1998b, Suwanda and Balke, 1993, Pabedinskas et al., 1994, Cheung and Balke, 1997), the final structure and characteristics of the extruded materials depends on the conditions used during the particular extrusion processes. In the gelatinization of starch during extrusion, it is important to have a strict control of the energy applied and the moisture content. The gelatinization process is depicted in Figure 2.2. The application of excessive heat and shear, such as that observed during extrusion processing of starch at low moisture content, leads to its thermo-mechanical degradation (Gomez and Aguilera, 1983, 1984,

Lai and Kokini, 1991). Products of starch degradation are mainly dextrins, and in more extreme cases oligomers and sugars (Gomez and Aguilera, 1983, 1984).

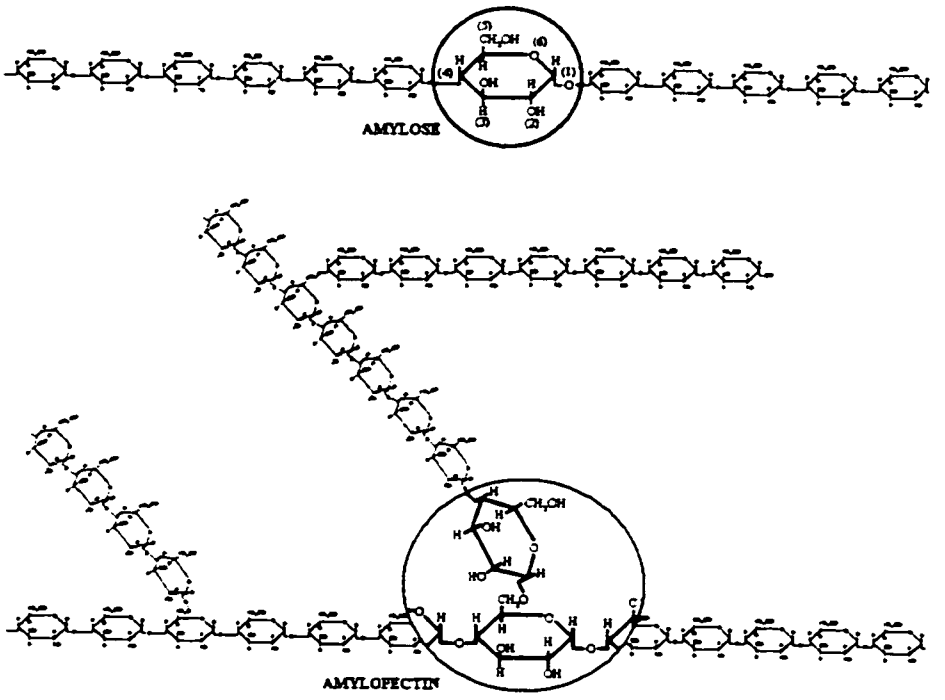

Figure 2.1 Schematic representation of starch molecules: amylose (top) and amylopectin (bottom) (Zobel, 1988).

Once starch granules are disrupted, the resulting gelatinized starch (GS) can be mixed with a suitable plasticizer to reduce its melting temperature and improve its processabillity. This material is known as thermoplastic starch (TPS). Water is a good plasticizer for TPS but its use leads to a high dependence of final properties to environmental conditions of humidity. Utilization of plasticizers other than water helps to stabilize the properties of TPS.

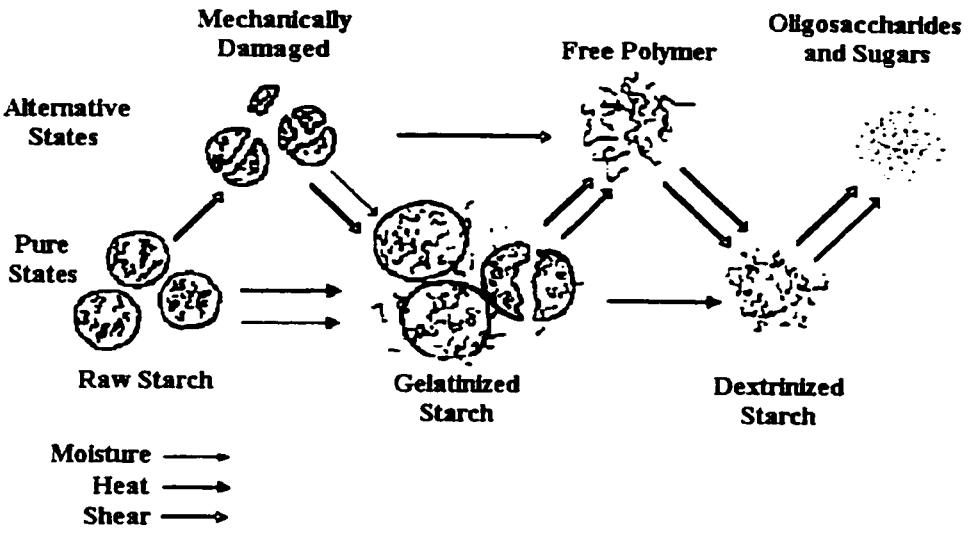

Figure 2.2 Schematic representation of starch gelatinization (Gomez and Aguilera, 1984).

2.1.3 Rheological properties of thermoplastic starch (TPS).

Rheological characteristics of extruded starch products have been studied from the point of view of polymer science (Della Valle et al., 1992, 1998, Willett et al., 1995, 1998, Aichholzer and Fritz, 1998). During extrusion, starch granules are exposed to high temperature and shear undergoing structural changes such as gelatinization and fractionation (Figure 2.2). Processing and physical properties depend on the extent of structural changes of the starch.

The on-line monitoring of the properties of molten polymeric materials during extrusion has been considered as an excellent alternative for the characterization and control of extrusion processes. It has been used for the control of polymer blend composition (Bains et al., 1994, Reshadat et al., 1995), for the detection of particulate contaminants in recycled plastic waste (Desa et al., 1995) and for-evaluation of the shear viscosity of polymeric melts. The apparent viscosity of TPS has been evaluated on-line during the extrusion process using capillary and slit dies attached to the processing device (Fletcher

et al., 1985, Senouci and Smith, 1988, Lai and Kokini, 1990, Della Valle et al., 1992, Willett et al., 1995, 1998, Aichholzer and Fritz, 1998). This direct measurement overcomes problems, such as plasticizer evaporation and moisture uptake, associated with batch testing processes such as capillary rheometry (Fletcher et al., 1985). However, several authors have reported the formation of bubbles at the exit of the die when water is used as plasticizer (Fletcher et al., 1985, Willett et al., 1995, Aichholzer and Fritz, 1998). Bubble formation appears at temperatures higher than 130°C for low moisture extrudates and at 100°C for materials having a moisture content of 30% (Willett et al., 1995). Shear viscosity of starch materials exhibits a power-law behavior at typical extrusion shear rate intervals (10^1 to 10^3 s^{-1}) and its values vary from 10^4 to 10^2 Pa-s depending on die temperature and plasticizer content.

Recently, rotational rheometry has been used to advance in the understanding of the viscoelastic behavior of starch-based materials in the melt (Della Valle et al., 1998, Dus and Kokini, 1990, Redl et al., 1999, Ruch and Fritz, 2000). As with many other biopolymers (Ross-Murphy, 1995), TPS has been found to display a gel-like viscoelastic behavior (Della Valle et al., 1998, Ruch and Fritz, 2000, Conde-Petit and Escher, 1995). Such rheological behavior is produced by an elastic network and has been related to the complexation of amylose molecules with lipid present in starch granules (Della Valle et al., 1998, Conde-Petit and Escher, 1995) and the physical entanglement of starch chains caused by its very high molecular weight (Ruch and Fritz, 2000).

2.2 Melt blending with starch.

Starch-based materials present two main drawbacks: brittleness (Stenhouse et al., 1993, Lawton and Fanta, 1994, Prinos et al., 1998, Averous et al., 2001a) and moisture sensitivity (Loomis et al., 1993, Shogren, 1993, Stenhouse et al., 1993, Van Soest and Borger, 1997). Melt blending of starch with ductile hydrophobic synthetic polymers may overcome such problems. A general review of melt blending with immiscible polymers and parameters that control the final morphology of immiscible polymeric blends will be

discussed in the next sections, followed by a review of studies where starch has been used as a blend component.

2.2.1 Melt blending with immiscible polymers.

Melt blending with immiscible polymers has been considered as an excellent approach to the development of new multi-phase materials (Utracki, 1989). Multi-phase systems are, in general, characterized by a dispersed component embedded in a continuous matrix, although other morphologies, such as composite droplets (Favis, 2000), highly-continuous (Favis et al., 1999), co-continuous (Favis et al., 1999) or layered structures (Balke et al., 1998, Karami and Balke, 2000), can also be developed. Mechanical performance of multi-phase systems is closely related to the size and shape of the dispersed domains. The morphology of immiscible polymer blends is determined by rheological (viscosity, elasticity, yield stresses and microscopic flow fields) as well as thermodynamic parameters, such as interfacial tension (Elemndorp, 1991). The mechanism of morphology development mainly involves the breakup and coalescence of dispersed domains.

2.2.1.1 Droplet Breakup.

Theories of droplet breakup initially focused on Newtonian fluids. Taylor (1932, 1934) in his classic work, observed that droplet breakup will occur at a certain shear rate and certain droplet size. He expressed the deformation degree of such a droplets, strained at low stress in a steady uniform shearing flow, by means of the capillary number,

$$Ca = \frac{\eta_m \dot{\gamma} R}{\sigma} \tag{2.1}$$

and the viscosity ratio:

$$p = \frac{\eta_d}{\eta_m} \tag{2. 2}$$

where η_d and η_m are the dispersed phase and matrix viscosity, respectively, $\dot{\gamma}$ is the shear rate, R is the radius of the drop, and σ is the interfacial tension. The critical conditions for droplet breakup are given by the critical capillary number (Ca_{crit}). If Ca is larger than Ca_{crit}, the droplet can further deform and breakup. Taylor derived a simple expression to calculate the Ca_{crit} of Newtonian systems under simple shear flow:

$$Ca_{crit} = \left(\frac{1}{2}\right)\left(\frac{16p+16}{19p+16}\right) \tag{2.3}$$

Several researchers continued Taylor's work. Rumscheidt and Mason (1961) proposed two basic breakup models for simple shear flow mixing based on the viscosity ratio: drop splitting and thread disintegration (Figure 2.3). At $p<0.1$ the droplets attains a sigmoidal shape and small drops are shed from the ends. At $0.1<p<2$, the droplets break up into daughter droplets. At $p>4$ there is no further breakup and the droplets just undergo deformation.

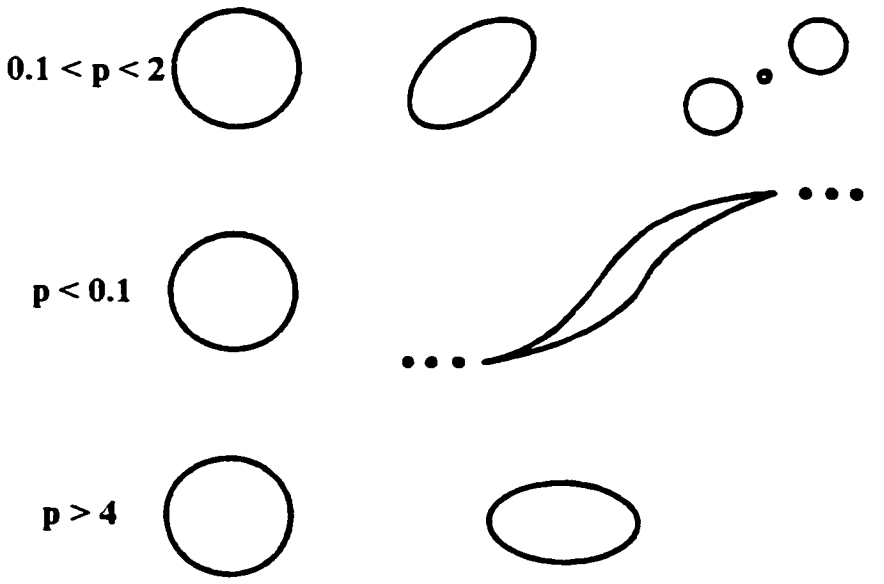

Figure 2.3 Modes of droplet deformation and burst at various viscosity ratios (λ) intervals proposed by Rumscheidt and Mason (1961).

Cox (1969) extended Taylor's theory to time-dependent flow fields. Later, Flumerfelt (1980) extended Cox's theory to fluids with well-defined viscoelastic interfaces. Grace (1982) performed a monumental work on breakup of Newtonian drops in both simple shear and extensional flows. For simple shear flow, he found that no further droplet breakup can occur above p=4, while for pure extensional flow, breakup is possible at all viscosity ratios (Figure 2.4).

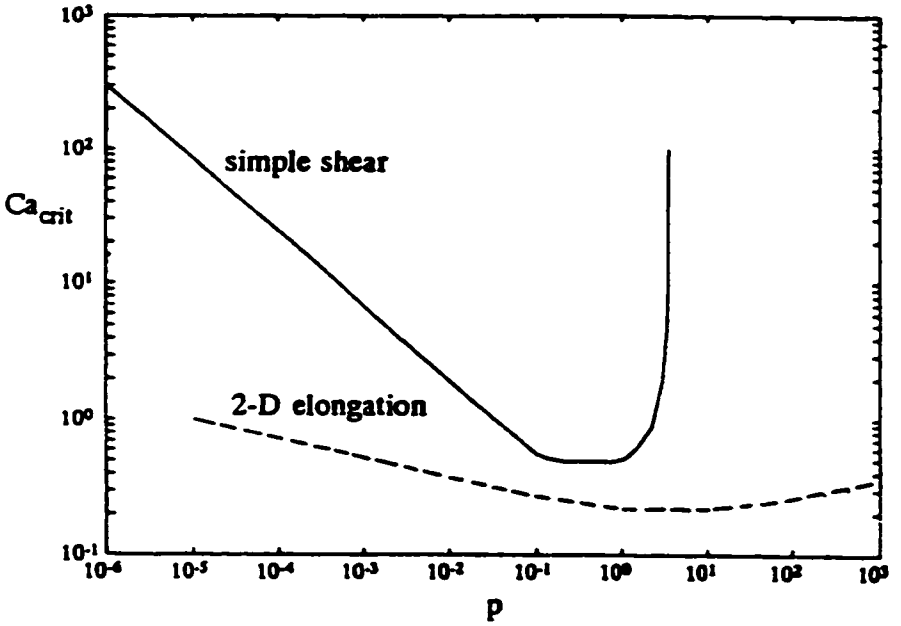

Figure 2.4 The effect of viscosity ratio (p) on the critical capillary number in shear and in elongational flow (Grace, 1982).

The final morphology of immiscible polymer blends has been evaluated as a function of their viscosity ratio (Wu, 1987, Favis and Chalifoux, 1987, Serpe et al., 1990, Everaert et al., 1999). Based on his experimental results, Wu formulated an empirical equation for the calculation of the final particle diameter:

$$d = \frac{4\sigma p^{\pm 0.84}}{\dot{\gamma}\eta_m} \qquad (2.4)$$

where the plus (+) sign of the exponent applies to p>1 and the minus (-) sign to p<1. The main deviation of Wu's equation from Taylor's theory is the relatively high dispersed phase concentration used by the former. Taylor worked with a single drop suspended in a fluid while in Wu's work, all blends contained 15wt % of the minor phase component.

Favis and Chalifoux (1987) studied the effect of viscosity ratio on the morphology of polypropylene (PP)/polycarbonate (PC) blends. Viscosity at 100 s^{-1} was used for the calculation of the viscosity ratio. The viscosity ratio of blends containing 7 and 23 vol% PC, in PP matrix (p>1), and PP, in PC matrix (p<1), were plotted against the volume average diameter (d_v) of the respective minor phase (Figure 2.5).

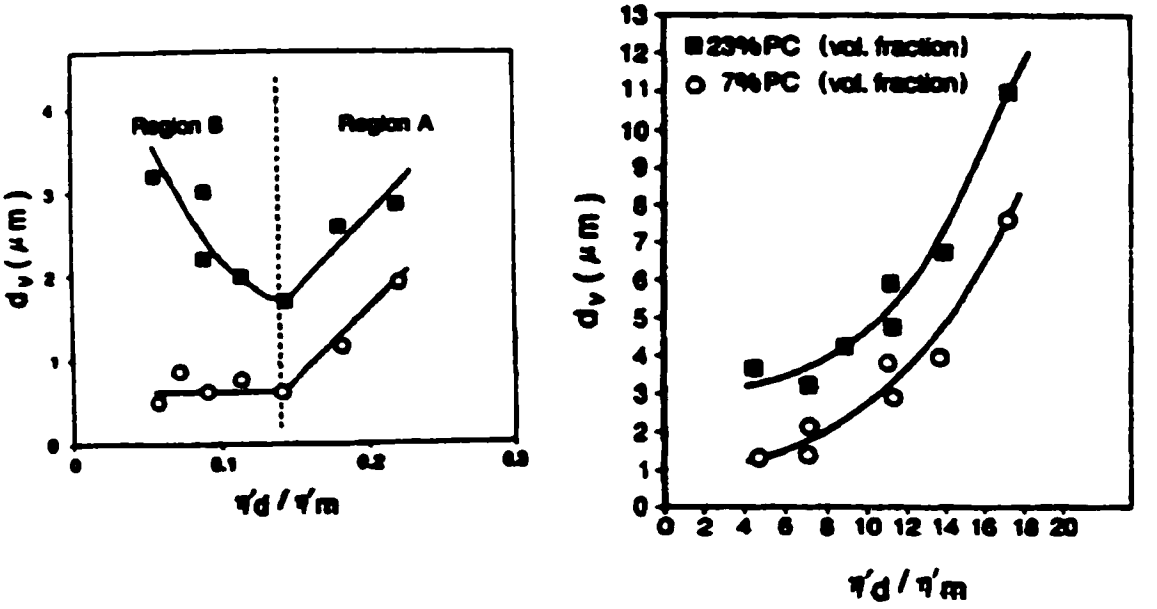

Figure 2.5 Volume average diameter versus the viscosity ratio of PP/PC blends at 7 and 23 vol% dispersed phase concentration. Left: p<1, PP dispersed in PC; right: p>1, PC dispersed in PP (Favis and Chalifoux, 1987)

Conversely to that observed with Newtonian fluids, the minimum average diameter is not located at a viscosity ratio of around 1. There is an upper limit at P>1 where the particle size is highly dependent of the viscosity ratio. This trend is not affected by the

increase in PC concentration from 7 to 23 vol%. At $p<1$, there is an important difference at the two concentrations of PP dispersed phase. A minimum average diameter is observed at $p\approx0.15$ for a composition of 23% PP in volume while at the same point the inflection to a plateau value is observed for a composition of 7 vol% PP. They demonstrated that the general consideration of a minimum occurring at $p=1$ is not universally true. Their results also demonstrate the effect of coalescence at high composition on the morphology of immiscible polymer blends.

2.2.1.2 Particle-Particle Coalescence

Particle-particle coalescence is a composition-related probabilistic phenomenon. Coalescence of Newtonian fluids mixtures has been studied by several researchers (Coulaloglou et al., 1977, Allan et al., 1984, Chen et al., 1984, Jeelani et al., 1991). Chen et al. (1984) found that the flow induced coalescence of two Newtonian fluids is dependent of the matrix viscosity, particle size of the dispersed droplet and density ratio between the matrix and the dispersed particles. The dynamic mechanism for the flow induced coalescence of two Newtonian fluids can be divided into three steps: the approach of two droplets; drainage of the film of the matrix phase between the two droplets; and rupture of the remainder of the continuous phase, usually by the creation of a "hole" in the thinnest interfacial section.

A number of studies have pointed out that the removal of the continuous phase in Newtonian systems is the major time-consuming step (Liem and Woods, 1974, Vijayan and Ponter, 1974, 1975). The hydrodynamics of this process is governed by the deformability of the dispersed particles and the mobility of the interfaces. The deformability of the dispersed particles can vary from fully deformable droplets to rigid particles. In the case of immiscible polymeric mixtures, the interfacial mobility of high viscosity polymer was considered as a relatively immobile interface which should result in long drainage times for the matrix film (van Gisbergen, 1991). However, Elmendorp and van der Vegt (1986) found experimentally that polymers had a high coalescence

probability during mixing and also that polymers had fully mobile interfaces. Elastic recoiling can make an important difference between the coalescence of polymeric and Newtonian fluids. It is expected to cause polymeric drops to separate during the initial step. Conversely to the expected reduction of coalescence, Roland and Böhm (1984) found that increasing shear rate increased the degree of coalescence.

Several theories have been developed to interpret the coalescence phenomenon. A composition-dependent theory for analysis of the size of dispersed particles in polymer blends was proposed by Tokita (1977). It was based on the equilibrium of drop diameter originating from the continuous breakup and coalescence of dispersed particles. He considered the total number of collisions per unit time proposed by Smoluchowski (1916, 1917)

$$N_T = \frac{4n\varphi_d\dot{\gamma}}{\pi} \tag{2.5}$$

where n is the number of particles. Assuming that coalescence is proportional to the total number of collisions, the reduction in the number of particles as a function of time can be represented by

$$\frac{dn}{dt} = -p_r N_T n \tag{2.6}$$

where p_r is the probability that a collision will result in coalescence. In the same way, the increment in the number of particles due to drop breakup as a function of time can be calculated with this expression:

$$\frac{dn}{dt} = n\left[\frac{\eta_m\dot{\gamma}^2}{E_{DK} + 6\sigma_{12}/d}\right] \tag{2.7}$$

where E_{DK} is the macroscopic bulk breaking energy. The particle size at the equilibrium conditions of droplet breakup and coalescence can be obtained from the combination of equation (2.6) and (2.7)

$$d_{eq} = \left(\frac{24 p_r \sigma_{12} \varphi_d}{\pi} \right) / \left[\eta_m \dot{\gamma} - \frac{4 p_r E_{DK} \varphi_d}{\pi} \right] \tag{2.8}$$

This equation suggests that the equilibrium drop size should increase with concentration and interfacial tension. On the other hand, particle size should decrease with shear stress which is in good agreement with Taylor's theory. One of the main contributions of this development is the consideration of the effect of composition on the drop size.

Following a procedure similar to that of Tokita, Fortelny et al. (1989, 1993) proposed an equation that considers both droplet breakup and coalescence to predict the equilibrium drop size,

$$r = r_c + \left(\frac{\sigma_{12} \alpha}{\eta_m f} \right) \varphi_d \tag{2.9}$$

where r_c represents the critical droplet radius as calculated from ca_{crit}; α is the probability of coalescence after collision; f is the function of Taylor capillary number (Ca) and rheological properties of the system. A disadvantage of this equation is the utilization of certain parameters that are not easy to quantify for the melt blending of viscoelastic polymers.

2.2.1.3 Capillary instabilities and formation of elongated morphologies.

Spherical particles can be deformed into threadlike shapes instead of disintegrating into drops when they are exposed to an elongational flow under specific conditions of deformation rates, viscosity ratio, and at relatively large particle sizes. Quantification of

these conditions requires knowledge of the stability of such liquid threads against interfacial tension-driven, capillary instabilities.

The theoretical basis for the study of the stability of a liquid cylinders surrounded by an immiscible matrix was established by Rayleigh (1892). Later, Tomotika (1935) extended Rayleigh's work to a Newtonian thread embedded in a Newtonian liquid. Tomotika found that the time required for breakup through the capillary instability mechanism depends on parameters such as interfacial tension, viscosity ratio and the initial thread diameter. Experimental work on the capillary instability of molten polymer systems demonstrated that both the growth and the wavelength of the dominant distortion are predicted satisfactorily by Tomotika's Newtonian developments.

The application of an elongational flow field has been found to be more effective for particle stretching that the application of a simple shear flow, especially at high viscosity ratio (Stone et al., 1986). Stretched particles can break up or maintain an elongated shape. The fibrillation-breakup process is controlled by interfacial tension, viscosity and elasticity ratios, the applied stress, and droplet particle size (Chapleau and Favis, 1995). Spherical particles can be transformed into ellipsoids or even long fibers under the influence of an elongational flow such as that exerted during passage through capillary dies (Favis and Therrien, 1991, Chapleau and Favis, 1995) or calendaring rolls (Gonzalez, et al., 1993, 1996). Favis and Therrien (1991) found that proximity to the die wall (high shear stress), high minor phase composition, and high viscosity/elasticity ratio enhance the formation of fiber-like morphologies. Chapleau and Favis (1995) studied the droplet-fiber transitions in immiscible polymer blends using capillary dies of different L/D ratios attached to a twin-screw extruder. They found that intensive deformation takes place in the elongation flow generated in the converging region of the capillary. In some cases they observed that the time required to develop these instabilities is very short. Coalescence of the dispersed phase was demonstrated at a concentration of 20%, for which fiber formation was enhanced. Coalescence phenomena appear to be dominant under these conditions. The addition of an interfacial modifier

results in a dramatic reduction of the dispersed phase size and, consequently, an important reduction of the deformation of the dispersed phase particles.

Gonzalez and coworkers (1993, 1996) studied the factors that influence the formation of elongated morphologies of hot-stretched immiscible polymer blends. They found that fiber formation is enhanced by increasing the hot stretch ratio (HSR) which is calculated from:

$$HSR = \frac{V_R - V_E}{V_E} \tag{2.10}$$

where V_R and V_E are the linear velocities of the calendar rolls and the extrudate, respectively (Gonzalez et al., 1993). They also studied the influence of coalescence on the morphology of melt-drawn polyamide-6 (PA-6)/HDPE blends (Gonzalez et al., 1996). Coalescence was suppressed by lowering the concentration of PA-6 (1%) in uncompatibilized blends or by the use of a compatibilizer in blends containing 20% PA-6, while an important coalescence effect was observed in uncompatibilized HDPE/PA-6 blends (80:20 in volume). A form factor ($F = 4\pi A / P^2$,where A and P are the surface area and perimeter) was calculated and plotted against HSR showing the presence of two deformation regions: region I, where there is deformation without coalescence, and region II dominated by deformation with coalescence (Figure 2.6). It is interesting to note that experimental data of blends where coalescence has been suppressed superimpose, region I in Figure 2.6. The relative role of coalescence and particle deformation on the final morphology of melt-drawn blends was demonstrated quantitatively in this work.

The presence of elongated elliptical or fiber-like particles can render the quantification of the dispersed phase dimensions difficult (Favis and Chalifoux, 1988). Elongated morphologies have been characterized by image analysis (Gonzalez et al., 1996, Luciani and Jarrin, 1996, Kelnar et al., 2001) or even by matrix extraction followed by the

separate quantification of spherical and fiber-like particles (Luciani and Jarrin, 1996). In the latter, the size of small particles (spherical and ellipsoidal) is determined with a particle counter. Only the volume percent of fibers is evaluated. The main disadvantages of this method are that small particles are all considered as spherical and that the size of single fibers is not determined. In some cases of image analysis, a relative volume (Gonzalez et al., 1996) or major axis-minor axis ratio (Kelnar et al., 2001) of elongated dispersed phase particles has been reported in comparison with the equivalent average spherical particle diameter. However, at the moment there is no method that allows the quantification of the size of single particles in elongated morphologies.

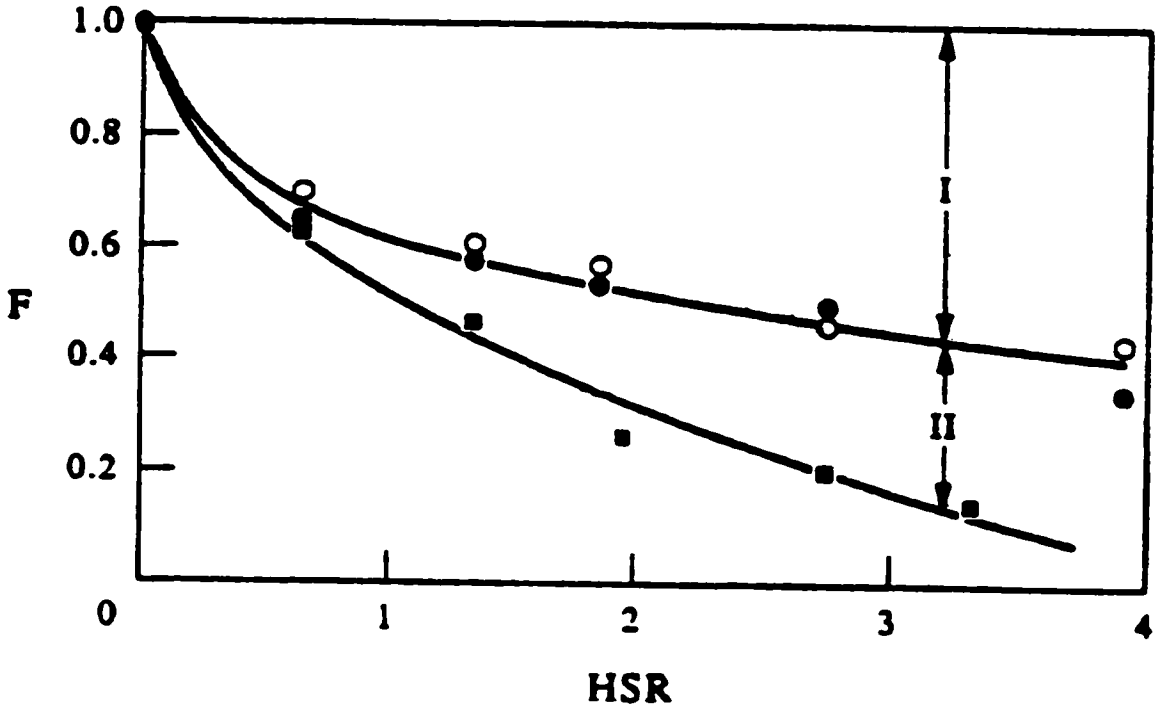

Figure 2.6 Form factor (F) vs. hot stretch ratio (HSR) of blends of PA-6 in HDPE: (O) 1% PA-6 (uncompatibilized), (●) 20% PA-6 (compatibilized) and (■) 20% PA-6 (uncompatibilized) (Gonzalez et al., 1996).

2.2.1.4 Continuity and phase inversion.

The co-continuous structure is a unique feature of immiscible polymer blend morphology. The evolution of this structure involves the transition from one minor phase dispersed in another matrix to dual phase continuity. The transition process can be explained by percolation theory. The percolation concept deals mainly with the value of the percolation threshold, p_c, at which an infinite connectivity of occupied sites (or bonds) first occurs, and the probability of finding such a connectivity as a function of p. The evolution of dispersed particle to a co-continuous morphology can be related to percolation theory (Figure 2.7). Starting with a simple homopolymer, we begin adding particles of a component. At low volume fraction of minor phase, the particles are disconnected and separated from one another (Figure 2.7A). As the volume fractions of minor phase increases, the particles start to become interconnected, as shown progressively by compositions B and C. Eventually, continuity is established throughout, as shown in D.

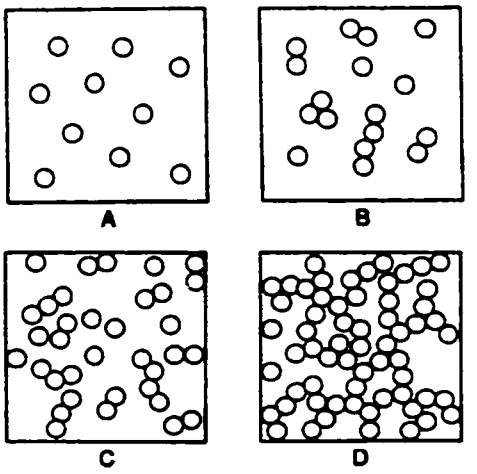

Figure 2.7 Schematic illustration of percolation theory (Hsu and Wu, 1993)

Stauffer (1980) presented a detailed review on scaling theory of percolation clusters. Through computer simulations (Monte Carlo method, series expansion, renormalization

group technique and exact inequality), the results demonstrate that there is a qualitative difference of cluster structures above and below p_c and suggest that for large clusters near the percolation threshold, p_c, the number of average clusters n_s, varies as an expression,

$$n_s \propto s^{-\tau} f(z) \tag{2.11}$$

with $z = (p - p_c)s$

where, s, is the number of the sites, f(z), the scaling function and τ, σ, the free exponents. Some researchers (Margolina et al, 1988, 1990, Hsu and Wu, 1993, Arends, 1992) have applied the percolation concept to interpret the change in mechanical properties in the transition region as function of morphology in polymer blends. They showed that percolation concepts could be successfully used to analyse the data and explain the transitions.

Percent continuity can be defined as the volume of one component involved in the continuous path divided by the total volume of that component. Phase inversion refers to a transition composition, at which a dispersed phase becomes continuous. In the literature the terms co-continuity and phase inversion has been erroneously used interchangeably. Co-continuity can exist in a composition range, whereas phase inversion occurs at a certain composition.

Several models have been proposed to predict the formation of interpenetrating co-continuous structures. Based on percolation theory Jorgensen and Utracki (1991) formulated an equation in which they suggested that, two types of domains, led by the coalescence and break-up process in simple shear flow and low volume fraction, are coexistent. One is small and nearly spherical, and the other, larger and nearly cylindrical. The critical concentration at which percolation occurs can be expressed as follows,

$$Q_{cr} = 1/z \tag{2.12}$$

where, z: average co-ordination number per domain, and z = z (Q_l, Q_s, P), Q_l and Q_s are the fractions of cylindrical and spherical domains, respectively, and P is the average number of spherical domains into which a cylinder can decompose. Using this model, they examined a polymethyl methacrylate (PMMA)/polystyrene (PS) blend system at a critical phase inversion point. The observed value was 0.113, compared with the predicted one of 0.109. Of course, this model can also be used to estimate the critical transition composition of spherical domains, especially, for the polystyrene/high density polyethylene (PS/HDPE) system. The observed value was 0.15, while the predicted value was 0.156. Thus the experimental result correlates well with the predicted value. From the above two systems, it appears that the percolation threshold can be decreased when clusters are composed of non-spherical domains.

Arends (1992) investigated percolation in injection molded polymer blends (polycarbonate (PC)/ poly (styrene-co-acrylonitrile) (SAN)). He measured the variation of blend modulus with composition at temperatures between the glass transition temperatures of the two components. He compared the injection molded modulus to the compression molded one, and found that the former is a factor of three higher than the latter. He ascribed this variation to the difference in connectivity between minor components, and modelled the morphologies of these materials using percolation theory. In his Monte Carlo simulation (Figure 2.8), it can be observed that extrinsic factors, such as the state of dispersion, particle shape, and orientation can significantly affect the percolation threshold.

A parameter, R, is defined as the ratio of the inclusion length to the effective domain size in the percolation direction. It was found that for small R (0.028) the threshold approaches 0.31, and for large R (0.22), the threshold reduces to 0.22, indicating that the higher the R, the lower the critical concentration for percolation. It is quite evident that the shape of the domain should have a significant effect on the percolation phenomenon.

Increasing the inclusion length reduces the critical concentration for percolation.

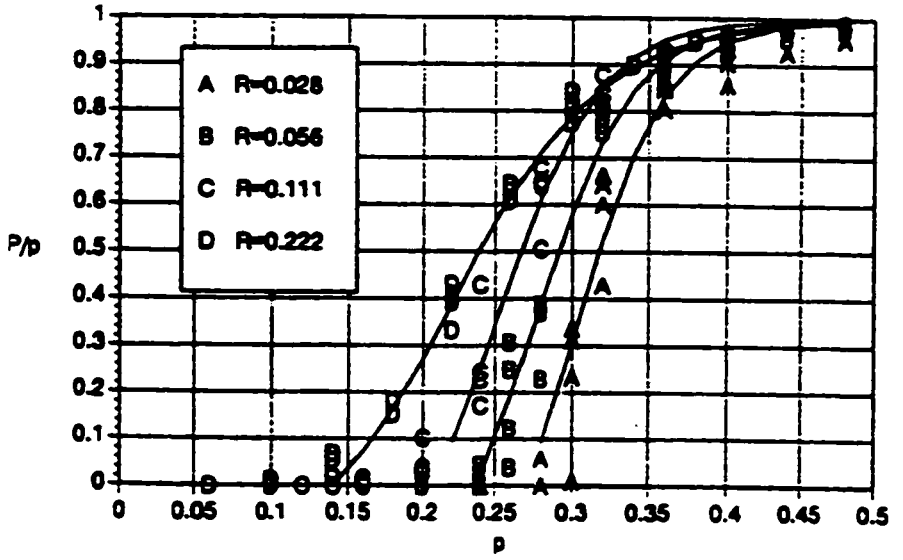

Figure 2.8 Effect of finite size on percolation : R is the ratio of inclusion to domain size in the percolation direction (Arends, 1992)

2.2.1.5 Factors influencing co-continuity

It has been well documented that several basic parameters are very important in controlling the morphology of polymer blends during processing. These include composition, viscosity ratio of the molten components, melt elasticity ratio, interfacial tension and processing history (Allen, 1985, David, 1993, Jorgensen and Utracki, 1991, Favis, 1992).

2.2.1.5.1 Viscosity Ratio and Composition

In 1975, Avgeropoulos et al. studied the influence of torque ratio and composition on the phase continuity of EPDM/polybutadiene blends. They found that there is a competition between the effects of the compositional and the rheological parameters. It appears that as the torque ratio approaches unity, the "conversion" region

is characterized by samples with co-continuous phases.

Paul and Barlow (1980) formulated a model based on observations made by Avgeropoulos indicating that the condition for phase inversion can be expressed as

$$\frac{\eta_1}{\eta_2} = \frac{\phi_1}{\phi_2} \tag{2.13}$$

where, ϕ_i is the composition at phase inversion and η_i is the viscosity of phase i.

Metelkin and Blekht (1984) proposed another expression for the prediction of dual phase continuity, which is based on Tomokita's theory of capillary instabilities. The phase inversion concentration for component 1 can be calculated from:

$$\phi_1 = \left[1 + \frac{\eta_1}{\eta_2} F\left(\frac{\eta_1}{\eta_2}\right)\right]^{-1} \tag{2.14}$$

$$\text{where } F\left(\frac{\eta_1}{\eta_2}\right) = \left[1 + 2.25\log\left(\frac{\eta_1}{\eta_2}\right) + 1.81\left(\log\left(\frac{\eta_1}{\eta_2}\right)\right)^2\right]$$

Utracki (1989) found good consistency between equation (2.13) and (2.14). In further work, he proposed an equation based on an emulsion model (1991)

$$\frac{\eta_1}{\eta_2} = \left[\frac{\phi_m - \phi_2}{\phi_m - \phi_1}\right]^{[\eta]\phi_m} \tag{2.15}$$

where, ϕ_m refers to the volume fraction of the matrix at the percolation point, and $[\eta]$ refers to intrinsic viscosity. A correction was applied to avoid prediction of co-continuity below its percolation threshold. It is important to mention that equations (2.13), (2.14) and (2.15) predict that the less viscous component tends to encapsulate the more viscous phase.

Jordhamo et al (1986) reported that the region of dual phase continuity of polybutadiene/polystyrene (PB/PS) obeyed the rheological viscosity/volume fraction equation

$$\frac{\eta_1}{\eta_2}\frac{\phi_2}{\phi_1}\begin{cases} > 1 \ phase\ 2\ continuous \\ = 1 \ dual\ phase continuity \\ < 1 \ phase\ 1\ continuous \end{cases} \tag{2.16}$$

Miles and Zurek (1988) examined the co-continuity of three thermoplastic blend systems (PS/PB, PS/PMMA and PMMA/EPR) with the above equation and found good consistency with their experimental results. Recently, Willemse et al. (1999) developed a semi-empirical relation based on geometrical requirements for the formation of co-continuous structures:

$$\frac{1}{\phi_d} = 1.38 + 0.0213\left(\frac{\eta_m \dot{\gamma} R_0}{\sigma}\right)^{4.2} \tag{2.17}$$

where ϕ_d is the volume fraction of the dispersed phase, η_m is the viscosity of the matrix, $\dot{\gamma}$ is the shear rate, σ is the interfacial tension and R_o is the radius of the thread. This relation gives the lower and upper limit, respectively, of the range of volume fractions within which a co-continuous structure can exist. A disadvantage of this model is that it cannot be used in a predictive manner because the thread radius has to be determined experimentally first.

Fortelny et al (1992) studied the composition dependence of phase structure of PP/EPR blends with various rheological properties of the components. They discovered that neither the empirical rule regarding the effect of the ratio of viscosities of the components on the ratio of their volume fractions at which the inversion of phases takes place, nor Van Oene's theory regarding the effect of elastic properties of the components on phase structure of the blend, is generally valid. Although a number of hypotheses

have been discussed and successfully applied to experimental results, discrepancies often arise.

2.2.1.5.2 Elasticity ratio

The influence of the elasticity on the morphology of polymer blend remains poorly understood. In his classical studies, Van Oene (1972) formulated an expression to describe the elastic contribution to the interfacial tension under dynamic conditions.

$$\sigma_{eff} = \sigma + \frac{d}{12}\left[(N_1)_d - (N_1)_m\right] \tag{2.18}$$

where, σ and σ_{eff} are the interfacial tension and effective interfacial tension, respectively. D is the droplet diameter. $(N_1)_d$ and $(N_1)_m$ are the first normal stress difference of dispersed phase and matrix, respectively. Van Oene's theory predicts the equilibrium between normal forces of the droplet phase and those of the matrix. He suggested that the interfacial tension term should be replaced by an effective interfacial tension which involves first normal stress differences. Under such considerations, the more elastic phase will tend to encapsulate the less elastic one to lower the overall surface energy. This was experimentally proven by Favis et al. (1988), who found that the more elastic polycarbonate encapsulates the less elastic polypropylene.

Levitt et al. (1996) studied the influence of elasticity ratio on the evolution of dispersed phase in immiscible polymer blends at low shear rate. At low shear rate and low frequency, the primary stress difference is approximately twice the storage modulus (G'). They observed that the minor phase changes from droplets to sheets, and then the sheets contract to fibers under the effect of interfacial tension. They proposed that the width of the flattened drops can be related to the difference in elasticity between matrix and drop, and is proportional to the first normal stress difference of the two phases. They proposed an analytical relationship between the first normal stress difference of the phases and the degree of widening. The degree of widening calculated in such a way

results in an area larger than the value calculated for a similar deformation.

Ghodgaonkar et al. (1996) proposed a quantitative model for the calculation of the dispersed phase size which was based on proportionality between viscoelastic and thermodynamic forces. The force balance best predicts the behaviour at low concentration of PP in PS blend since the force balance is for a single polymer drop in a polymer matrix, and thus matches the results for the very dilute blend system. The minima are independent of the weight fraction of the dispersed phase in this region. However, no minimum was observed for 20% PP in PS blend, and they suggested that this may be due to greater coalesence at this high concentration. Droplets and fibers coexist, causing the morphology to be more complex.

Bourry et al. (1997) studied the effect of the elasticity ratio on the level of co-continuity for PS/HDPE blends prepared in a twin-screw extruder. They proposed a equation for the prediction of phase inversion:

$$\frac{\phi_1}{\phi_2} = \frac{G_2'(\omega)}{G_1'(\omega)} \tag{2.19}$$

where, ϕ_i is the composition of phase inversion, G_i' is the elasticity of phase i (storage modulus) at a given frequency (ω). Observing the phase inversion in the PS/HDPE blend system, they found the predicted value from their equation ($\phi_{PS(th)}$=0.67) is in accordance with the observed composition ($\phi_{PS(ex)}$=0.7) at high shear rate, while the viscosity ratio models failed. It is indicated that the viscosity ratio models can only predict accurately the observed phase inversion region at very low shear rates, and fail to do so under the vigorous mixing conditions of a typical twin-screw extruder.

2.2.1.5 Granular starch-filled composites.

Native starch has been used as filler of polymer composites. In pioneering work, Griffith (1977) reported the preparation of starch-filled polyethylene (PE) composites. Ductile

films could be prepared at low starch loading, but films became paperlike when starch content exceeded 15%. As with mineral fillers, the addition of granular starch to PE results in a reduction of the tensile strength (σ_{max}) and elongation at break (ε_b) while the elastic modulus (E) increases (Willett, 1994, Kim et al, 1995, Chandra and Rustgi, 1997). Increment of σ_{max} and E can be achieved by the improvement of the interface between the non-polar polyolefin and the polar granular starch.

2.2.1.6 Gelatinized Starch/Polyethylene Blends.

Extensive work has been devoted to the development of materials containing gelatinized starch (GS). Otey et al. (1980, 1982) developed GS/EAA cast films that presented good transparency, flexibility and good mechanical properties. Starch and EAA were mixed with the other additives in a long initial process. The resultant dough was then extruded several times to improve the homogeneity and the moisture content reduced to the desired value. Blown films of GS/EAA blends, optionally compounded with low-density polyethylene (LDPE) and/or polyvinyl alcohol (PVA), were extruded in a further step. The addition of LDPE led to the reduction of both σ_{max} and ε_b, but, surprisingly, improved biodegradability. The incorporation of PVA increased the ε_b of starch-based films. Otey's process was improved (Otey et al., 1987) and modified by other authors (Wool et al., 1990, Shi and Seib, 1995). The use of the original formulation or a slight modification was a characteristic of such works. Subsequent work on this polymeric system was devoted to the fundamental understanding of the interactions between starch components and EAA. Several techniques have been used to study the complexation reaction of amylose and amylopectin with EAA. Such techniques were solvent extraction (Fanta et al., 1990), X-ray diffraction (Shogren et al., 1991a), CP/MAS solid state NMR (Shogren et al., 1991a), FTIR (Shogren, et al., 1991a), optical rotation (Shogren et al., 1991b), bacterial degradation (Shogren et al, 1992), fluorescence microscopy (Shogren et al, 1992), DSC (Shogren et al, 1992). These works demonstrated that amylose and amylopectin form V-type inclusion complexes with EAA. The hydrophobic segment of EAA molecules is trapped into the hydrophobic core

of starch helix. Amylose/EAA complexes are highly crystalline and, consequently, resistant to enzymatic attack. Conversely, amylopectin/EAA complexes are poorly crystalline and are susceptible to amylolytic attack. The morphological evaluation of those blends showed the continuous nature of the GS phase. That can be advantageous for the bacterial attack, but it can also lead to the embrittlement of films due to the stiff nature of GS. They finally propose the utilization of other compatibilizers, different than EAA, to improve the interfacial adhesion with PE and to reduce the GS particle size without promoting the formation of starch complexes.

2.2.1.7 Thermoplastic Starch Blends.

Blending TPS with synthetic polymers have shown the typical characteristics of immiscible polymer blends (St-Pierre et al, 1997). The melt blending of TPS with synthetic polymers has given place to a series of scientific and technologic developments. Such works differed in the mixing protocol and the type of additives used. Some authors proposed the use of two steps for the preparation of TPS-based blends (Aburto et al., 1997, Bikiaris et al., 1997a, 1997b, 1998, Prinos et al., 1998, Fritz et al, 1995, Ruch and Fritz, 1999, Averous et al., 2000a, 2000b, 2001b, 2001c, Martin and Averous, 2001) while other preferred just one-step processes (Dehennau and Depireux, 1993, St-Pierre et al., 1997). Starch-based blends prepared in two steps are generally characterized for the preparation of TPS in a separated extrusion step. St-Pierre and coworkers presented a blending process, in only one step, for TPS-based polymer blends (St-Pierre et al., 1997). They developed an extrusion system combining a TSE with a single-screw extruder (SSE). TPS was prepared in the SSE, and then it was blended with LDPE in the last sections of the TSE. Using such an extrusion system, they demonstrated experimentally that a certain morphological control of PE/TPS blends could be achieved by varying the TPS concentration from 0 to 22 wt%. Those blends showed an unusual high level of ductility.

2.3 Tensile properties of Thermoplastic Starch-based blends

Mechanical properties of starch-based materials are highly dependent of the nature of the starch dispersed phase. For instance, granular starch behaves as typical rigid filler increasing the elastic modulus but decreasing the stress and elongation at break of starch-filled polymeric composites (Willett, 1994, Ratto et al., 1999). Willett (1994) studied the influence of starch volume fraction, granule size and the presence of compatibilizer on the mechanical properties of LDPE/granular starch composites. He found that his experimental results fit quite well with theoretical predictions. Humidity and interfacial modifier did not affect the stress and elongation at break, while the improvement of interfacial adhesion increased the elastic modulus. Conversely, tensile properties of blends of synthetic polymer with TPS were highly sensitive to moisture, (water is a good plasticizer for starch) and other plasticizer content (Psomiadou et al., 1997, Martin et Averous, 2001). Final properties of TPS-based blends were also affected by the type and concentration of compatibilizers (Dehennau et Dipereux, 1993, Prinos et al., 1998).

Fracture mechanisms involved in failure during tensile testing are the key to prediction of the mechanical performance of multiphase systems. Bazhenov et al. (1994) and Li et al. (1994a) presented a series of papers devoted to the study of tensile properties of PETG filled with organic and inorganic fillers. They proposed five fracture modes based on the macroscopic stress-strain behavior and the surface fracture characteristics of specimens cryogenically fractured in the longitudinal direction (Li et al., 1994a). Only spherical particles of regular size were considered for the development of the fracture mode schemes. Particle coalescence (or agglomeration) was not considered. It is known that cohesive dispersed particles, such as thermoplastic polymers (Kunori et Geil, 1980a, 1980b, Favis et Chalifoux, 1988) and uncoated mineral fillers (Maiti et Mahapatro, 1991), tend to coalesce as the dispersed phase volume fraction (ϕ_d) increases. For that reason, these fracture modes should be considered for composite materials filled with

non-cohesive particles, but care must be taken when applying these fracture modes to immiscible polymer blends.

Fracture mechanism of multiphase polymeric systems has been related to macroscopic changes in the material structure, such as stress whitening. Stress whitening of immiscible polymer blends (Kunori et Geil, 1980b, , Liu et Truss, 1995) and composites (Bazhenov et al., 1994, Li et al., 1994b) has been related to cavitation and debonding of dispersed phase particle. Liu and Truss (1995) studied the tensile yielding and microstructure of isotactic PP/LLDPE blends. Tensile yielding of those blends was evaluated at different strain rates and different testing temperatures and compared to the Eyring's viscosity theory. The yielding mechanism was found to be related to both strain rate and temperature by means of Eyring's process I and II. When process I was dominating (low strain rate and high temperature) no stress whitening has been observed, whereas stress whitening was present when process II (high strain rate and low temperature) was dominating. SEM observations revealed that the surface of cryo-fractured unwhitened samples was smoother than that of whitened samples. It was also found that in both cases the originally spherical LLDPE particles became elongated under the action of shear stress transferred from the isotactic PP matrix. However, in the case of whitened samples an extensive debonding of LLDPE particles from isotactic PP matrix was observed. LLDPE debonding was accompanied by craze-like microstructures. They finally related the stress whitening to the presence of those micro-voids.

2.4 Biodegradability of Starch-Based Materials

Several authors have studied the biodegradability of granular starch-based composites (Tanna et al., 1992, Ramsay, et al., 1993, Chandra and Rustgi, 1997, Ratto et al., 1999) and polymeric blends (Shogren et al., 1991a, 1992, Psomiadou et al., 1997, Bikiaris et al., 1997b, 1998, Prinos et al., 1998). When starch is mixed with biodegradable polymers, a significant improvement in the biodegradation rate can be observed (Tanna

et al., 1992, Ramsay et al., 1993, Ratto et al., 1999). This has been attributed to the faster biodegradation rate/solubility of starch compared to other biodegradable polymers. The case of a starch/non-biodegradable polymer system is completely different because only the starch fraction is biodegradable. In such a system, the extent of starch biodegradation is dependent on the nature of the starch and its concentration, and on the presence of compatibilizer. Prinos et al. (1998) reported that LDPE blends prepared with TPS showed a higher biodegradation extent than those prepared with granular starch. This difference was explained on the basis of a more homogeneous distribution of TPS, which allowed a larger amount of starch to be available to microorganisms. It has been observed that below 30 wt% starch, only a limited amount can be degraded. That is in good agreement with the percolation threshold for the starch dispersed particles (volume fraction ≈ 0.31 calculated by Peanasky et al. (1991)). The addition of a compatibilizer has been reported to produce an adverse effect on the biodegradation extent (Chandra and Rustgi, 1997, Bikiaris et al., 1998, Prinos et al., 1998). It was stated that starch has strong interactions with polar compatibilizers, such as ethylene-acrylic acid copolymers (Otey et al., 1980). However, Bikiaris et al. (1988) proposed that it could be just due to the lower concentration of starch at the blend surface as a consequence of the better dispersion promoted by the compatibilizer. From these reasons, it can be concluded that starch biodegradation in partially degradable systems is dependent of the accessibility of starch domains and its continuity in the bulk. Arends (1992) stated that the presence of fiber-like structures can results in a higher continuity than its spherical counterpart at the same composition in immiscible polymeric systems. That suggests a good alternative to increase the biodegradation extent of starch-based materials.

2.7 Conclusion of Literature Review

Melt blending of starch with synthetic polymers is an excellent alternative to get less expensive materials which may also be environmentally benign. Mechanical properties and biodegradation of starch-based materials depends enormously on the blend morphology. However, for good control of the morphology of such immiscible blends,

an in-depth knowledge of the rheological properties of all blend components and other processing parameters that influence the breakup-coalescence equilibrium and the stability of elongated particles is required.

Among several processing techniques reported in the literature, the one-step process developed in this laboratory seems to be the most convenient for the preparation of highly ductile TPS-based blends. However, some modifications are required to improve the control of TPS properties, and consequently those of the final product.

Tensile properties of starch multiphase systems depends of several factors such as the nature of the starch (i.e. granular or thermoplastic, and the plasticizer content of the latter), starch concentration, the type and concentration of the compatibilizer and, of course, the properties of the pure synthetic polymer matrix. In the case of ductile synthetic polymers, elongation at break has been reported as the most critically affected property. The addition of concentrations higher than 30 wt% enormously reduces the ductility of starch multiphase systems, which in several cases has rendered impossible the extrusion of blown films. However, it has been reported that blends of LDPE with TPS prepared in a one-step process presented an unusually high ductility at low TPS concentrations.

The biodegradation extent of starch multiphase systems, especially when the synthetic polymer is non-biodegradable, depends on the concentration of starch. At concentrations up to 30 wt%, starch domains are mainly encapsulated in a non biodegradable matrix resulting in low biodegradation extents.

The above literature review suggests that a number of issue related to the formulation of starch-based materials and the characterization of its properties should be studied.

1. The development of an extrusion system that allows the preparation of highly ductile, highly continuous LDPE/TPS blends, preferentially in one step. This extrusion system must be flexible enough to allow the complete control of the

different stages of compounding process (starch gelatinization and plasticization and melt blending with LDPE). It should permit the full control of the plasticizer content in TPS, especially water.

2. The study of the physical properties of TPS, which would permit a deeper understanding of this system. TPS is a complex system of starch and plasticizers (generally water and glycerol). The study of the influence of plasticizer content on thermal and rheological properties can be useful for the understanding of the complex structure of TPS. It could be also useful for the comprehension of the effect of plasticizer content and mixing conditions (shear rate) on the morphology of LDPE/TPS blends.
3. The control of morphology to allow the evaluation of the effect of particle size and shape on the tensile properties and biodegradability of LDPE/TPS blends
4. Finally, the exhaustive analysis of the influence of several parameters such as the effect of glycerol content on TPS properties, and of blend morphology and ambient humidity on the tensile properties of LDPE/TPS blends. Special emphasis will be made on the study of the properties of such blends at high strain and the fracture mechanisms that allow high ductility.

CHAPTER 3. ORGANIZATION OF THE ARTICLES

The first paper, "High Performance LDPE/Thermoplastic Starch Blends: A Sustainable Alternative to Pure Polyethylene", presents an approach to preparing polyethylene/thermoplastic starch blends with exceptional properties. In this study a one-step combined twin-screw/single screw extrusion setup is used to carry out the melt-melt mixing of the components. Glycerol was used as the starch plasticizer and its content in the TPS is varied from 29 to 40%. Composition of TPS was varied in a range near the dual-phase continuous region. Blend morphology, tensile properties and percent continuity were directly related to the glycerol content in TPS and the polymer-polymer composition. Effective control of the glycerol content, TPS concentration and processing conditions can result in a wide variety of morphological structures including spherical, fiber-like, highly continuous and co-continuous morphologies. These various blend morphologies are shown to be the determining parameters with respect to the observed mechanical properties.

The thermal and rheological properties are important parameters in the control of final morphology. Since LDPE rheological behavior is already well known and since much effort is currently being devoted to melt blending of glycerol-plasticized TPS the purpose of "Study of the Rheological and Thermal Properties of Thermoplastic Starch" was to evaluate the thermal and rheological properties of TPS produced under typical melt blending conditions. TPS structure was evaluated by DSC and X-ray diffraction. Rheological properties in the shear and oscillation mode were determined on-line from the TSE and by using two oscillatory rheometers, respectively. TPS has excellent thermal stability at 150°C, but becomes unstable at temperatures above 180°C. The studies indicates that TPS stability was maintained for short time periods at temperatures up to 200°C. Both the shear and dynamic viscosities are dependent of glycerol content. Rheological studies in oscillation mode revealed the presence of a percolation threshold

of the well-plasticized glycerol-rich soft regions at concentration around 30%glycerol. The shear viscosity of this TPS was lower than that of LDPE while the opposite trend was observed in the oscillation mode probably due to the fact that the shear measurements were done out of the linear viscoelastic domain of TPS.

Tensile properties and biodegradation of partially biodegradable starch-based blends are dependant of the size, shape and distribution of starch dispersed domains. In "The Influence of Melt Drawing on the Morphology of One and Two-Step Processed LDPE/Thermoplastic Starch Blends", the morphology of LDPE/TPS blends prepared by a one-step extrusion/shaping process is compared to that obtained by reprocessing of the original blends. The influence of composition and melt drawing is examined. The evaluation of the morphology of immiscible polymer blends at high dispersed phase concentrations is often made difficult by the presence of elongated shapes. A novel methodology based on the form factor of the dispersed particle is used to estimate the equivalent spherical particle size of dispersed TPS. This approach allows for the quantitative comparison of average dispersed phase particles regardless of their shape. Blends prepared in the one-step extrusion process show increased levels of anisotropy as a consequence of a combination of coalescence and particle deformation during melt drawing. Re-processed materials demonstrate morphologies that are highly stable to a wide range of hot stretch ratio conditions. The TPS particles of re-processed blends show no-coalescence and a low degree of deformation. This phenomenon is explained by plasticizer evaporation resulting from the second processing step.

One of the most interesting characteristics of PE/TPS blends prepared in the one-step process is the unusually high ductility presented by these blends. Annex I, "Ductility of LDPE/Thermoplastic Starch Blends", presents a study devoted to the analysis of the mechanisms that allow such amazing feature of this polar-no polar immiscible system. The relationship between the morphology and fracture mechanisms of PE/TPS blends was evaluated by observation of the evolution of the microstructure of tensile tested samples. Those observations reveal not just the influence of particle size

and particle size distribution on the fracture mechanism but also the effect of humidity on the energy dissipation mechanism. Fracture mechanisms composed of three stages (debonding, void growth and failure) are proposed. The completion and extent of those stages are dependent on the morphology.

Annex II presents a study of the biodegradability of PE/TPS blends in an activated sludge reactor. Biodegradability of starch domains is evaluated as a function of starch content and blend morphology.

Annex III explains more in detail the methodology developed for the evaluation of elongated morphologies.

In short, this work shows a novel technology for the development of well characterized PE/TPS blends in only one extrusion step. It also provides a very complete study that allows a better understanding of this complex system. The control of the morphology of PE/TPS blends offers an excellent alternative for the development of low-cost tailored partially biodegradable materials. PE/TPS immiscible system can be a powerful model system for the study of the energy dissipation mechanisms via the control of plasticizer (water and/or glycerol) content.

CHAPTER 4

HIGH PERFORMANCE LDPE/THERMOPLASTIC STARCH BLENDS: A SUSTAINABLE ALTERNATIVE TO PURE POLYETHYLENE.

4.1 Abstract

This paper presents an approach to preparing polyethylene/thermoplastic starch blends with exceptional properties. Thermoplastic starch (TPS), as opposed to dry starch, is capable of flow and hence when mixed with other synthetic polymers can behave in a manner similar to conventional polymer-polymer blends. In this study, a one-step combined twin-screw/single screw extrusion setup is used to carry out the melt-melt mixing of the components. Glycerol was used as the starch plasticizer and its content in the TPS is varied from 29 to 40%.

Under the particular one-step processing conditions used it is possible to develop continuous TPS (highly interconnected) and co-continuous polymer/TPS blend extruded sheet which possess a high elongation at break, modulus and strength in the machine direction. The PE/TPS (55:45) blend prepared with 36% glycerol content maintains 94% of the elongation at break and 76% of the modulus of polyethylene. At a composition level of 71:29 PE/TPS for the same glycerol content, the blend retains 96% of the elongation at break and 100% of the modulus of polyethylene. These exceptional results are achieved in the absence of any interfacial modifier and despite the high levels of immiscibility in the polar-nonpolar TPS-PE system. The 55:45 blend possesses a 100% continuous or fully interconnected TPS morphology, as measured by hydrolytic extraction. This TPS configuration within the blend enhances its potential for environmental biodegradation which is an additional potential feature of the system. The elongation at break in the cross direction of these materials, although lower than the machine direction properties, also demonstrate ductility at high TPS concentrations. At

a glycerol content of 36% in the TPS, the blends demonstrate only very low levels of sensitivity to moisture. A high degree of transparency is maintained over the entire concentration range due to the similar refractive indices of PE and TPS and the virtual absence of interfacial microvoiding.

Effective control of the glycerol content, TPS concentration and processing conditions can result in a wide variety of morphological structures including spherical, fiber-like, highly continuous and co-continuous morphologies. These various blend morphologies are shown to be the determining parameters with respect to the observed mechanical properties.

Considering the significantly lower cost of starch as compared to polyethylene, this material represents a serious potential route towards polyethylene replacement. Furthermore the material has the added benefit of containing large quantities of a renewable resource and hence represents a more sustainable alternative to pure synthetic polymers. Since the starch can be fully interconnected through morphology control, it is also completely accessible for biodegradation.

4.2 Introduction.

Starch is a natural carbohydrate storage material accumulated by green plants in the form of granules. It is composed of linear polysaccharide molecules (amylose) and branched molecules (amylopectin) and is an inexpensive, renewable and natural polymer. It can be added to synthetic polymers to lower the cost of the final product. Numerous studies have shown that the addition of dry starch granules to low density polyethylene (LDPE) follows the general trend for filler effects on polymer properties (Evangelista, 1991, Willett, 1994). The modulus increases due to the stiffening effect of the starch granules and the elongation decreases as the starch content is increased. In pioneering work, Griffith (1977) reported on the preparation of starch-filled polyethylene (PE) composites. Ductile films could be prepared at low starch loading, but the films became paper-like when starch content exceeded 15% (Griffith, 1977). In a

fashion typical of that observed for mineral fillers, the addition of granular starch to PE results in a severe reduction of tensile strength (σ_{max}) and elongation at break (ε_b), while the elastic modulus (E) increases (Willett, 1994, Kim et al., 1995, Chandra and Rustgi, 1997). Some improvement of σ_{max} and E can be achieved through modification of the non-polar polyolefin and the polar granular starch interface (Willett, 1994, Chandra and Rustgi, 1997).

Native starch granules swell when they absorb water through hydrogen bonding with their free hydroxyl groups, but they still retain their order and crystallinity. However, when these swollen starch granules are heated, hydrogen bonding between adjacent glucose units is disrupted and the crystallinity is progressively destroyed. This process is called gelatinization (French, 1984). The processing of starch and water in a heated extruder is an efficient way to obtain gelatinized starch (GS) since the high shear that can be generated in the extruder disrupts the starch granules.

Extensive work has been devoted to the development of materials containing gelatinized starch (GS). Otey et al. (1980, 1982) developed GS/EAA cast films that demonstrated good transparency, flexibility and mechanical properties. Blends of GS with other polymers were prepared by first mixing starch, ethylene-acrylic acid copolymer (EAA) and other additives in a long initial process. The resultant dough was then extruded several times to improve the homogeneity and to reduce the moisture content to the desired value. Blown films of these GS/EAA blends, compounded with LDPE and polyvinyl alcohol (PVA), were extruded in a further step. The addition of LDPE led to the reduction of both σ_{max} and ε_b. The incorporation of PVA increased the ε_b of starch-based films. Otey's process was improved (Otey et al., 1987) and modified by other authors (Wool et al., 1990, Shi and Seib, 1995). The use of the original formulation or a slight modification thereof was a characteristic of the subsequent works. Detailed studies on this polymeric system were devoted to the fundamental understanding of the interactions between starch components and EAA. Solvent extraction (Fanta et al.,

1992), X-ray diffraction (Fanta et al., 1992, Shogren et al., 1991a), CP/MAS, solid state NMR (Shogren et al., 1991a), FTIR (Shogren et al., 1991a), optical rotation (Shogren et al., 1991b), bacterial degradation (Shogren et al., 1992), fluorescence microscopy (Shogren et al., 1992) and DSC (Shogren et al., 1992) were used to study the complexation reaction of amylose and amylopectin with EAA. Those works demonstrated that amylose and amylopectin form V-type inclusion complexes with EAA. The hydrophobic segment of EAA molecules is trapped into the hydrophobic core of the starch helix. Amylose/EAA complexes are highly crystalline and resistant to enzymatic attack. Conversely, amylopectin/EAA complexes are poorly crystalline and are susceptible to amylolytic attack. These findings led to the proposal that compatibilizers other than EAA should be employed to improve interfacial adhesion with PE and reduce the GS particle size, without promoting the formation of starch complexes (Shogren et al., 1992).

Addition of a plasticizer such as glycerol can further improve the ductility of GS. Plasticized GS is known as thermoplastic starch (TPS) and is capable of flow. Thus, mixtures of TPS with other polymers have the potential to behave in a manner similar to conventional polymer-polymer blends. The melt blending of TPS has been studied with polyethylene (Dehennau and Depireux, 1993, Aburto et al., 1997, St-Pierre et al., 1997, Bikiaris, 1997a, 1997b, 1998, Prinos, 1998 and biodegradable polyesters such as polycaprolactone (Averous et al., 2000a, 2001b, 2001c), polyesteramide (Averous et al., 2000b, 2001b, 2001c), polylactic acid (Averous et al., 2001c, Martin and Averous, 2001), poly(butylene adipate-co-terephtalate) (Averous et al., 2001c, Martin and Averous, 2001) , and poly(butylene succinate adipate (Averous et al., 2001c, Martin and Averous, 2001). The tensile properties of these blends decreased significantly as TPS content increased. The elongation at break is the most adversely property affected by the presence of TPS particles and typically ductile polymers, such as polyethylene and polycaprolactone, became fragile with the addition of 20-30 wt% TPS.

TPS/polyolefin blends have not been frequently studied since the general bias in the literature is that the two materials are too dissimilar and none of the above papers have attempted to systematically control the TPS morphology. St-Pierre and coworkers (St-Pierre et al., 1997) reported on a one-step blending process for TPS/polyethylene blends. They developed an extrusion system combining a twin-screw extruder (TSE) with a single-screw extruder (SSE). TPS was prepared in the SSE, and then it was blended with LDPE in the final sections of the TSE. The LDPE/TPS morphology displayed the typical characteristics of immiscible polymer blends where the particle size increased as the TPS content increased. The mechanical properties showed a small reduction in the Young's Modulus and strength at yield with TPS concentration. On the other hand, the elongation at break dropped dramatically at TPS contents greater than 10%. The highest TPS loading used in that work was 22 wt%. They demonstrated that the dispersed phase particle size could be controlled as a function of the TPS concentration.

In this work an improved and much more highly effective one-step process for the preparation of LDPE/TPS blends is presented. The purpose of this study was to analyze the effect of processing conditions, glycerol content and TPS composition on the morphology and properties of LDPE/TPS blends. An emphasis was placed on controlling highly continuous dispersed TPS phase morphologies.

4.3 Experimental.

4.3.1 Materials.

Two commercial LDPE resins, LDPE2040 (MFI = 12g/10min) and LDPE2049 (MFI = 20g/10min), were supplied by Rexene Chemical Co (now Huntsman). They are referred to as PE1 and PE2 respectively. Supergell 1203-C wheat starch obtained from ADM/Ogilvie was composed of 25% amylose and 75% amylopectin. TGA measurements showed that the water content in the starch granules was 7.1%. The water content of glycerol (SIMCO Chemical Products Inc.) was determined by its refractive index to be 5.9%.

4.3.2 Processing.

Starch suspensions were prepared using the ratios of starch, glycerol and water listed in Table 4.1. Starch granules were gelatinized, plasticized and blended with LDPE in a one step process. The extrusion system (Figure 4.1) was composed of a single-screw extruder (SSE) connected to a Leistritz AG 34 mm co-rotating twin-screw extruder (TSE) composed of eight zones. The starch suspension was fed in the 1st zone of the TSE. Three suspension compositions were used and are shown in Table 4.1. Native starch was gelatinized and plasticized in zones 2 to 4 of the TSE. Volatiles were extracted in the 4th zone at a temperature of 110°C by venting under vacuum. Molten LDPE (T=150°C) was fed from the SSE to the 5th zone of the TSE using an adapter designed specially for that purpose. The mixing of TPS with LDPE (T=150°C) started in the same (5th) zone and continued to the 7th zone of the TSE. The last (pumping) zone was used to increase the pressure of the extrudate (T=150°C). The TSE screw speed for all blends was 150 rpm. Blends were extruded through a 2.5 x 32mm rectangular die. The extrudate was quenched in a calendar to form ribbons of about 2mm thickness. A draw ratio (Gonzalez et al., 1996) of approximately 2 was applied to these blends. LDPE/TPS blends were prepared containing 27% to 53% starch by weight. More details concerning the extrusion process are reported elsewhere (Favis et al., 1999).

Table 4.1 Composition of starch suspensions.

Code	Starch (%)	Glycerol (%)	Water (%)
TPS40	48	32	20
TPS36	48.5	27.5	24
TPS29	50	20	30

Vapor extracted during extrusion was mainly composed of water, most of which was removed during the venting process. For that reason, the TPS can be considered as a

binary blend of starch and glycerol. Under such conditions, the glycerol content of the final TPS material can be estimated directly from the glycerol content in the initial suspension. Hence, the final glycerol content of the extruded TPS material prepared from suspensions containing 32%, 27.5 and 20% glycerol was 40%, 36%, and 29%, respectively. Thermoplastic starch materials prepared at these glycerol contents are referred to as TPS 40, TPS36 and TPS 29 in this study.

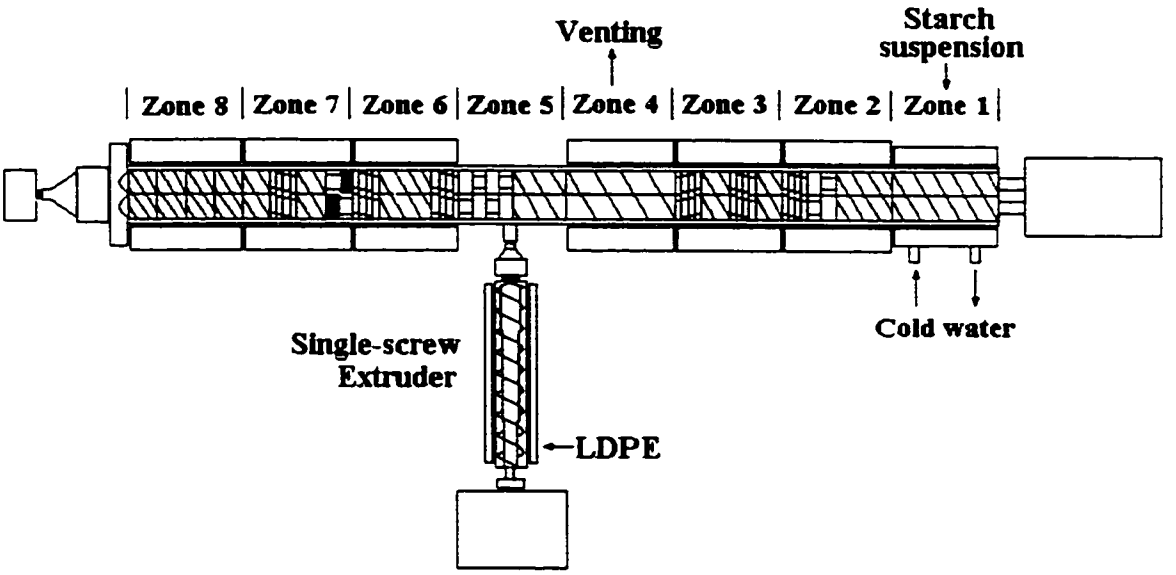

Figure 4.1 Schematic representation of the one-step extrusion system used for the preparation of PE/TPS blends.

4.3.3 On-line viscosity measurements.

The extruder configuration was modified to evaluate the viscosity of pure components under the same conditions used for melt blending. Zones 5 to 7 were not present and the 8^{th} zone was connected to the 4^{th} one. This allowed the estimation of the apparent viscosity of the PE and TPS at the same point at which mixing takes place. The rectangular die replaced by a series of capillary dies (H1, H2, H3) that have an internal diameter of 0.328cm. The L/D ratios of the capillary dies were 9.658, 15.491 and 23.183

for H3, H2, and H1, respectively. The flow rate of the starch suspension was fixed at 40gr-min^{-1}, while the flow rate of TPS extrudate was varied using a valve placed on the extruder head. Pressure and temperature sensors (Dynisco, Franklin, MA) were placed far ahead from this valve to avoid flow disturbances. Pressure values were measured each 5 sec while the TPS mass flow was determined at intervals of 30 sec once the pressure was stable. Figure 4.2 indicates the shear viscosity of PE1, PE2, TPS36 and TPS40.

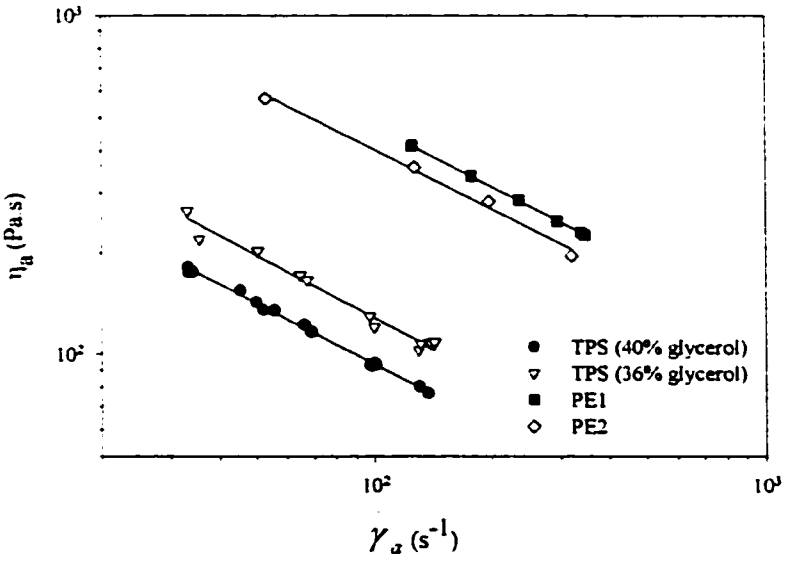

Figure 4.2 Shear viscosity as a function of apparent shear rate for PE1, PE2, TPS36 and TPS40 determined on-line from a five section twin-screw extruder at 150°C.

4.3.4 Scanning Electron Microscope.

PE/TPS blend ribbons were cryogenically microtomed to obtain smooth axial surfaces. Fractured samples were coated with a gold/palladium alloy and further observed in a JSM-820 SEM.

4.3.5 Thermogravimetry.

The LDPE concentration was measured using a TGA 2950 (TA Instruments), equipped with a computer for data acquisition (Thermal Analysis 2000). The temperature was varied from 30 to 600°C at a heating rate of 20°C-min^{-1}. Three well-defined shifts were observed in the TGA curves (Figure 4.3). The first shift, at around 100°C, was produced by water evaporation. The second shift started at *ca.* 180°C and was due to the evaporation of glycerol. This continues gradually up to 300°C where the thermal decomposition of starch occurs. Signal overlap preludes the direct calculation of the glycerol content by this technique. The last shift, at around 400°C, is caused by the thermal decomposition of LDPE. TPS and PE/TPS blends produced a black residue after each measurement, which was related, but not directly proportional, to the thermal decomposition of starch. The LDPE concentration in the blend can be measured from the difference in weight at 400°C and 575°C.

4.3.6 Tensile testing.

PE/TPS blends were tested according to the ASTM D-638 method. Tensile specimens of type IV were cut longitudinally from the recently prepared PE/TPS ribbons. In order to evaluate the effect of minor phase orientation, samples (type V) were cut parallel and perpendicular to the machine direction. Tests performed with those samples will be referred to as microtensile tests. Tensile samples were conditioned at ambient humidity following the ASTM standard. Microtensile samples were conditioned at 0% and 50% relative humidity (RH) during 48 hr. All samples were strained at 10mm-min^{-1} on a M30K machine (JJ Instruments) equipped with a 5kN cell and a data acquisition system. The average values of the Young's modulus and elongation at break were calculated from at least 12 measurements.

4.3.7 Percent continuity.

A sample of 1mm length (machine direction) x 7.5mm width x 2mm thickness was cut from PE/TPS ribbons. Hydrolytic degradation of starch domains in those samples was carried out at 60°C in a solution of HCl 6N for 96 hours. Extracted samples were vigorously washed with distilled water and dried at 60°C in a vacuum oven for 48 hrs. The extraction percentage was determined by the weight loss.

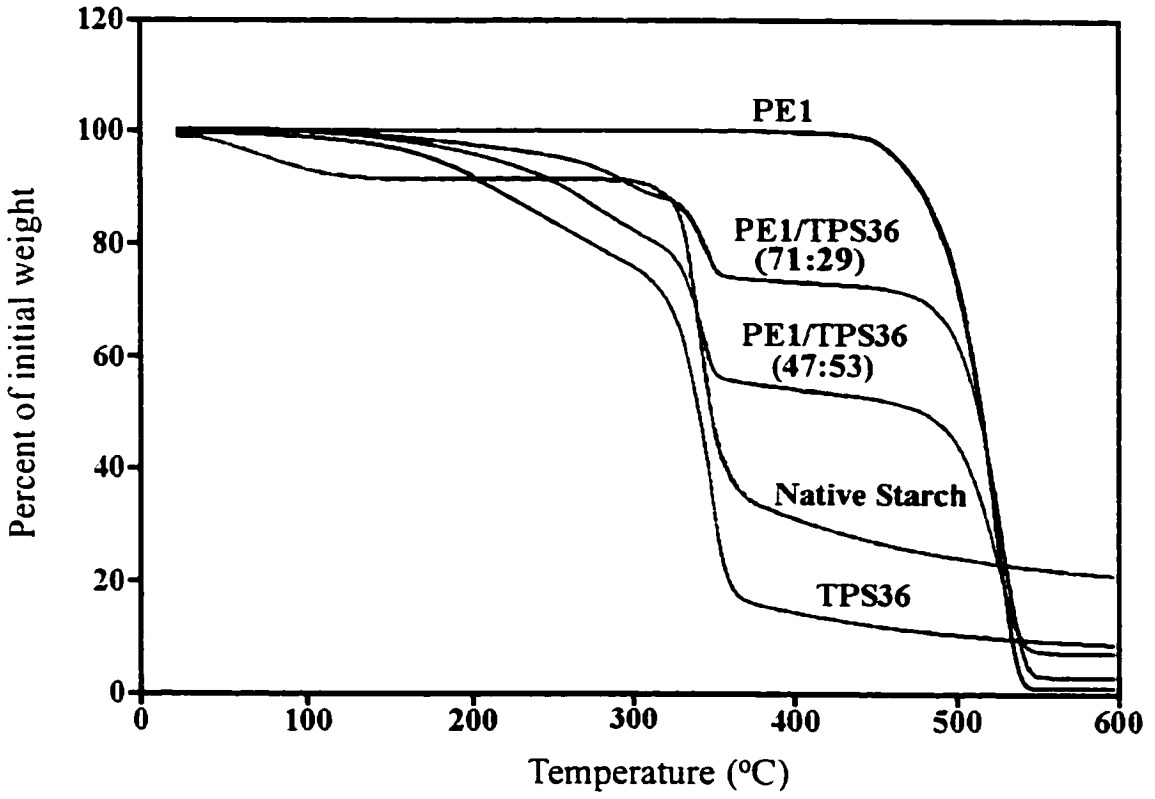

Figure 4.3 Typical TGA curves of native starch, PE1, TPS36 and PE1/TPS36 blends measured from 30° to 600°C at a heating rate of 20°C-min^{-1}.

4.3.8 TPS refractive index.

The average index of refraction (η) of TPS samples was measured at 23°C according to ASTM Standard Test Method D524-90. Thin films of around 100μm were prepared by

compression molding at 70°C using a dried TPS sample. Isopropylaniline (η = 1.53, at 25°C) was used as the contacting liquid.

4.4 Results and discussion.

4.4.1 Effect of glycerol content on morphology.

PE/TPS blends display a discrete morphology where LDPE is the matrix, especially at low TPS content. The combined effect of glycerol content and the elongational flow exerted on PE/TPS blends (TPS concentration ≈ 30 wt%) during quenching can be observed in Figure 4.4. PE1 blends prepared with TPS40 and TPS36 (Figures 4.4a and 4.4b) show a high level of deformation in the machine direction. Conversely, blends compounded with TPS29 show very little deformation (Figure 4.4c) and even less when prepared with PE2 (Figure 4.4d). The singular morphologies displayed by PE/TPS blends are closely related to the differences in viscosity of both TPS and PE. The rheological properties of TPS materials have been studied and it was found that 30% glycerol is required to effectively plasticize starch (Rodriguez et al., 2001a). From Figure 4.4, it can be seen that below that limit, the viscosity and elasticity of TPS are too high to allow the LDPE matrix to greatly deform the TPS dispersed phase. When the lower viscosity PE2 is used it can be seen in Figure 4.4d that the dispersed particles of TPS are of a spherical nature and that the particle size has increased compared to those in Figure 4.4c. These results clearly demonstrate that a high degree of morphological control is possible for this system and that the full range from spherical dispersed phase to that of a highly deformed fibrillar phase can be obtained at a given TPS concentration level. In fact, it is apparent that the control of the glycerol concentration allows one to modify the state of the starch from that of a solid particle to that of a quasi crosslinked dispersed phase to that of a highly deformable material. It will be shown below that these different structures have an important influence on the mechanical properties.

4.4.2 Effect of TPS concentration on morphology.

The axial direction morphology of PE1/TPS36 blends was a combination of large fiber-like structures with small spherical-like particles (Figure 4.5). Increasing the TPS concentration reduces the number of small spherical particles due to particle-particle coalescence. The larger particle size of the TPS domains plus particle coalescence leads to the lengthening of TPS fibers in the machine direction. At high TPS loadings (above 45 wt%), it was difficult to distinguish whether LDPE or TPS constituted the matrix. Both components appear to be fully continuous in the axial draw direction. The orientation imposed by the elongational flow field at the die exit plays an important role in the continuity development of starch in these PE/TPS blends.

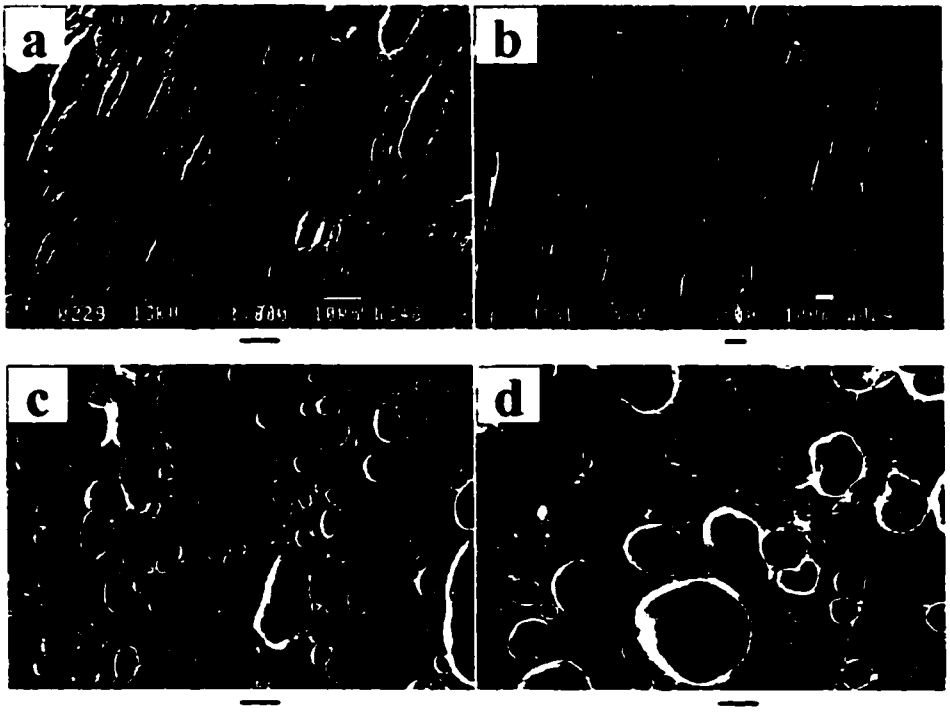

Figure 4.4 Effect of glycerol content and LDPE viscosity on the morphology of microtomed PE/TPS (70/30) blends. PE1/TPS blends: a) 40% glycerol, b) 36% glycerol, and c) 29% glycerol. d) PE2/TPS at 29% glycerol content. The black bar below the micrographs represents 10μm.

The starch domain size increases in PE1/TPS29 as the TPS29 content increases (Figure 4.6). In contrast to the high continuity observed for the low-viscosity low-elasticity TPS36, TPS29 particles remain dispersed in a PE1 matrix, even at high loadings (conc. of TPS ≈ 49 wt%). It can be observed from Figure 4.6 that increasing the concentration of the TPS at low glycerol contents has little effect on the particle shape.

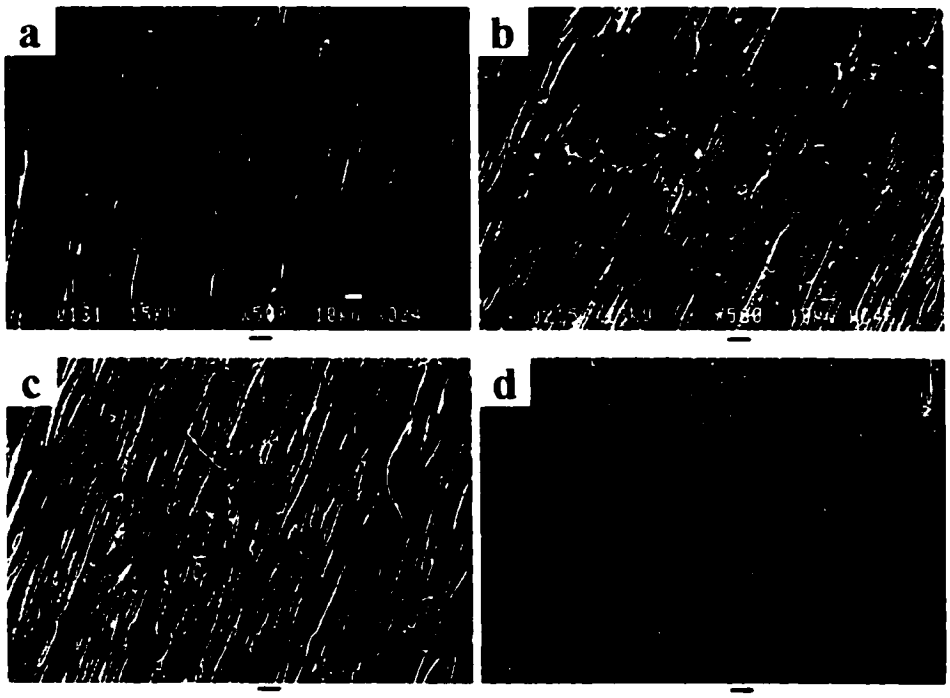

Figure 4.5 Influence of TPS concentration on the morphology of PE1/TPS36 blends. a) 29 wt% TPS, b) 36 wt% TPS, c) 45 wt% TPS, and d) 53 wt% TPS. The black bar below the micrographs represents 10μm.

4.4.3 TPS continuity.

Blends of PE/TPS having higher glycerol contents showed a fiber-like morphology in the machine direction. Consequently, a higher percent of continuity in the axial direction can be expected. In order to quantitatively determine the extent of this continuity,

samples were exposed to hydrolytic extraction and the percent continuity was measured as a function of weight loss. The percent continuity as a function of TPS content for PE1/TPS36 and PE2/TPS29 blends is plotted in Figure 4.7.

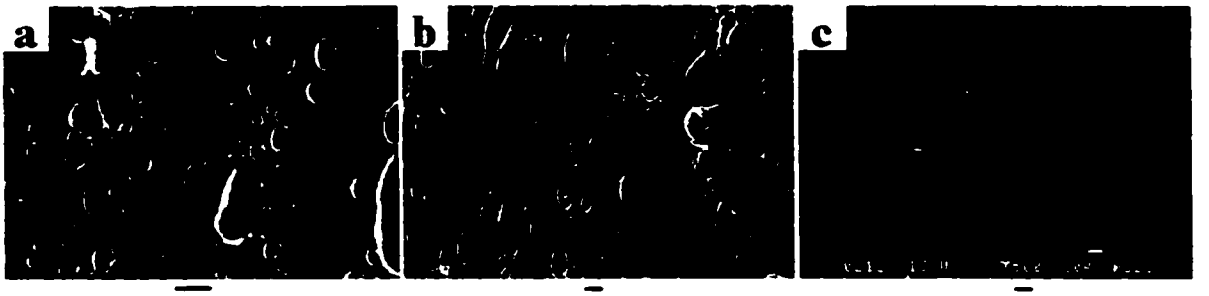

Figure 4.6 Influence of TPS concentration on the morphology of PE1/TPS29 blends. a) 30 wt% TPS, b) 41 wt% TPS, and c) 49 wt% TPS. The black bar below the micrographs represents 10μm.

In all cases, the percent of continuity of starch domains increases as TPS concentration increases and reaches 100% at the phase inversion region. In PE1/TPS36 blends, the starch phase could be completely extracted, an indication of very high continuity in the axial direction. It is interesting to note that the TPS continuity development for the PE2/TPS29 system is shifted to higher TPS concentrations. This is a result of the dominance of droplet morphologies discussed above. The TPS36 is highly elongated and percolates more readily while PE2/TPS29 develops continuity through essentially spherical particle-particle interactions and coalescence (Li et al., 2002).

The high degree of TPS continuity demonstrated in this work indicates that these blend systems have the potential to render all starch domains in the blend accessible for biodegradation. The potential environmental implications are considerable.

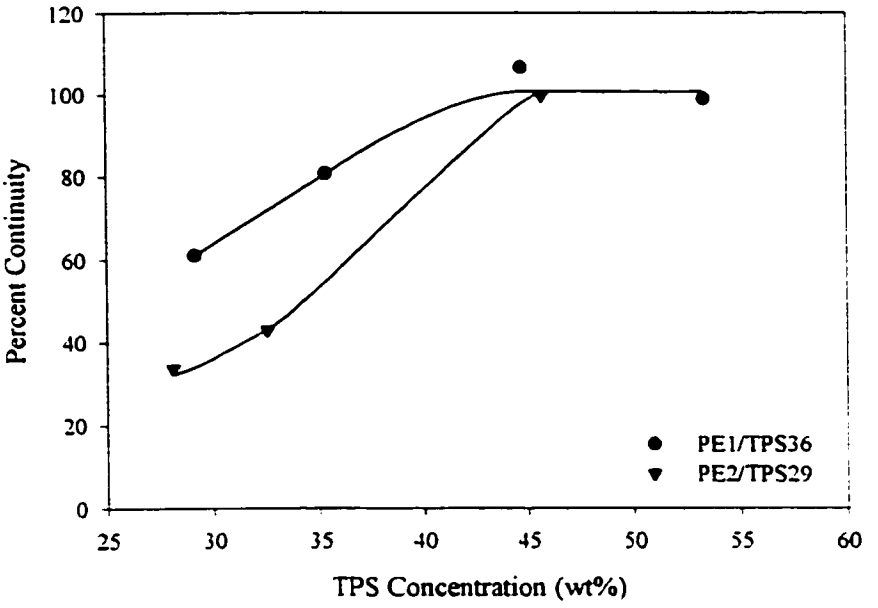

Figure 4.7 Effect of glycerol content, PE type and TPS concentration on the percent continuity of PE1/TPS36 and PE2/TPS29 blends.

4.4.4 Mechanical properties.

4.4.4.1 Elongation at break (ε_b).

The relative elongation at break ($\varepsilon_b/\varepsilon_{b0}$) in the machine direction of PE1/TPS blends is shown in Figure 4.8a and raw data are given in Table 4.2. The results are remarkable and demonstrate that at high glycerol contents (36% and 40%), the blends have an ε_b comparable to the virgin polyethylene (ε_{b0}) even at 53 wt% TPS. The ε_b values of PE1 blends drop with the addition of TPS29. If these data are compared with the morphology results from the previous section, it is clear that the high ε_b for blends with TPS36 and TPS40 is closely related to the ability to deform the TPS phase.

In St-Pierre's work (1997), PE/TPS blends presented a maximum in the ε_b at around 10 wt% TPS followed by a dramatic drop at 22 wt%. In this work, the improved extrusion

process and the controlled deformation of the TPS phase yields an important improvement in the ε_b of PE/TPS blends as a function of composition, as observed in Figure 4.8a. Such an improvement in ε_b is also, in part, due to a highly effective removal of water by venting before blending with polyethylene. In St-Pierre's process, TPS was blended with LDPE and then passed through the venting section. At low concentration, TPS was probably encapsulated into a LDPE matrix, which impeded proper water removal. The presence of water at the blending temperature (150°C) can lead to the formation of bubbles in the extrudate, which weakens the final product (Verhoogt et al., 1995). In the present system, water was almost completely devolatilized from TPS before mixing with polyethylene (Gonzalez et al., 1996). Thermogravimetric analysis indicates the presence of only 1% of water in the final extruded product from the current work.

Table 4.2 Tensile properties of PE1/TPS blends in the machine direction.

Material	TPS (wt%)	ε_b (%)	$\varepsilon_b/\varepsilon_{b0}$[a]	E (MPa)	E/E_0[a]
PE1	0	482	1.00	55.9	1.00
PE1/TPS40	31	465	0.97	44.0	0.79
	46	449	0.93	44.4	0.79
	50	415	0.86	41.2	0.74
PE1/TPS36	29	464	0.96	60.0	1.08
	36	427	0.89	50.1	0.90
	45	453	0.94	42.4	0.76
	53	388	0.80	34.2	0.61
PE1/TPS29	30	400	0.83	60.2	1.08
	41	345	0.72	64.4	1.15
	49	230	0.48	66.2	1.19

[a] Relative values were determined as a function of PE1.

4.4.4.2 Young's Modulus.

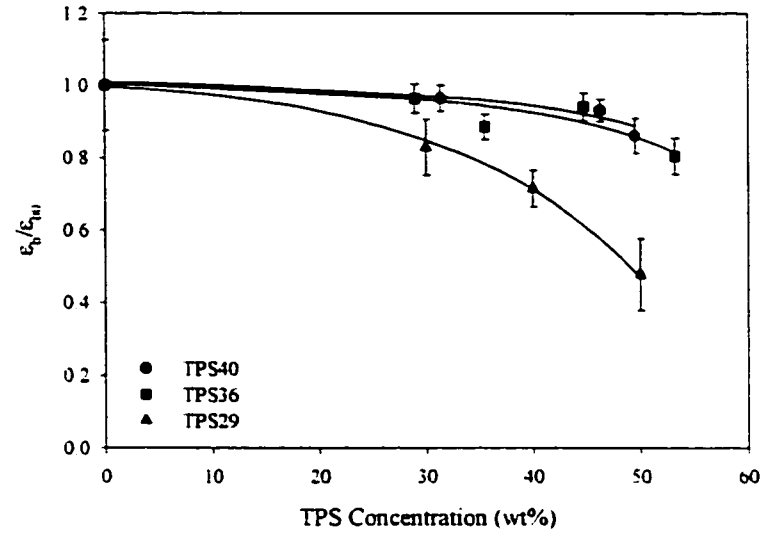

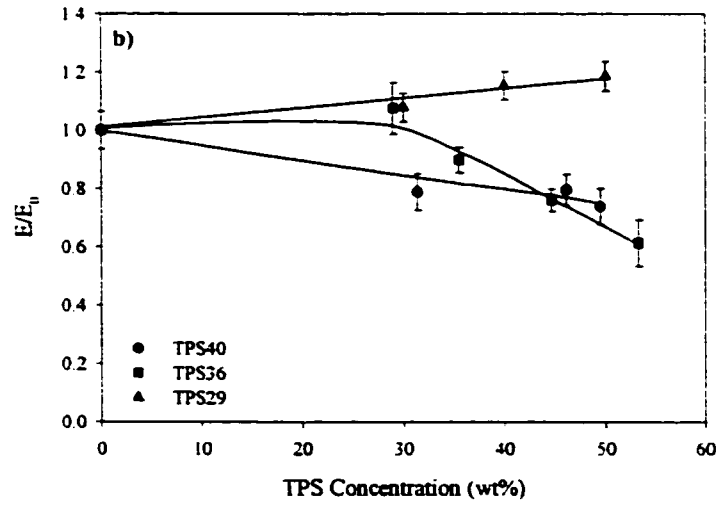

Figure 4.8 a) Relative elongation at break ($\varepsilon_b/\varepsilon_{b0}$) and b) relative Young's Modulus (E/E_0) of PE1/TPS blends as a function of TPS concentration (wt%). Terms with subscript 0 refer to the pure LDPE.

The relative Young's modulus (E/E_0) is demonstrated in Figure 4.8b and the raw data are given in Table 4.2. Once again the results are excellent. The E can be maintained at high levels even at high loadings of TPS36 and TPS40. At lower levels of glycerol (TPS29) the E of the blend can be seen to even exceed that of the neat polyethylene. These are unusual results considering the high levels of immiscibility between PE and TPS. The results also indicate the potential of tailoring the mechanical properties of the blend through an appropriate glycerol content. This unexpected result can be explained by good interfacial contact. Leclair and Favis (1996) found that the compression exerted by a crystalline matrix (HDPE), during crystallization, on an amorphous dispersed phase (PC) can result in good interfacial contact and a higher elastic modulus. They also observed that this effect had a positive influence on the modulus only when the contraction took place on a smooth, non-deformable surface. The mirror-like quality of the TPS surface is demonstrated in Figure 4.9.

4.4.4.3 Effect of humidity on axial and cross properties.

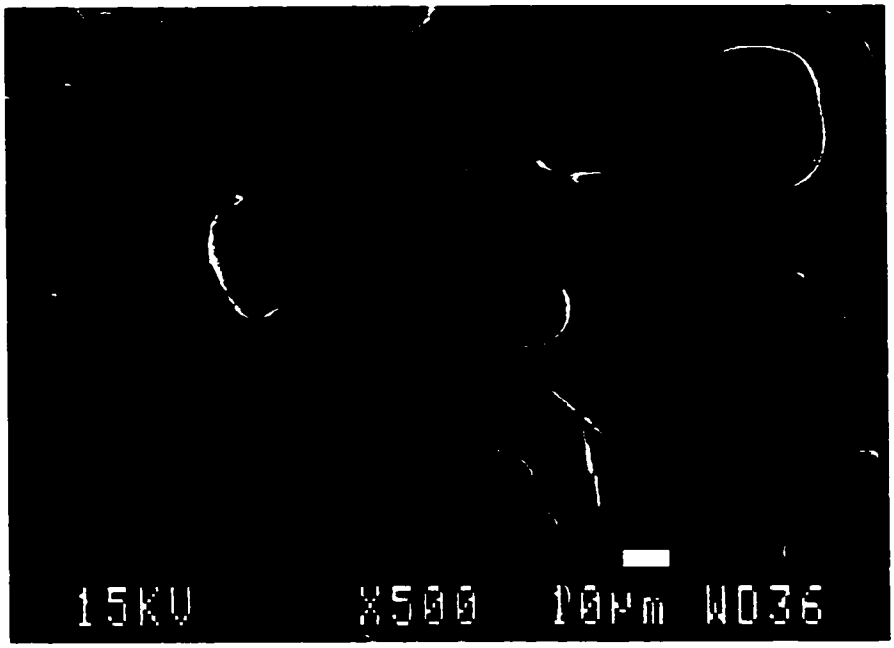

Figure 4.9 SEM cryofracture surface of PE1/TPS40 demonstrating excellent interfacial contact and mirror-like surface of the TPS phase.

Microtensile samples cut in the machine direction (Figure 4.10) showed a similar trend as that observed for the standard tensile test (Figure 4.8). The humidity conditioning of blends compounded with high glycerol contents (36% and 40%) at 0% and 50% of relative humidity (RH) has little effect on the tensile properties. This is a critical finding since it indicates that a control of glycerol levels in the TPS can dramatically reduce the sensitivity of these types of materials to humidity in the environment. This opens up a wide range of application areas. On the other hand, blends containing 29% of glycerol are more sensitive to humidity. When the relative humidity increased from 0% to 50%, the εb increased (Figure 4.10a) and the E decreased (Figure 4.10b) because of the softening effect of water on the TPS dispersed phase.

The mechanical properties of microtensile samples cut in the cross direction are listed in Table 4.3. Due to the axial orientation imposed during calendaring, the cross properties of PE1 and PE1/TPS microtensile samples display a reduction with respect to those in the axial direction (Table 4.2). For instance, values of ε_b and E for the pure PE1 conditioned at 0% RH drop from 625 to 222 and from 54.1 to 43.3 respectively. In the case of the PE1/TPS36 blends, the elongation at break values are significantly less than that observed in the longitudinal direction. Nevertheless under all conditions studied, and despite the applied longitudinal draw ratio, the PE1/TPS36 blends demonstrate ductile behavior in the cross direction. These are excellent results considering that no interfacial modifier was used in these blends. Under all conditions, PE1/TPS29 blends demonstrate higher elongations at break in the cross direction. Because of its isotropic structure composed of spherical dispersed TPS particles, the cross direction properties of PE1/TPS29 blends are less affected than the blends exhibiting a fiber-like structure. As mentioned above, the spherical dispersed phase morphology in PE1/TPS29 blends results from its less deformable TPS phase. These results clearly demonstrate that the morphology of the TPS dispersed phase plays a very important role on the cross microtensile properties of PE1/TPS blends. The reduction in the section area, transverse to the machine direction, presented by fiber-like domains leads to the drop in the ε_b of

PE1/TPS36 blends. Conversely, spherical particles have the same surface area in both axial and cross direction, which permitted a good balance of tensile properties in both testing directions. These results indicate that a significant degree of property manipulation can be achieved through morphology control via the melt draw ratio and the glycerol content in the TPS.

Table 4.3 Tensile properties of PE1/TPS microtensile specimens in the cross direction conditioned at 0% and 50% RH.

Material	TPS (wt%)	ε_b (%)	$\varepsilon_b/\varepsilon_{b0}$[a]	E (MPa)	E/E_0[a]
Axial/0%RH					
PE1	0	625	---	54.1	---
Cross/0%RH					
PE1	0	222	1.00	43.3	1.00
Cross/0%RH					
PE1/TPS36	29	85	0.38	36.0	0.83
	36	62	0.28	35.0	0.81
	45	43	0.19	25.3	0.58
	53	33	0.15	24.5	0.57
PE1/TPS29	30	163	0.73	42.7	0.99
	41	84	0.38	40.7	0.94
	49	41	0.19	43.8	1.01
Cross/50%RH					
PE1/TPS36	29	90	0.40	31.3	0.72
	36	71	0.32	27.0	0.62
	45	49	0.22	18.1	0.42
	53	39	0.18	14.0	0.32
	30				
PE1/TPS29	41	454	2.05	33.8	0.78
	49	256	1.16	30.8	0.71
		205	0.92	24.5	0.57

[a] Relative values were determined as a function of PE1 (cross) conditioned at 0% RH

4.4.5 Interfacial structure.

In addition to the high ductility shown by the one-step processed LDPE/TPS blends in this work, these blends also demonstrated high levels of transparency even at high loadings of TPS. Opacity in immiscible polymer blends originates from two possible sources: different refractive indexes (η) between the two domains or scattering of light due to interfacial voids. This is depicted in Figure 4.11. The η has been related to the molecular arrangement and orientation of polymer chains (Seferis and Samuels, 1979). As the molecular packing increases, such as is found in crystalline structures, the η increases. In the case of semi-crystalline polymers, such as PE, the η is reported as the average between the crystalline (1.560) and amorphous (1.476) regions. The average η of PE1, considering its density (ρ = 0.920 g-cm^{-3}) should be around 1.514 (Brandrup and Immergut, 1989). Comparing that value with those determined for TPS40 and TPS36 (1.489 ± 0.001 and 1.491 ± 0.001, respectively), a difference of *ca.* 0.024 was obtained. This difference would be even smaller if amorphous LDPE was preferentially located at the interface with TPS. This difference in refractive index is similar in magnitude to the refractive index difference between water (η=1.333) (Budavari, 1989) and glass (η=1.356, glass standard #1, ASTM D542-90) and represents too small a value to result in opacity.

The other potential cause of opacity in immiscible polymer blends is the formation of microvoids at the interface resulting from poor surface adhesion and the different thermal expansion coefficients of matrix and dispersed phase. As previously discussed, PE/TPS blends display an excellent interfacial contact. This is likely due to the contraction of the semi-crystalline polyethylene about the amorphous TPS during cooling. Previous work has shown that such a contraction can significantly reduce interfacial voiding (Leclair and Favis, 1996). The micrograph in Figure 4.9 demonstrates the excellent interfacial contact.

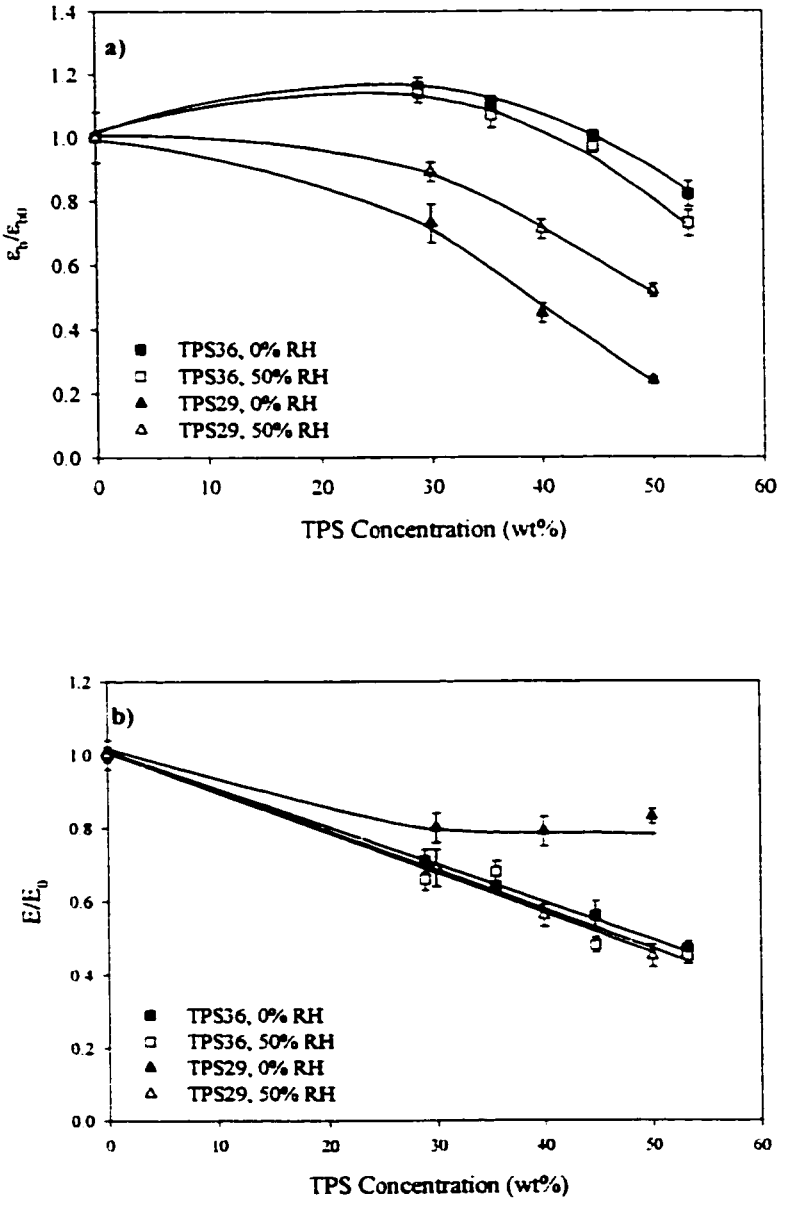

Figure 4.10 Effect of humidity on a) the relative elongation at break ($\varepsilon_b/\varepsilon_{b0}$) and b) the relative Young's Modulus (E/E_0) of PE1/TPS36 and PE1/TPS29 microtensile samples (machine direction). Filled symbols: conditioned at 0% RH; open symbols: conditioned at 50% RH.

An argument could be raised that very small microvoids might be still present beyond the range of typical microscopic techniques. Even if very small microvoids existed at the interface it is highly probable that a very thin glycerol layer coats the surface of TPS in these materials. Since TPS is a miscible starch/glycerol mixture and since the glycerol/PE and starch/PE surface energies are quite similar (23.17 and 23.95 mN m^{-1}, respectively) it is very likely that some low molecular weight glycerol migrates to the TPS/PE interface in order to reduce the overall surface free energy of the blend system as predicted by Harkin's equation rewritten by Hobbs and coworkers (Hobbs et al., 1988). This phenomenon would have the effect of even further reducing the optical effects due to interfacial voiding.

It is apparent from this work that a combination of excellent interfacial contact and very similar refractive index values are responsible for the high levels of transparency demonstrated by this immiscible polymer blend (Figure 4.11).

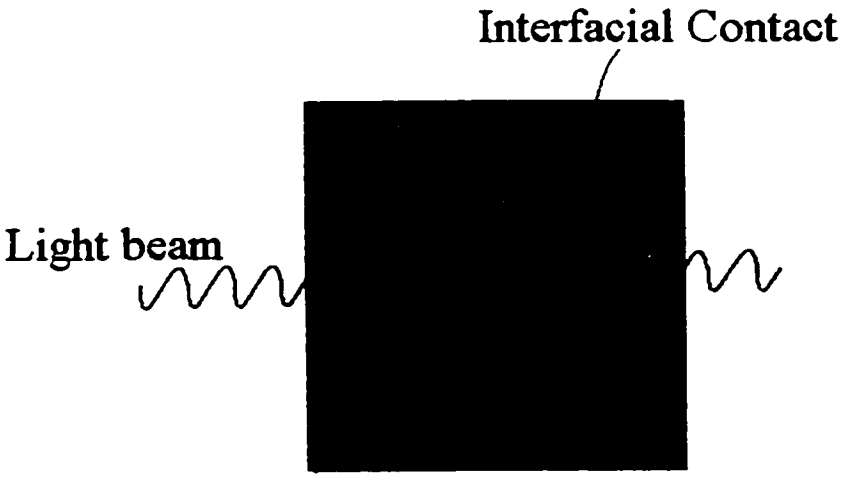

Figure 4.11 Schematic representation of the PE/TPS interface. These blends demonstrate high levels of transparency at high TPS loadings due to similar refractive index values for the PE and the TPS as well as due to the high level of interfacial contact (very little interfacial microvoiding).

4.5 Conclusions.

This study reports on a polymer blend material comprised of polyethylene and thermoplastic starch possessing highly unusual properties prepared using a novel one-step process. The PE/TPS blends demonstrate levels of ductility and modulus similar to the virgin polyethylene even at very high loadings of TPS without the addition of any interfacial modifier. The remarkable properties are a combination of both the melt blending process and a sophisticated morphology control. Furthermore, the material demonstrates very high levels of transparency even at 50:50 concentrations of PE/TPS.

The melt blending is carried out on the twin-screw extruder to produce ribbon extrudates and the first part of the process converts a starch-water-glycerol slurry into a virtually water-free thermoplastic starch. Polyethylene is added to the thermoplastic starch as a melt using a single-screw extruder connected midway on the twin-screw. The latter part of the twin-screw blends the two melts through intensive mixing zones. Using this approach it is possible to achieve blends where the thermoplastic starch morphology can be effectively controlled yielding a wide range of highly sophisticated morphological states.

Through a control of the glycerol content and thermoplastic starch volume fraction, the above process can result in morphological structures, which run the full range of those observed in classical blends of synthetic thermoplastics. Spherical, fiber-like and co-continuous morphologies are observed. Control of the glycerol content of the starch allows one to control the properties of starch from that of a solid filler through to that of a highly deformable thermoplastic material. A wide range of potential properties can be exploited for this type of material.

At 55:45 PE/TPS, and when the thermoplastic starch in the blend is highly continuous, the blend material at 36% glycerol content maintains 94% of the elongation at break and 76% of the modulus of polyethylene without the addition of any interfacial modifier. At a composition level of 71:29 PE/TPS for the same glycerol content, the blend retains

96% of the elongation at break and 100% of the modulus of polyethylene. These properties far surpass any results ever achieved through the addition of dry granular starch and is a remarkable result considering the high levels of immiscibility in the polar-nonpolar TPS-PE system. Even the properties in the cross- direction demonstrate ductility at these high concentrations. At 36% glycerol contents in the TPS, the blend system demonstrates only very low levels of sensitivity to moisture. A high degree of transparency is maintained over the entire concentration range due to the similar refractive indices of PE and TPS and the virtual absence of interfacial voiding.

Considering the significantly lower cost of starch as compared to polyethylene, this material represents a serious potential route towards polyethylene replacement. Furthermore the material has the added benefit of containing large quantities of a renewable resource. Since the starch can be fully interconnected through morphology control, it is also completely accessible for biodegradation.

This approach to blending with TPS is currently being adapted to other polymers such as polypropylene and biodegradable polyester materials and will be discussed in future papers.

CHAPTER 5

STUDY OF THE RHEOLOGICAL AND THERMAL PROPERTIES OF THERMOPLASTIC STARCH.

5.1 Abstract.

This work is part of a series of papers devoted to the study of LDPE/thermoplastic starch (TPS) blends. In this paper, the thermal and rheological properties of TPS (glycerol content 29 to 40%) prepared in a TSE were analyzed and compared to those of LDPE. DSC analysis revealed the presence of a glass transition temperature (Tg) below ambient temperature, which indicated the complete gelatinization of starch granules. The Tg decreased from –45.6°C to –56.2°C as glycerol content increased from 29% to 40%.

Rheological properties in the shear and oscillation mode were determined on-line from the TSE and by using two oscillatory rheometers, respectively. Time sweep measurements demonstrated that TPS has excellent thermal stability at 150°C, but becomes unstable at temperatures above 180°C. The studies indicate however that TPS stability was maintained for short time periods at temperatures up to 200°C. These results are important since they indicate that the potential exists to prepare stable TPS materials at high temperature by maintaining short residence times during processing. The shear viscosity of TPS (at ~ 130 s^{-1}) decreased 20% when the glycerol content was increased from 36 to 40%. Similarly, G' and G" decreased as glycerol content increased with a particularly dramatic reduction around 30% glycerol. This suggested the percolation threshold of the well-plasticized glycerol-rich soft regions. The shear and oscillation viscosities of TPS (40% glycerol) were compared with that of LDPE. The shear viscosity of this TPS was lower than that of LDPE while the opposite trend was observed in the oscillation mode probably due to the fact that the shear measurements were done out of the linear viscoelastic domain of TPS.

5.2 Introduction.

Extrusion of starch-based products is common in the food industry (Gomez and Aguilera, 1983, 1984). In the polymer field, interest in this biopolymer has been recently renewed due to its abundance, low-cost, biodegradability and the possibility of processing using conventional polymer processing equipment.

The physicochemical and rheological characteristics of extruded starch products have been studied from the point of view of both food (Gomez and Aguilera, 1983, 1984, Baird and Labropoulos, 1982, Fletcher et al., 1985, Senouci and Smith, 1988, Lai and Kokini, 1990, 1991) and polymer science (Della Valle et al., 1992, 1998, Willett et al., 1995, 1998, Aichholzer and Fritz, 1998). During extrusion, starch granules are exposed to high temperature and shear and undergo structural changes such as gelatinization, melting and fractionation. The ability to process starch and the resulting physical properties depend on the extent of structural changes of the starch. During gelatinization, starch molecules are released from the granule structure (Gomez and Aguilera, 1983). The addition of a plasticizer to gelatinized starch allows free starch molecules to behave in a similar fashion to common thermoplastic synthetic polymers. Starch prepared in this fashion is known as thermoplastic starch (TPS).

The apparent viscosity of TPS has been studied directly during the extrusion process using capillary and slit dies attached to the processing device (Fletcher et al., 1985, Senouci and Smith, 1988, Lai and Kokini, 1990, Della Valle et al., 1992, Willett et al., 1995, 1998, Aichholzer and Fritz, 1998). This direct measurement overcomes problems such as plasticizer evaporation and moisture uptake, associated with batch testing processes such as capillary rheometry (Fletcher et al., 1985). However, several authors have reported the formation of bubbles at the exit of the die when water is used as a plasticizer (Fletcher et al., 1985, Willett et al., 1995, Aichholzer and Fritz, 1998). Bubble formation appears at temperatures higher than 130°C for low moisture extrudates and at 100°C for materials having a moisture content of 30% (Willett et al., 1995). The shear

viscosity of TPS exhibits power-law behavior at typical extrusion shear rate intervals (10^1 to 10^3 s^{-1}) and its values vary from 10^4 to 10^2 Pa-s depending on die temperature and plasticizer content.

Recently, rotational rheometry has been used to advance the understanding of the viscoelastic behavior of starch-based materials in the melt (Della Valle et al., 1998, Dus and Kokini, 1990, Redl et al., 1999, Ruch and Fritz, 2000). As with many other biopolymers (Ross-Murphy, 1995), TPS has been found to display a gel-like viscoelastic behavior (Della Valle et al., 1998, Ruch and Fritz, 2000, Conde-Petit and Escher, 1995). Such rheological behavior has been related to the formation of a crystalline elastic network produced by the complexation of amylose molecules with lipids (Della Valle et al., 1998, Conde-Petit and Escher, 1995) and the physical entanglement of starch chains caused by its very high molecular weight (Ruch and Fritz, 2000). Knowledge of the rheological properties of TPS, such as viscosity and elasticity, are important parameters for the prediction of the phase inversion region and co-continuity of TPS/thermoplastic polymer mixtures (Paul and Barlow, 1980, Metelkin and Blekht, 1984, Utracki, 1991, Bourry and Favis, 1998).

This paper is one in a series devoted to the study of polyethylene/thermoplastic starch blends from this laboratory. The work has demonstrated that a one-step combined twin-screw/single screw extrusion processing protocol could be used to prepare highly continuous thermoplastic starch blends. In another paper, the effect of a hot stretch draw ratio on the thermoplastic starch morphology was examined.

In this work the influence of the glycerol content and operating temperature on the thermal and rheological properties of thermoplastic starch are examined in detail. Since our previous work has centered on polyethylene/thermoplastic starch blends, the polyethylene rheology is also shown. Previously, LDPE has been melt blended in a one-step process with TPS plasticized with glycerol, in this laboratory (Favis et al., 1999, Rodriguez et al., 1999, 2001b). The blend morphology was dependent on the LDPE/TPS

ratio, LDPE melt index, glycerol content of TPS and the hot-stretch ratio. Since LDPE rheological behavior is already well known and since much effort is currently being devoted to melt blending of glycerol-plasticized TPS (Dehennau and Depireux, 1993, Aburto et al., 1997, Bikiaris et al., 1997a, 1998, St-Pierre et al., 1997, Prinos et al., 1998, Favis et al., 1999, Rodriguez et al., 1999, 2001b), the purpose of this work was to evaluate the thermal and rheological properties of TPS produced under typical melt blending conditions.

5.3 Experimental.

5.3.1 Materials.

An LDPE resin (LDPE2040, referred to as PE1) from Rexene Chemical Co. was used as a reference for the rheological properties of TPS. Wheat starch (Supergell 1203-C) was kindly supplied by ADM/Ogilvie. This starch is composed of 25% amylose and 75% amylopectin. The original moisture content was around 7.1%. The glycerol was obtained from SIMCO Chemical Products Inc. and contained about 5% water as determined by refractive index measurements. Starch, glycerol and distilled water were mixed to form the suspensions used in melt blending experiments. The water content of glycerol was considered in the calculations of the proportions of the suspensions listed in Table 5.1.

Table 5.1 Composition of the starch suspension

Starch	Glycerol	Water
48	32	20
48.5	27.5	24
50	20	30

5.3.2 Thermoplastic starch (TPS) preparation.

In previous work, PE1/TPS blends have been prepared in a one-step process using a co-rotating twin-screw extruder (TSE) and a single-screw extruder to feed molten LDPE (Favis et al., 1999, Rodriguez et al., 1999, 2001b). In this process, starch is gelatinized and plasticized in the first zones of the TSE, then mixed with molten LDPE in the last zones. In order to evaluate the characteristics of the TPS prepared in such conditions, the TSE configuration was re-arranged to contain only the section for starch gelatinization and plasticization and the pumping section. The processing temperatures in these sections were the same as those used in the LDPE/TPS blend preparation (Favis et al., 1999). The screw speed was 150 rpm. The starch suspension of was fed into the first zone of the extruder. Water used for gelatinization was almost entirely removed during the pass through the venting zone (Favis et al., 1999). For that reason, this TPS can be considered as a binary system of starch and glycerol and, consequently, the glycerol content of the materials studied is 40%, 36%, 33% and 29% for TPS40, TPS36, TPS33 and TPS29, respectively. The TPS materials were extruded through a rectangular die to form ribbons having *ca.* 2 mm of thickness. TPS ribbons were cooled using a three-roll calendar at the minimal draw-ratio to avoid longitudinal orientation. Samples were stored in LDPE bags to reduce water absorption.

5.3.3 Analysis.

5.3.3.1 On-line viscosity measurements.

TPS viscosity was measured directly from the TSE by replacing the rectangular die used for sample preparation with a series of capillary dies. Three capillary dies having the same diameter (0.328cm) but different lengths were used. The L/D ratios of the capillary dies were 9.658, 15.491 and 23.183. The flow rate of the starch suspension was fixed at 40 g-min^{-1}, while the flow rate of TPS extrudate was varied using a valve placed on the extruder head. Pressure and temperature sensors (Dynisco, Franklin, MA) were placed far ahead from this valve to avoid causing flow disturbances. Pressure values were

measured each 5 sec while the TPS mass flow was determined at intervals of 30 sec once the pressure was stable. Bagley's correction was performed using the data from the three capillary dies. Power-law parameters were calculated by linear regression (Sigma Plot V.4.0 software, Chicago, Illinois).

5.3.3.2 DSC measurements.

Samples were taken from TPS ribbons and conditioned for at least one week in a dessicator at 0% R.H. The thermal properties were measured using a Differential Scanning Calorimeter Pyris 1 from Perkin Elmer. Samples were heated and cooled at 10°C/min. Glass transition temperatures (Tg) were scanned from –170° to 40°C. Higher thermal transitions, such as fusion and crystallization, were scanned from 25° to 200°C. The thermal transitions were calculated from the second heating cycle.

5.3.3.3 Glycerol evaporation measurement.

TPS samples maintained at ambient humidity were cut into small pieces (around 20 mg) for thermogravimetric analysis (TGA) evaluation. Another series of samples having dimension around 2×2×3.5 mm and the same weight were also cut and heated at 150°C and maintained at this temperature during 40 min (heat rate to isotherm 20°C min^{-1}). During the heating ramp (around 375 sec), a large weight loss was produced by water evaporation (absorbed during exposition to ambient humidity). Once the moisture in TPS was lost, glycerol evaporation proceeded at a lower rate than water evaporation (around 5 wt% in 25 min). It was observed that both the extent and rate of evaporation depended on the sample surface area.

5.3.3.4 X-ray diffraction.

X-ray diffraction analysis was performed in a Siemens D5000 diffractometer operating at 30kV, 25mA and over a scattering angle (2θ) range of 5° to 30° at 0.6°/min.

5.3.3.5 Rheological measurements.

Round samples (25mm diameter) were cut directly from the TPS ribbons (around 2mm thickness). Samples were dried in a dessicator for at least one week and maintained under these conditions until testing. The rheological properties were measured in the oscillation mode using two rheometers (a CSM Bohlin and an SR-5000 from Rheometrics). They were equipped with a 25-mm plate-plate configuration. All measurements were carried out under N_2 atmosphere. A seal of silicon grease was used to eliminate the evaporation of plasticizer, except in tests where the influence of plasticizer evaporation was examined. Tests devoted to the evaluation of the viscoelastic domain and of the thermal stability of TPS were carried out at a frequency of 1 Hz.

5.4 Results and discussion.

5.4.1 TPS extrusion and on-line viscosity measurement.

TPS materials extruded in the TSE at 150°C were transparent with a light yellow color that became darker as glycerol content decreased. Room temperature TPS40 extrudates were flexible and slightly sticky. Both flexibility and adhesion decreased as glycerol content decreased.

The pressure readings of TPS36 and TPS40 at 150°C were quite regular while those of TPS29 were mostly irregular. For this reason only TPS36 and TPS40 were evaluated. As observed by other authors (Senouci and Smith, 1988, Lai and Kokini, 1990, Della Valle et al., 1992, Willett et al., 1995, 1998, Aichholzer and Fritz, 1998), the shear viscosity (η_a) of both TPS and PE1 melts display a power-law (shear thinning) behavior at the shear rate (γ_a) interval developed over die extrusion conditions (Figure 5.1).

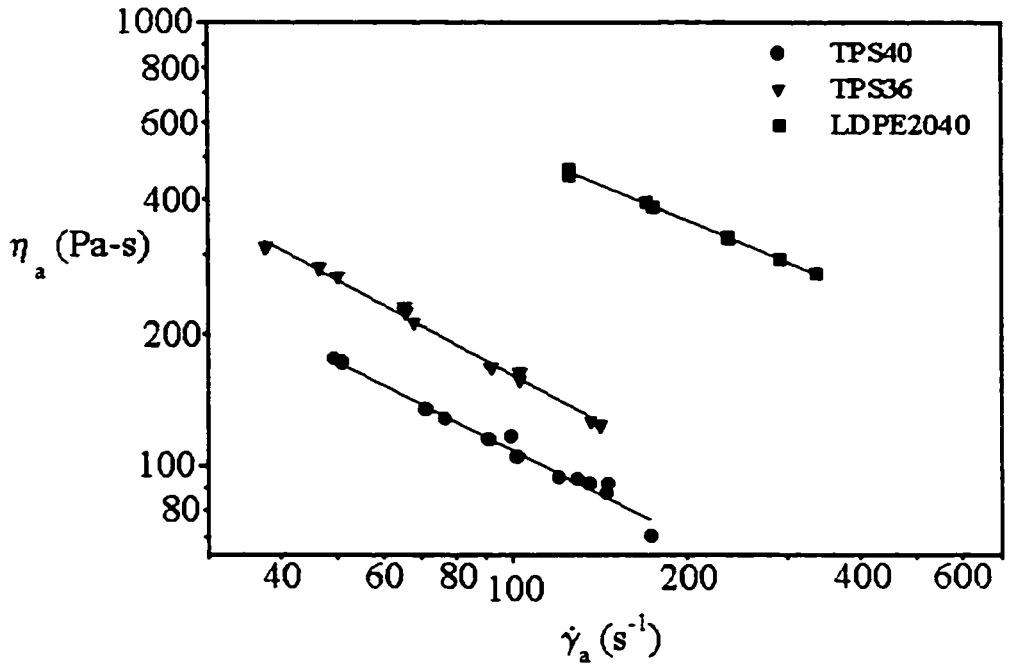

Figure 5.1 Comparison of the shear viscosity of TPS40, TPS36 and PE1 measured on-line in the TSE at 150°C.

The η_a of TPS materials depended on the plasticizer content. An increment of glycerol content from 36% to 40% resulted in a reduction of 20% of η_a of TPS36 (at $\gamma_a \sim 130\ s^{-1}$). At the same γ_a, PE1 showed a η_a 4 and 5 times higher than TPS36 and TPS40, respectively. The Power-law index (*m*) and consistency (K) of TPS melts were calculated from the data in Figure 5.1 and are listed in Table 5.2. The reduction of the TPS consistency has been attributed to the plasticizing effect of glycerol (Lai and Kokini, 1990, Della Valle et al., 1992, Willett et al., 1998, Aichholzer and Fritz, 1998). Nevertheless, there are discrepancies in the changes in power-law index. There is a decrease of *m* as glycerol content increased, similar to that found in a study of the extrusion of waxy maize (Lai and Kokini, 1990). During the study of the shear viscosity of cornstarch, Willett *et al.* found that *m* varies slightly at different water contents (Willett et al., 1995). However, an important decrease of *m* was observed when the

content of certain co-plasticizers was increased. In a further work, Willett and coworkers reported that m increases as the water content of waxy maize increases (Willett et al., 1998). It seems that the relationship between m and the plasticizer content is quite complex and depends on a number of parameters such as processing history, plasticizer type, and the presence of other additives.

Table 5.2 Properties of the components of LDPE/TPS blends.

Code	Melt index (gr-(10min^{-1}))	Glycerol (wt%)[a]	Consistency K (Pa-s^m)	Power Law index m
PE1	12	---	5957	0.531
PE2	20	---	---	---
TPS29	---	29	---	---
TPS36	---	36	4140	0.705
TPS40	---	40	2275	0.659

[a] Estimated the from preliminary results.

5.4.2 Thermal properties of TPS.

Knowledge of the structural changes produced by melt processing and of the effect of additives on thermal transitions is necessary for the prediction of the mechanical and rheological behavior of starch-based materials. Techniques such as DSC, DMTA, X-ray diffraction and NMR have been used to evaluate structural changes (Della Valle et al., 1998, Lourdin et al., 1997, Kalichevsky et al., 1993, Van Soest and Borger, 1997). Slade and Levine (1987) used a fringed micelle model to describe the partial crystallinity of starch. In this model, starch is conceptualized as a three-dimensional network composed of microcrystalline regions that behave as physical cross-linking points for an amorphous matrix (Slade et al., 1988). Three characteristic thermal transitions may exist for such semi-crystalline polymers: a glass transition for the amorphous fraction (Tg), a

thermal transition for the melting of crystallites (Tm) and a transition due to crystallization (Td). DSC analysis below ambient temperature shows that the Tg of TPS decreases as glycerol content increases (Figure 5.2).

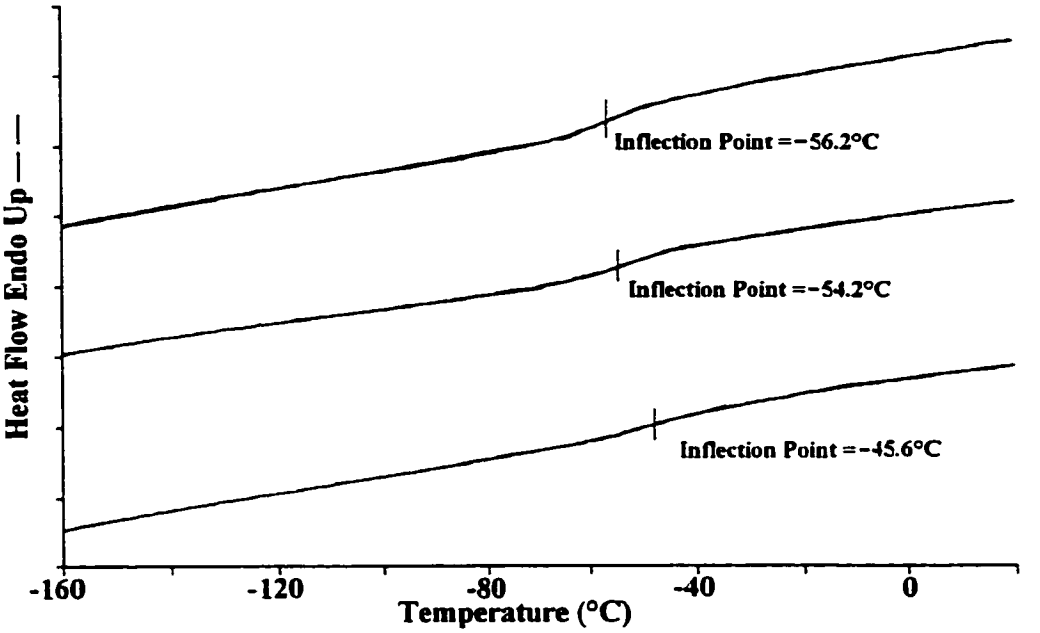

Figure 5.2 DSC thermograms of TPS samples conditioned for 24h at 0% R.H. The glycerol content in TPS is 40, 36 and 29% from the top to the bottom.

DSC scans of TPS above room temperature reveal no observable thermal transitions between 25° and 200°C (not shown). Disruption of the crystalline region, such as occurs during starch gelatinization (Donovan, 1979), leads to the disappearance of thermal transitions above Tg. However, X-ray diffraction showed the presence of crystalline regions (Figure 5.3). Other authors have observed the same signs of ordered regions in glycerol-plasticized wheat starch (Della Valle et al., 1998). Those peaks have been related to the presence of lipids in wheat starch granules, which have the ability to form complexes with amylose (Della Valle et al., 1998, Conde-Petit and Escher, 1995). The size of starch crystalline domains in TPS may typically be in the order of 15 to 30Å

(Della Valle et al., 1998). The DSC is likely not sensitive enough to detect the presence of such small crystalline regions formed by amylose-lipid complexes.

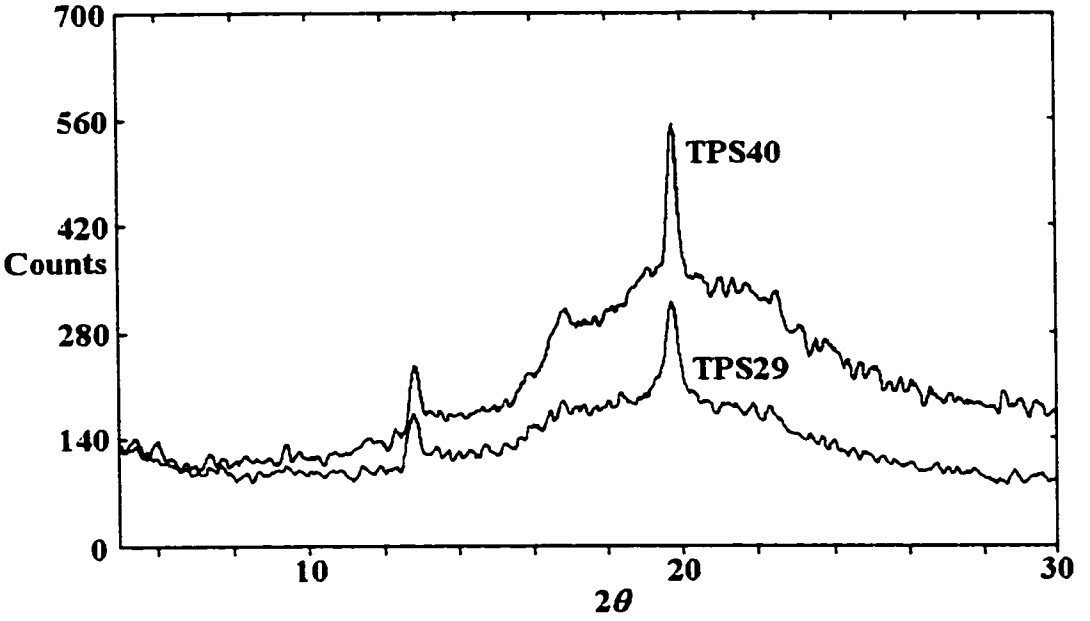

Figure 5.3 X-ray diffraction patterns of extruded and dried TPS compounded with 29% and 40% glycerol.

5.4.3 Thermal stability and linear visco-elastic domain.

In order to correlate the structure of extruded starch materials with their rheological properties it is necessary to evaluate the viscoelastic properties of TPS materials.

TPS was found to be highly stable at 150°C (Figure 5.4) with only a slight reduction (*ca.* 2.33%) in complex modulus (G*) after almost two hours. On the other hand, TPS becomes unstable at 180° and 200°C. A reduction of 10% of the complex modulus of TPS was observed at 25.5 min at 180° and after 11 min at 200°C.Nevertheless, these data are very important since they indicate that blends of TPS and other polymers may be produced even at temperatures close to 200°C, if short residence times are maintained. Our previous work has reported on a one-step processing technique for the blending of

thermoplastic starch with synthetic polymers which allows for the possibility of very short residence times at high temperature (Bourry and Favis, 1997).

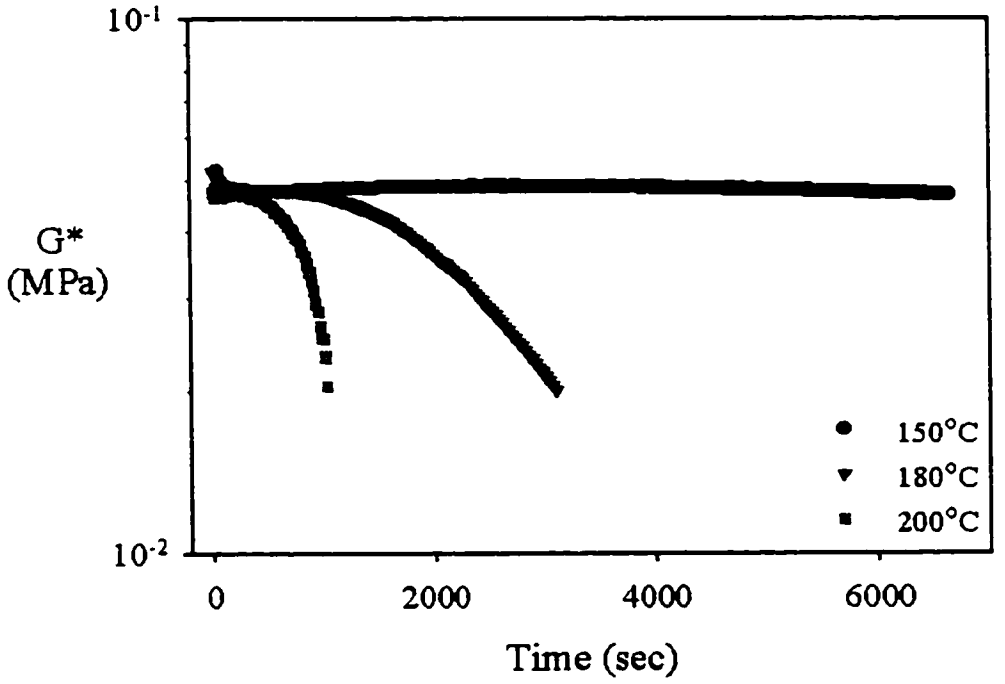

Figure 5.4 Thermal stability of TPS40 evaluated at a frequency of 1Hz and different temperatures (150°, 180° and 200°C).

The linear visco-elastic domain of TPS evaluated at a frequency of 1 Hz extends to deformation values (γ) of around 0.02 (Figure 5.5). This value is one decade larger than that reported in the literature (Della Valle et al., 1998) and, may be related to the significantly lower glycerol content (27%) of their testing sample in that previous work.

5.4.4 Effect of plasticizer evaporation.

The re-processing of LDPE/TPS blends (TPS with 40% glycerol) in a twin-screw extruder was examined in a recent paper from this laboratory (Rodriguez et al., 2001b). The TPS particles of original blends showed an excellent elongational deformability while dispersed particles of re-processed blends were not able to deform. Reduced

deformability of re-extruded TPS was related to glycerol evaporation during the pass through the vacuum venting zone at 150°C. TGA measurements corroborated the possibility of glycerol evaporation at such low temperature. In order to evaluate the effect of glycerol evaporation on the rheological properties of TPS, experiments were carried out in the rheometer without the silicon grease seal.

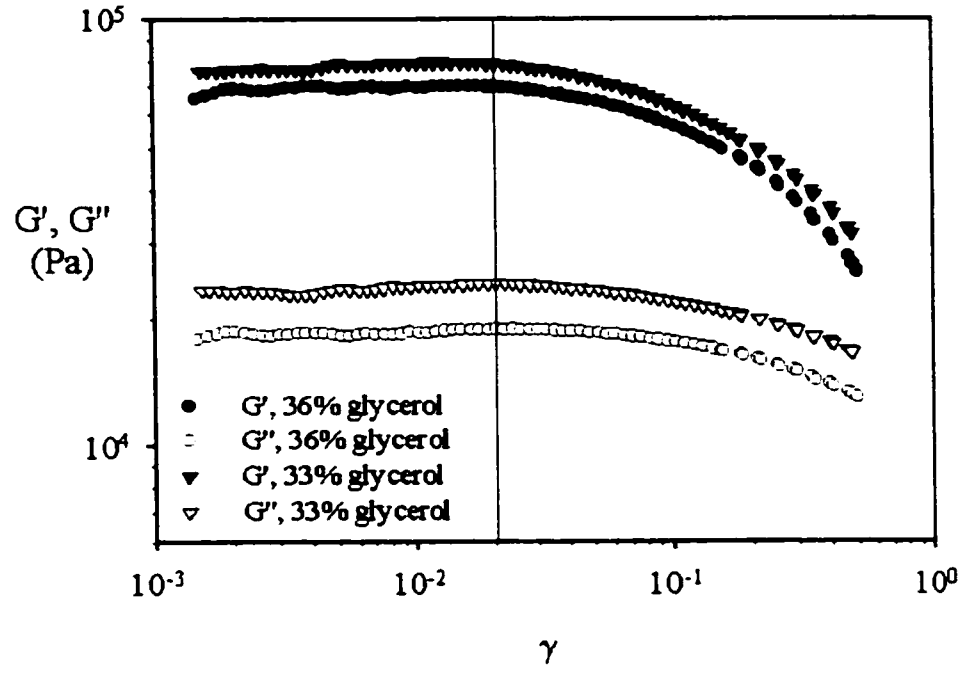

Figure 5.5 Stress sweep tests of TPS compounded with different glycerol concentrations. Tests were carried out at 150°C and at a frequency of 1Hz.

Both the storage and loss modulus increase with time due to the evaporation of glycerol (Figure 5.6). Although glycerol is lost only through the gap between the two plates, glycerol diffusion promoted by test shearing renewed the plasticizer content in the outer surface. A similar response was observed during the evaluation of the rheological properties of TPS containing different moisture contents (Della Valle et al., 1998). In that work, moisture was lost even below the water boiling point temperature (90°C).

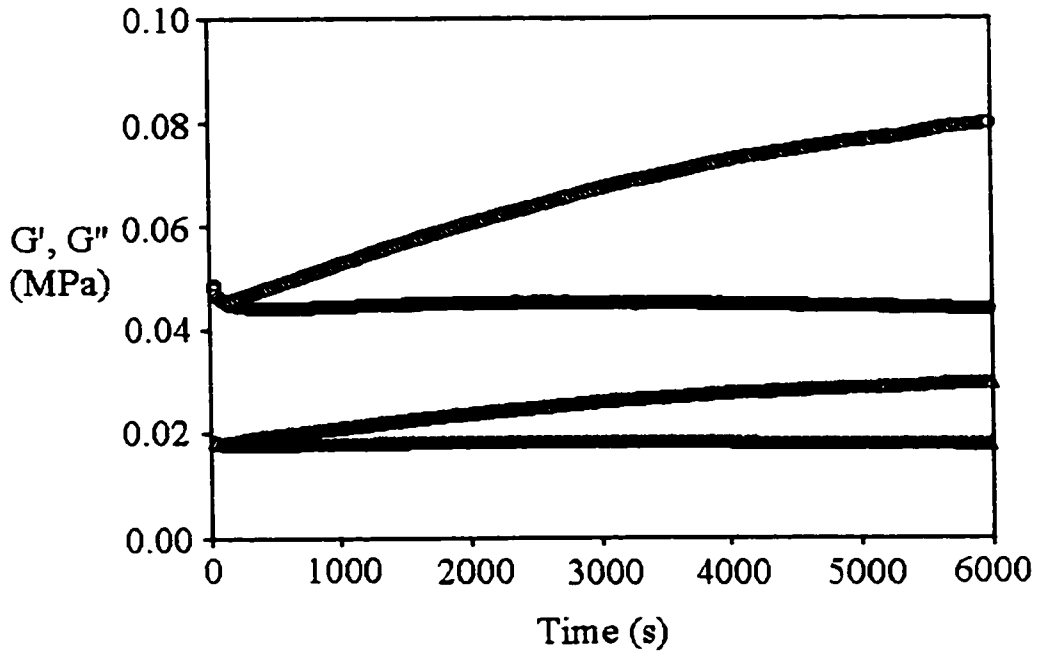

Figure 5.6 Effect of plasticizer loss on G' (●,○) and G" (▲,△) of TPS40 at 150°C and a frequency of 1Hz. TPS40 was coated with (dark symbols) and without (light symbols) silicon grease.

5.4.5 Effect of glycerol content.

TPS exhibits the rheological behavior of a typical gel (Figure 5.7) as characterized by a storage modulus (G') larger than the loss modulus (G") and with both moduli largely independent of frequency over the amplitude of the experimental window (Ross-Murphy, 1995). This behavior is produced by the presence of an elastic network embedded in a softer matrix. The rigidity in those regions can be produced by chemical or physical crosslinking. The structure of the elastic network has been related to the crystallinity derived from the complexation reaction between amylose and lipids (Della Valle et al., 1998, Conde-Petit and Escher, 1995), and the physical entanglement of the high molecular weight polysaccharides (Della Valle et al., 1998, Ruch and Fritz, 2000).

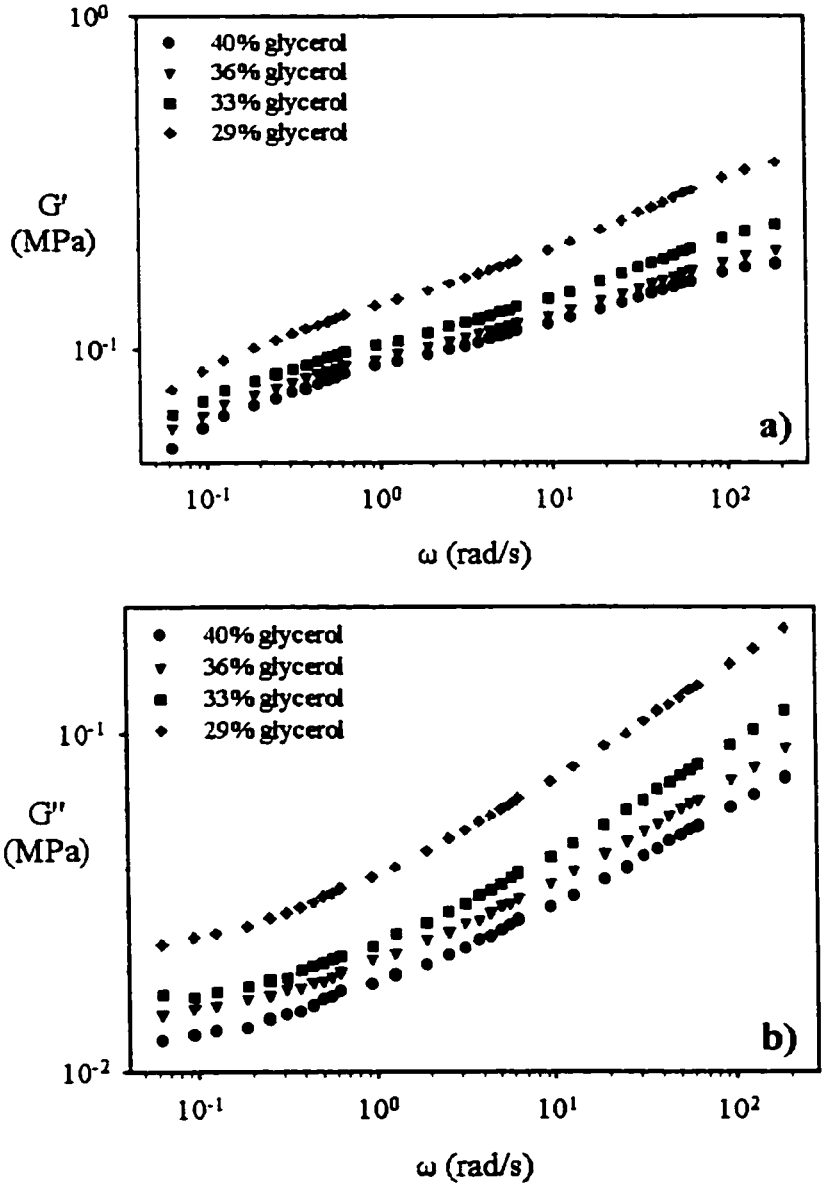

Figure 5.7 Effect of glycerol content on (a) elastic modulus (G') and (b) loss modulus (G") of TPS materials evaluated at 150°C.

As expected, the augmentation of the glycerol content in TPS results in a reduction of both G' and G". However, the trend in the modulus curves was nearly the same, regardless of the glycerol content. From the study of low-concentration starch

dispersions, Conde-Petit and Escher showed that the formation of amylose-emulsifier complexes modifies the viscoelastic response of potato starch dispersions (Conde-Petit and Escher, 1995). Crystalline regions produced during the amylose-emulsifier complexation form an elastic network, which is responsible for the liquid-like to solid-like viscoelastic modification. From the similarity of the trend of the G' curves it can be inferred that glycerol modification does not affect the nature of the hypothetical crystalline elastic network, it just plasticizes the amorphous fraction of starch. This statement was corroborated by the comparison of X-ray diffraction patterns between TPS40 and TPS29 (Figure 5.3), where no change of the crystalline to amorphous fraction ratio occurs. It appears that crystalline regions created by the amylose-lipid complex are not uniquely responsible for the viscoelastic behavior shown by TPS material, although it must be an important part of it as demonstrated by Della Valle *et al.* (1998) from the comparison of waxy maize and high amylose maize.

The reduction of G' at different glycerol contents was similar to that observed in starch gel systems (Kulicke et al., 1996). The reduction of the glycerol content from 40% to 33% results in a quasi-linear increment of G', while the reduction from 33% to 29% glycerol produces a larger variation in G'. In the case of the elastic modulus of polymer composites, percolation theory explains the non-linearity produced by the phase inversion effect at high filler content (Willett, 1994). The limit of glycerol plasticization that produces the non-linearity observed in the G' of TPS at a concentration around 30% glycerol can be explained in a similar way. TPS can be considered as a homogeneous system composed of a hard elastic network and soft amorphous regions. Amylose complex crystallites, highly entangled starch molecules, poorly plasticized starch-rich sites, or a combination of them could compose the hard elastic network. Soft amorphous regions could be composed of well-plasticized glycerol-rich starch. Even though the elastic network was present at 33% glycerol, the soft amorphous regions dominate the viscoelastic response. The increment of glycerol content produces a relatively small reduction in the rheological parameters. Around 30% glycerol, phase inversion occurs

resulting in the domination of the viscoelastic response by the hard elastic network, which is in good agreement with percolation theory. That suggests a glycerol plasticization threshold at a concentration around 30%. A more in-depth study of starch microstructure is necessary to determine the actual components of the hard elastic network and the soft amorphous regions in TPS materials.

5.4.6 Comparison of TPS viscosity measured in oscillation and shear modes.

The real component of the viscosity ($\eta' = G''/\omega$) of PE1 and TPS40 was compared with the respective values of η_a (Figure 5.8). It is evident that PE1 obeys the Cox-Merz rule while TPS40 does not. The Cox-Merz rule indicates that η_a and η' should converge at high shear rate/frequencies (Dus and Kokini, 1990). The deviation of TPS rheological properties from the Cox-Merz rule has already been observed by other authors (Della Valle et al., 1998). It can also be inferred from the results published by Fritz and coworkers (Aichholzer and Fritz, 1998, Ruch and Fritz, 2000). Another important result evidenced by Figure 5.8 is the inversion of the trend observed in Figure 5.1, where η_a of TPS < η_a of PE1. Deviation of TPS viscosity from the Cox-Merz rule may be the cause of this trend inversion. It appears that viscosity values measured in the capillary die (TSE) were out of the linear viscoelastic domain of TPS. In order to prove that, γ was gradually increased above the linear viscoelastic domain ($\gamma \sim 2\%$). At high γ, the G" drops giving place to a reduction of the η' (Figure 5.9). At 10 rad-sec^{-1}, for instance, η' drops from 14100 to 3109 Pa-s as γ increases from 1 to 50%. A crossover point between η_a and η' can be observed at a sufficiently high γ. That is extremely important considering that the rheological properties of TPS are fundamental for the theoretical prediction of the morphology of TPS-based blends.

5.5 Conclusions.

The thermal and rheological properties of TPS materials prepared in a TSE were analyzed. The study of the thermal transition of TPS proved that granular starch was

completely disrupted. The TPS showed a thermal transition below room temperature corresponding to the glass transition temperature and this Tg was dependent on glycerol content. Even though no thermal transition was observed above room temperature, a crystalline structure, which can be related to the complexation of amylose with lipids present in wheat starch granules, was detected by X-ray diffraction.

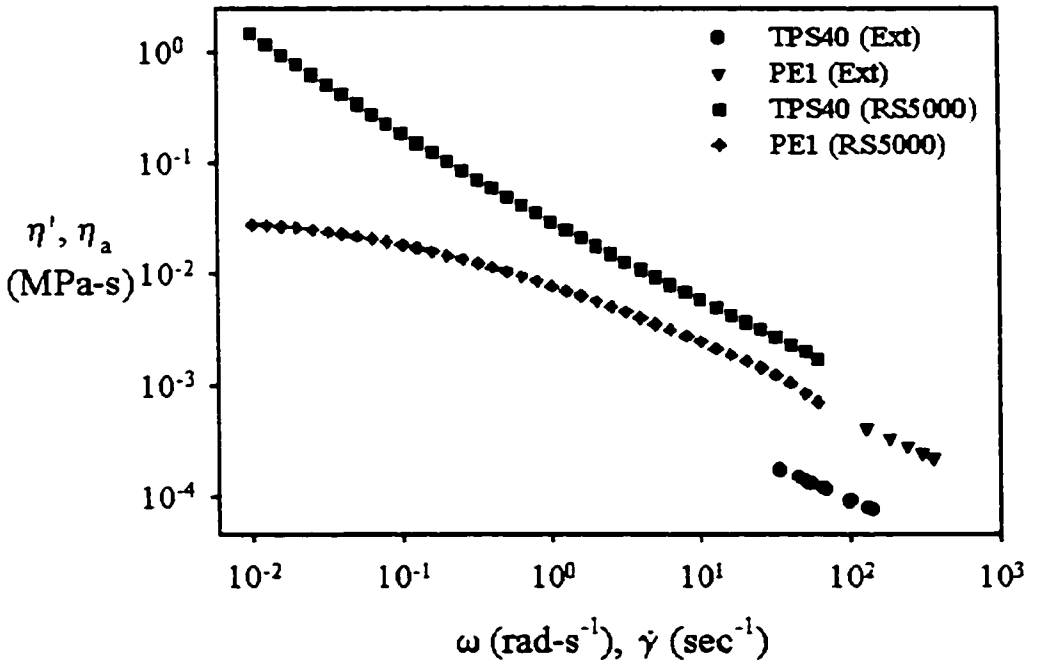

Figure 5.8 Comparison of the dynamic viscosity (η') measured in the oscillation mode (Rheometer RS5000) and the shear viscosity (η_a) of PE1 and TPS40 measured on-line in the TSE.

During rotational rheometry, TPS demonstrated an excellent thermal stability at 150°C but became unstable at temperatures above 180°C. The studies indicate however that TPS stability was maintained for short time periods for temperatures up to 200°C. These results are important since they indicate that the potential exists to prepare stable TPS materials at high temperature by maintaining short residence times during

processing. The linear viscoelastic domain of TPS extended to $\gamma \sim 0.02$ due to the restricted motion imposed by the presence of an elastic network. The evaporation of glycerol leads to a gradual increase in the rheological properties of TPS due to the stiffening of TPS.

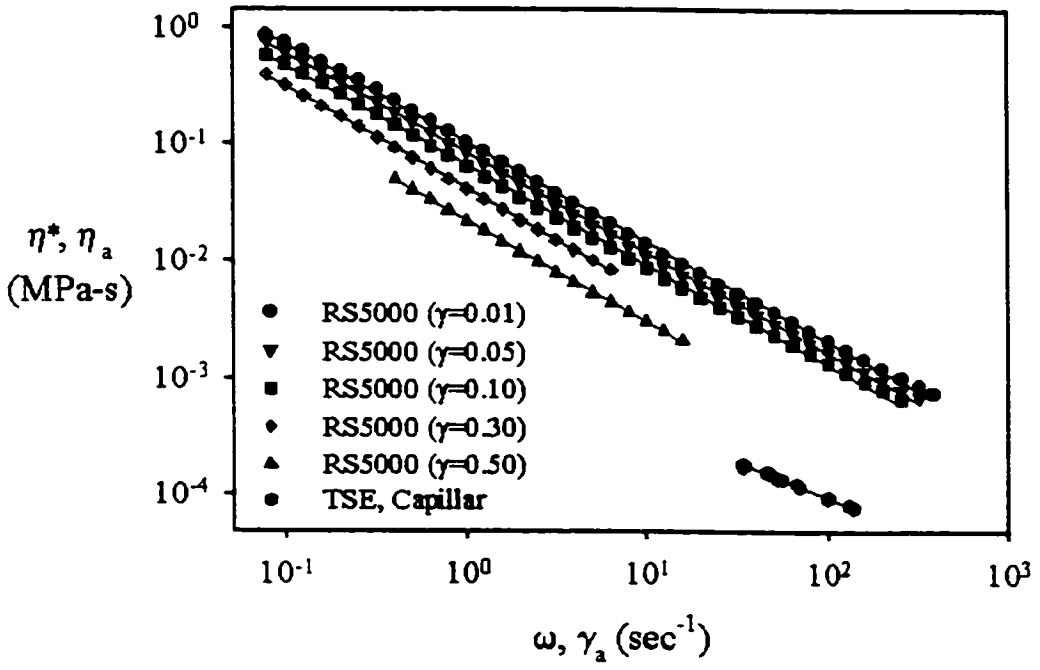

Figure 5.9 Comparison of η' of TPS40 measured at 150°C for different deformations (γ) in a RS5000 rheometer and η_a determined on-line in the TSE at 150°C.

As was observed for the thermal properties, the rheological properties were also highly dependent on glycerol content. The shear viscosity of TPS decreased 20% when the glycerol content was increased from 36 to 40%. In the same way, G' and G" also decreased as glycerol content increased. However, a particularly dramatic variation was observed when the glycerol content was varied from 29% to 33%. These latter results suggest a phase inversion from a hard elastic network to soft amorphous regions. The glycerol plasticization threshold thus occurs at a content of approximately 30%.

Comparison of the shear and dynamic viscosity of TPS40 and PE1 show important differences in the viscosity ratio for this polymer pair. Under shear conditions, LDPE was more viscous than TPS while in the oscillation mode the trend is reversed. The lower shear viscosity displayed by TPS can be attributed to the very high deformation, out of the TPS linear viscoelastic domain, undergone by this material during the pass through the capillary die.

CHAPTER 6

THE INFLUENCE OF MELT DRAWING ON THE MORPHOLOGY OF ONE AND TWO-STEP PROCESSED LDPE/THERMOPLASTIC STARCH BLENDS

6.1 Abstract

In this study the morphology of LDPE/TPS blends prepared by a one-step extrusion/shaping process is compared to that obtained by reprocessing of the original blends. The influence of composition and melt drawing is examined. A novel methodology based on the form factor of the dispersed particle is used to estimate the equivalent spherical particle size of dispersed TPS. This approach allows for the quantitative comparison of average dispersed phase particles regardless of their shape. Blends prepared in the one-step extrusion process show increased levels of anisotropy as a consequence of a combination of coalescence and particle deformation during melt drawing. Re-processed materials demonstrate morphologies that are highly stable to a wide range of hot stretch ratio conditions. The TPS particles of re-processed blends show no-coalescence and a low degree of deformation. This phenomenon is explained by plasticizer evaporation resulting from the second processing step. The TPS is transformed from a highly deformable phase to one resembling a partially crosslinked material. These data indicate that the one-step processing of LDPE/TPS blends can be used to generate a wide range of highly elongated morphological structures. A two-step approach, analogous to typical compounding and shaping operations and involving controlled glycerol removal in the second step can be used to prepare a wide range of highly stable, more isotropic, dispersed particle morphologies.

6.2 Introduction

Starch is of interest to the plastics industry because it is a biodegradable renewable resource of very low cost. Native starch granules are solid particles that can be used as a filler while thermoplastic starch (TPS) behaves as a deformable plastic material. TPS is

produced by the breakdown of the crystalline structure of native starch through the application of heat, shear and water (gelatinization). The amorphous state can be stabilized by the addition of a plasticizer such as glycerol. Although it does not possess highly desirable mechanical properties itself, thermoplastic starch can be melt blended with other polymers to produce partially or completely biodegradable materials whose properties resemble certain commercial plastics (Favis et al., 1999, Rodriguez et al., 1999, 2002a).

Partially biodegradable materials can be produced by the melt blending of starch with non biodegradable polymers such as polyethylene (PE) (Otey et al., 1980, Shogren et al., 1992, Bikiaris et al., 1997, 1998, Favis et al., 1999, Rodriguez et al., 1999, 2002a). The biodegradability of gelatinized starch domains has been shown to be dramatically reduced, in spite of the high starch content, when a copolymer of ethylene-acrylic acid was added. This is due to the formation of amylose complexes with the copolymer, which are resistant to bacterial attack (Otey et al., 1980, Shogren et al., 1992). LDPE blends prepared with TPS concentrations up to 30 wt% have been reported to demonstrate a very low biodegradation extent (Bikiaris et al., 1998). An even lower biodegradation extent was observed when a maleic anhydride-grafted polyethylene was added as a compatibilizing agent. Highly continuous or co-continuous morphologies of starch domains in partially biodegradable blends are essential to assure enzymatic access to the starch biodegradable phase. The connectivity of the TPS minor phase can be improved by the presence of elongated fiber as demonstrated by work from this research group (Favis et al., 1999, Rodriguez et al., 1999, 2002a).

PE and TPS form immiscible blends due to the high interfacial tension between a non-polar polymer and a highly polar one. Spherical droplets can be stretched under the action of a flow field. However, the application of an elongational flow field is more effective for particle stretching than the application of simple shear flow, especially at high viscosity ratio (Stone et al., 1986). Spherical particles can be transformed into ellipsoids or even long fibers under the influence of an elongational flow such as that

exerted during the pass through capillary dies (Chapleau and Favis, 1995) or calendaring rolls (Gonzalez, et al., 1993, 1996). Once deformed, the particles can breakup or maintain the elongated shape. The fibrillation-breakup process is controlled by interfacial tension, viscosity and elasticity ratios, the applied stress, and droplet particle size (Chapleau and Favis, 1995). The presence of elongated elliptical or fiber-like particles can render the quantification of the dispersed phase dimensions difficult. In some cases, a relative volume (Gonzalez et al., 1996) or major axis-minor axis ratio (Kelnar et al., 2001) of elongated dispersed phase particles have been reported as a comparison with the equivalent average spherical particle diameter.

In typical polymer processing operations, both a one-step compounding/shaping approach and a two-step protocol are used routinely. The objective of this work is to evaluate the morphology development in these two environments under a variety of melt drawing conditions and TPS concentrations.

6.3 Experimental

6.3.1 Materials

The polyethylene used is an LDPE2040 supplied by Rexene Chemical Co (PE1). Wheat starch, Supergell 1203-C, was supplied by ADM/Ogilvie. Supergell 1203 contains 25% amylose and 75% amylopectine. The purity of glycerol (SIMCO Chemical Products Inc.) was determined by refractive index measurements. In this work a starch/glycerol/water suspension (48:32:20 weight ratio) was fed to the first step extrusion system.

6.3.2 One-Step Extrusion Process

PE1/TPS blends, containing 30% and 45% by weight of TPS, were prepared in a one-step extrusion system composed of a co-rotating twin-screw extruder (TSE) and single-screw extruder (SSE). Volume fractions of TPS (ϕ_{TPS}) were calculated based on the densities of PE1 (0.920 g-cm^{-3}) and TPS (1.410 g-cm^{-3}). The starch suspension was

pumped into the first zone of the TSE while PE1 was fed into the 5th zone of the TSE via the SSE. The TSE was equipped with a venting zone attached to a vacuum system. Water was extracted at mid-stream of the TSE just before the zone where molten PE1 was fed. A more detailed description of this extrusion system is reported elsewhere (Favis et al., 1999). The melt mixing of TPS with PE1 was performed at 150°C with the screw speed maintained at 150 rpm. PE1/TPS ribbons were extruded through a rectangular die (32 X 2.1 mm). The extrudates were cooled and drawn using a three-roll water-cooled calendering unit. The maximum gap between the rolls was 1.65 mm. The hot-stretch ratio (HSR) was calculated from the difference between the linear velocity of the rolls (V_R) and the linear velocity of the extrudate (V_E), $HSR = (V_R - V_E)/V_E$ (Gonzalez et al., 1993).

6.3.3 Re-Processing

Some of the PE1/TPS blends prepared in the one-step process were pelletized and mixed with additional PE1 to produce blends containing 1%, 10%, 30% and 45% TPS by weight. To achieve this, PE1/TPS pellets were dried at 60°C under vacuum for 24 hours and dry mixed with PE1 pellets before being fed to the TSE via a hopper. The TSE had the same screw and barrel configurations as those used in the one-step process. The temperature was maintained at 150°C throughout the TSE and the screw speed was 150 rpm. Blends extruded in this way were cooled and stretched through the three-rolls calendaring unit as described above.

6.3.4 Analysis

6.3.4.1 Morphological Analysis

Specimens of PE1/TPS ribbons were cut in both the longitudinal and transversal directions. These specimens were cryogenically microtomed under a liquid nitrogen flow using a Reichert Jung Supercut 2050 equipped with a glass knife. Once microtomed, TPS was extracted with 6N HCl at 60°C for 48 hours. The samples were

then washed several times with distilled water and dried in a vacuum oven at 60°C for 24 hours. Dried samples were coated with a gold-palladium alloy and observed with a Jeol 35 CF scanning electron microscope (SEM).

6.3.4.2 Image analysis

The area and perimeter of TPS domains were measured using a digitizing table controlled by a Sigma Scan Pro 5 system. In the cases of 1% and 10% TPS at least 3 sets of fields of view of around 200 particles each were analyzed for HSR in order to have enough particles for a statistical evaluation. For the other blend compositions, five fields of view (more than 400 particles per field of view) were analyzed for each HSR. The degree of deformation was measured using the form factor (F) as an index of reference. $F = 4\pi A/P^2$, where A is the area and P is the perimeter of the particle. For a perfect sphere F = 1 and for the maximum deformation, F = 0 (a very long fiber with a vanishing diameter).

In order to quantify the volume changes regardless of the distinct particle shapes, a novel methodology was proposed. This volume can be calculated using the formula of the volume of an ellipsoid ($V = {}^4/_3\pi abc$, where a and b are the minor axes, and c is the major axis of the ellipsoid). For a sphere, a = b = c = r where r is the radius. For a fiber, c is the fiber length in the longitudinal direction and a and b can be calculated from the fiber dimensions in the cross-section. Assuming unidirectional deformation, i.e. a = b, the volume of an ellipse in revolution is given by ($V=4/3\ \pi a^2 c$). It is only dependent on particle dimensions in the longitudinal section (a and c). Several equations to find a relationship between 1/F to the form ratio (c/a) were analyzed. The nonlinear regression of a hyperbola (double rectangular of 5 parameters) fits perfectly using a log-log scale. That expression is:

$$y = \frac{b_1 x}{b_2 + x} + \frac{b_3 x}{b_4 + x} + b_5 x \qquad (1)$$

where b_1, b_2, b_3, b_4, and b_5 are constants. Their values were determined to be 0.0736, 0.0024, 0.2643, 0.0931, and 0.9858, respectively, using Sigma Plot software. In order to handle the results in a more robust fashion, independent of the degree of deformation, volumes were considered as the volume of an equivalent sphere. Using that assumption, the equivalent average diameters in number ($D_{n,equiv}$) and in volume ($D_{v,equiv}$) of TPS domains were calculated. It should be noted that $D_{n,equiv}$ and $D_{v,equiv}$ as defined here are related to the average volume of the particles. An increase of those averages indicates coalescence phenomenon. $D_{v,equiv}$ tracks the larger particles and $D_{n,equiv}$ tracks the smaller ones.

6.4 Results and discussion

6.4.1 Effect of HSR on the morphology

6.4.1.1 One-step extrusion process

In this work, the effect of HSR on the morphology of PE1/TPS blends was evaluated by varying the rotational speed of a three-roll calendaring unit which also served to quench the extruded ribbons. The influence of the melt drawing on the morphology of PE1/TPS blends prepared in a one-step extrusion process can be observed in Figure 6.1. At the low HSR, there is a large population of small round particles dispersed around some large TPS particles that show an important deformation in the strain direction. As HSR increases, the concentration of large elliptical particles and fibers increases, which in the case of ϕ_{TPS} = 0.32 form elongated structures with lengths of 300 μm or larger (Figure 6.1, bottom-right). The deformation values of TPS domains are quantitatively reported in Figure 6.2. Both volume fraction blends demonstrate a reduction of F. At ϕ_{TPS} = 0.32, a combination of particle deformation and fiber coalescence render this reduction more dramatic. It is known that fiber formation is enhanced by the combination of particle coalescence and particle deformation (Gonzalez et al., 1996, Tsebrenko et al., 1989, Champagne et al., 1996, Favis and Therrien, 1991). The reduction of F values is less than expected probably due to the influence of a large population of small particles. The

capillary number from Taylor's theory predicts that large particles are more easily deformed than small ones. It is important to notice that the values of F at low HSR are lower than unity. That suggests a deformation process that occurs before melt drawing and is likely related to the elongational deformation imposed by the reduction in the transverse section area when the blend melt passes from the extruder head to the rectangular die. The elongational deformation imposed by this extrusion system is similar to that produced by a capillary die (Chapleau and Favis, 1995). Although it is evident that HSR has an important effect on the deformation of TPS dispersed phase particles, the elongational deformation imposed by the pass through the die is even more marked (Figure 6.2).

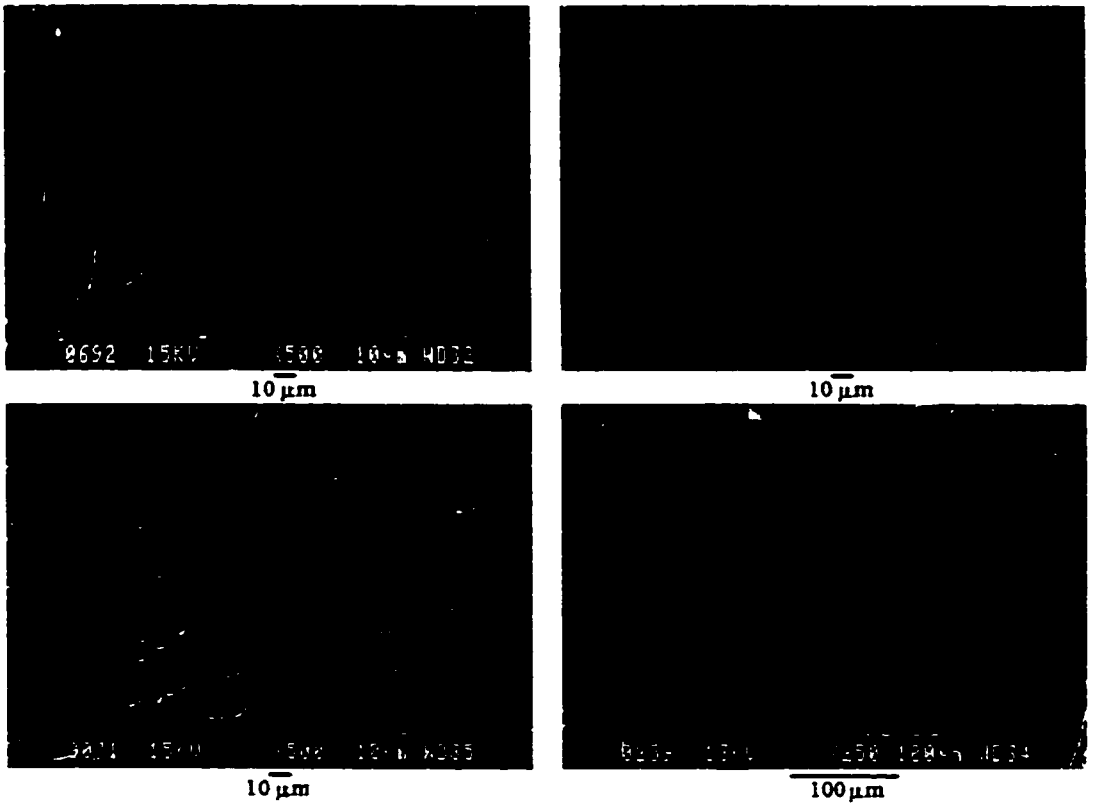

Figure 6.1 Influence of hot-stretching on the longitudinal morphology of cryogenically microtomed PE1/TPS blends (ϕ_{TPS} = 0.20, left and ϕ_{TPS} = 0.32, right) prepared in one-step process at 150°C. Top: low HSR, bottom: high HSR.

An inhomogeneous particle size distribution is evidenced in Figure 6.1. This broad particle size distribution could potentially mask the effect of the hot stretch ratio applied onto those blends. In order to separate out the effect of particle size distribution on the response to elongational deformation, individual particle volume intervals were analyzed separately (Figure 6.3). As predicted by Taylor's theory, F is dependant on the particle size. The form factor of small particles, having a volume under 20 μm^3, was independent of the applied hot stretch ratio. Particles in the interval of volume between 20 and 300 μm^3 were shown to be clearly dependant on HSR. However, particles greater than 300 μm^3 were unexpectedly independent of the hot stretch ratio. It is probable that these larger particles undergo such high level of deformation in the die that the effect of subsequent melt drawing is minimal. Those results suggested that there was an onset of particle deformation at particle volumes somewhere between 20 – 30 μm^3.

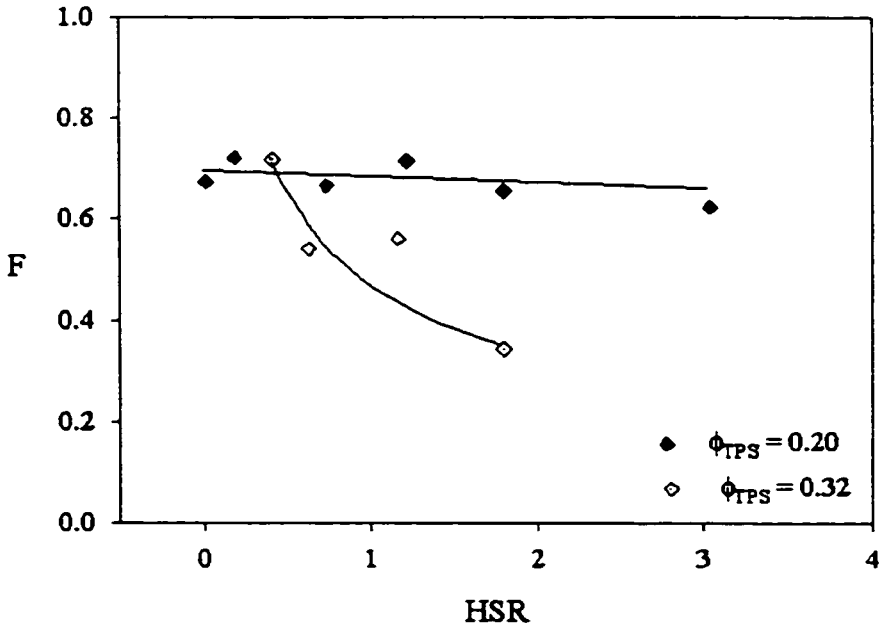

Figure 6.2. Form factor (F) *vs.* HSR of LDPE/TPS blends prepared in a one-step process at 150°C.

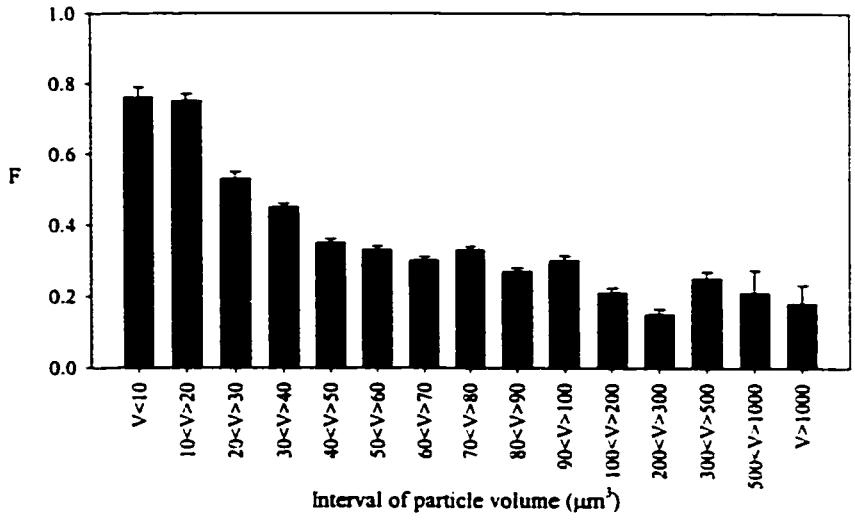

Figure 6.3. Histogram of the F of LDPE/TPS blends prepared in a one-step process (ϕ_{TPS} = 0.20) *vs.* the interval of particle volume.

6.4.1.2 Re-processing

The influence of HSR on the morphology of re-processed PE1/TPS blends is shown in Figure 6.4. As in a typical immiscible polymer blend, the particle size increases with composition of the minor phase. The TPS domains at low volume fraction of thermoplastic starch are spherical even at high HSR. Moreover, the particle size distribution of starch domains is quite homogeneous. The particle size population of the ϕ_{TPS} = 0.20 and 0.32 samples is more heterogeneous. At those concentrations, there is a large quantity of small particles, in general spherical, and some larger elliptical particles or short fibers. The drawing applied during calendaring does not appear to significantly influence the morphology in the case of re-processed blends. A quantitative evaluation of TPS deformation is shown in Figure 6.5.

In all cases, the F values suggest that the morphology has not been altered by increasing HSR, even at high ϕ_{TPS}. PE1/TPS blends compounded with ϕ_{TPS} = 0.006 and ϕ_{TPS} = 0.06

show values of F close to unity. At higher TPS content, re-processed blends do not demonstrate any deformation due to HSR. However, the elongational flow imposed by changes in the channel sections in the extrusion die markedly affect the large TPS domains (Figure 6.4).

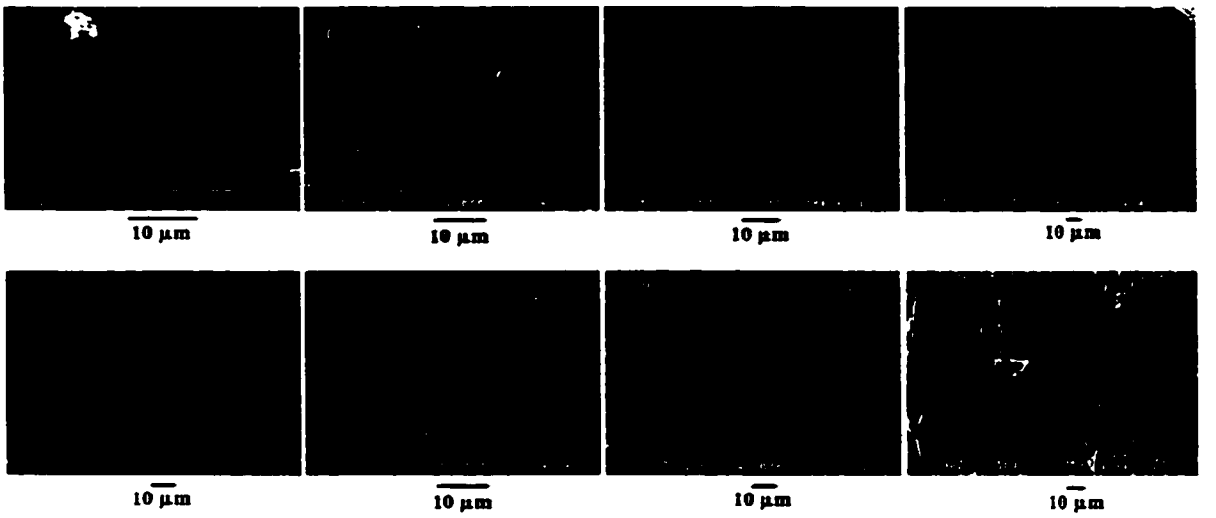

Figure 6.4. Influence of hot stretching on the longitudinal morphology of cryogenically microtomed PE1/TPS blends re-processed at 150°C. ϕ_{TPS} from left to right: 0.006, 0.06, 0.20 and 0.32. Top: low HSR, bottom: high HSR.

6.4.2 Influence of TPS concentration and HSR on the coalescence

6.4.2.1 One-step extrusion process

Several authors have studied the effect of minor phase concentration and melt drawing on the morphology of immiscible polymer blends (Gonzalez et al., 1996, Tsebrenko et al., 1989, Champagne et al., 1996). Particle-particle coalescence has been indirectly inferred through an increase in fiber formation (Tsebrenko et al., 1989, Champagne et al., 1996) or an augmentation of the relative volume of dispersed phase particles (Gonzalez et al., 1996). In this work, the effect of TPS volume fraction and HSR on the particle-particle coalescence of PE1/TPS blends prepared in a one-step extrusion process

is directly related to the evolution of $D_{n,equiv}$ and $D_{v,equiv}$ of starch domains (Figure 6.6). As mentioned in the experimental, a novel methodology based on the form factor of the dispersed particle is used to estimate the equivalent spherical particle size of dispersed TPS. This approach allows for the quantitative comparison of average dispersed phase particle volume regardless of particle shape. $D_{n,equiv}$ and $D_{v,equiv}$ as defined here are related to the average volume of particles under a given condition. An increase of those averages indicates coalescence phenomenon. $D_{v,equiv}$ tracks the larger particles and $D_{n,equiv}$ tracks the smaller ones.

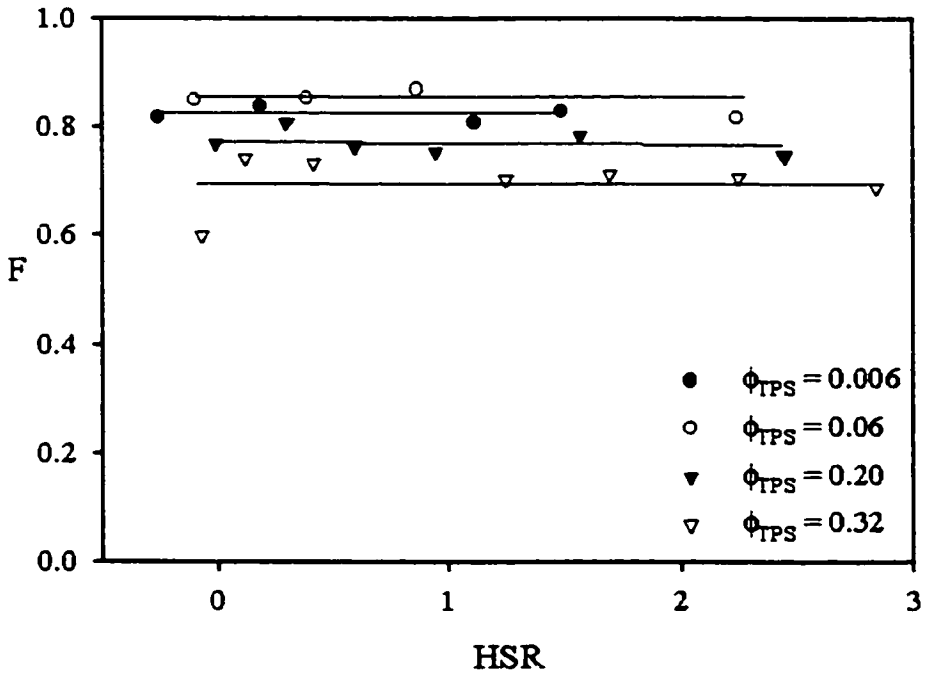

Figure 6.5 Form factor *vs.* HSR of LDPE/TPS blends prepared in a two-step process.

Figure 6.6 indicates that at ϕ_{TPS} =0.20, coalescence effects for the blends prepared by the one-step process as a function of hot stretch ratio are not very evident. Melt drawing as carried out in these experiments is essentially an elongational flow field. The values of $D_{n,equiv}$ at all HSR values seem to be the same, while the values of $D_{v,equiv}$ show a gradual increase as the HSR increases. In general, Dn is related to the total number of particles,

whereas Dv is more influenced by the largest particles. The blends prepared at ϕ_{TPS} =0.32 show a dramatic increase in coalescence with HSR. At low hot stretch ratio, the particle diameters for both volume fraction blends are similar. As the hot stretch ratio is increased, significant differences in coalescence effects between the two different volume fraction blends becomes apparent. These results appear to indicate that a critical interparticle distance exists below which coalescence effects are dramatically increased.

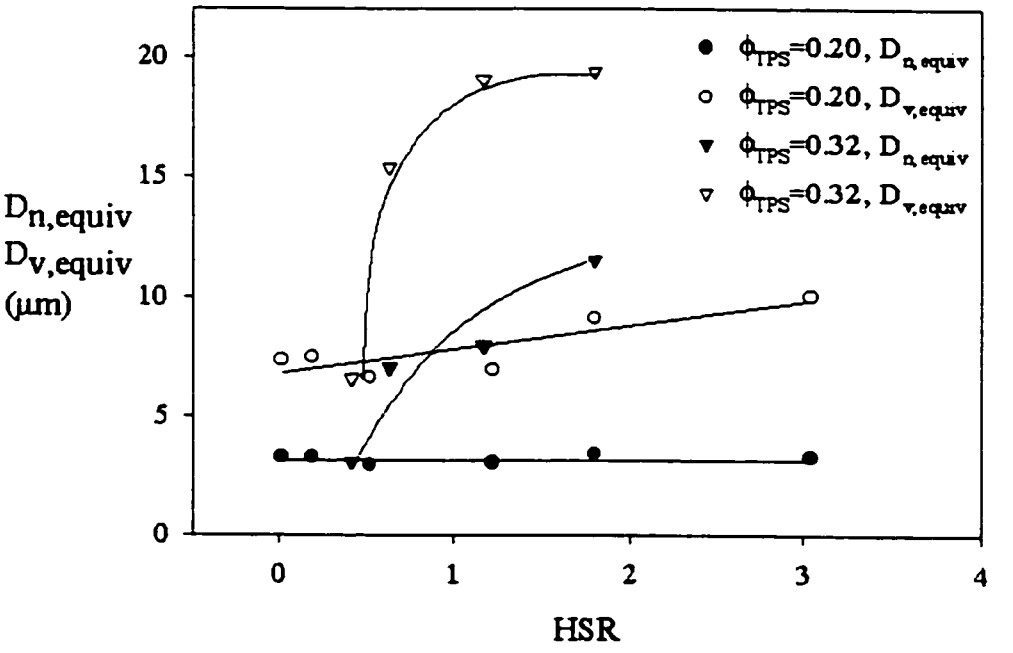

Figure 6.6 Effect of composition and HSR on starch particle size(volume) of LDPE/TPS blends prepared in a one-step process at 150°C. Filled symbols: $D_{n,equiv}$; open symbols: $D_{v,equiv}$.

6.4.2.2 Re-processing

PE1/TPS blends prepared in a one-step extrusion process were pelletized and re-extruded. In some cases more PE1 was added to have ϕ_{TPS} of 0.006, 0.06, 0.20 and 0.32. There is no increase of starch particle size with melt drawing at any of the volume

fractions in Figure 6.7. Even in the case of high ϕ_{TPS} (0.20 and 0.32) the re-extruded PE1/TPS blends demonstrate no increased coalescence with hot-stretch ratio. These results are important since they indicate that a wide range of highly stable TPS morphologies can be obtained via the two-step process. The elongational flow field produced during melt drawing is generally considered as one of the most effective flow fields in perturbing dispersed phase morphologies for typical polymer blends. Since these morphologies are stable even to the elongational flow field produced during melt drawing, this strongly indicates that compounded granules of PE/TPS prepared under these conditions could result in stable morphologies for a wide range of subsequent polymer shaping operations.

The explanation for the reduced coalescence observed in Figure 6.7 is related to the intrinsic nature of TPS. In the first step TPS is prepared from a former suspension of starch/glycerol/water. During the one-step process, most of water is extracted during the pass through the venting zone (at 110°C) resulting in a system composed only of starch and glycerol (Favis et al., 1999). Assuming that all water was extracted and that 100% of starch and glycerol remains, the actual glycerol content in the TPS should be 40% after the first processing step. During re-processing in the twin-screw extruder, PE1/TPS blends pass through the venting zone, which was under vacuum, at 150°C. It is probable that some glycerol is eliminated during re-processing leading to the stiffening of the TPS dispersed phase as observed in previous work.[16,17] In that study it was shown that glycerol evaporation results in a marked increment of both storage and loss moduli of TPS (40% glycerol) measured at 150°C and at a frequency of 1Hz. Moreover, it has been observed that at high glycerol content (36% and 40% glycerol) TPS demonstrates a lower apparent shear viscosity than PE, which results in highly elongated particles, whereas TPS compounded with 29% glycerol results in stiffer non deforming particles (Favis et al., 1999, Rodriguez et al., 1999, 2002a). These results demonstrate that at high levels of glycerol, TPS behaves as a typical thermoplastic material demonstrating high levels of coalescence and deformation after melt drawing. At low levels of glycerol, the

TPS phase behaves in a similar fashion to a partially crosslinked material and demonstrates low levels of deformation and virtually no coalescence during hot melt stretching. A second conclusion that can be draw from the above results is that the deformation resulting from the elongational flow generated through the die was larger than the melt drawing with the calendaring unit.

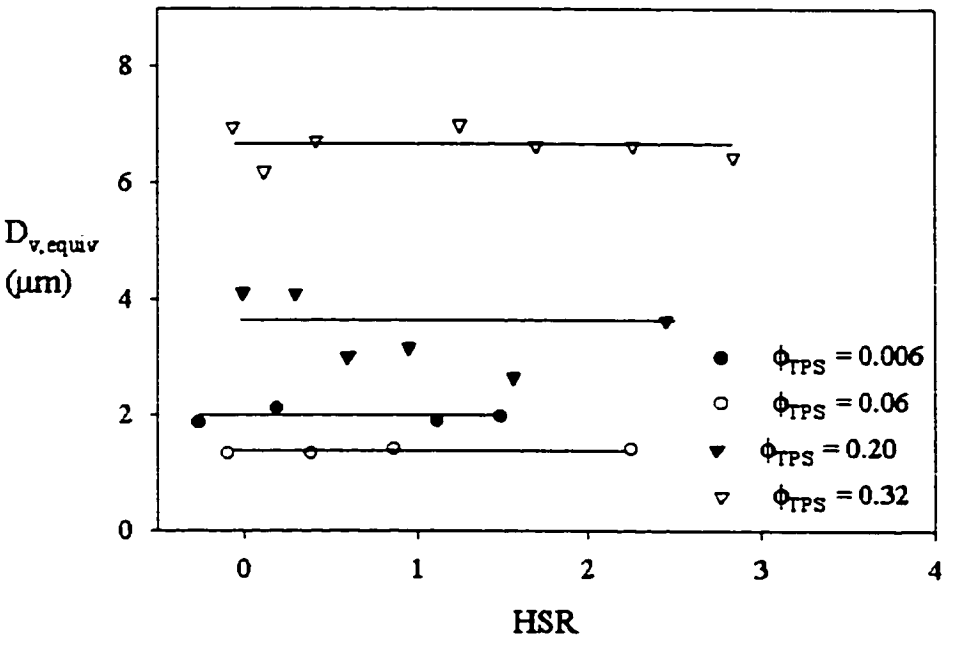

Figure 6.7 Effect of composition and HSR on the starch particle size(volume) of LDPE/TPS blends re-processed at 150°C

Control of the glycerol content either at the onset of the two-step process or through controlled glycerol evaporation (use of melt seals, selective venting) can thus allow for the obtention of a dispersed phase that runs the full range from solid particle to fully thermoplastic material. The morphological versatility of such a system, in the absence of any necessary chemical reactions or interfacial modifier, is unmatched in the entire polymer blend literature.

6.5 Conclusion

PE1 was blended with TPS in a one-step extrusion process at 150°C and then re-processed at the same temperature. Blends prepared in a one-step extrusion process behave as typical thermoplastic immiscible blends exposed to an elongational flow. Under such conditions, the TPS dispersed phase particles stretch producing a gradual increment in the form factor as HSR increases. The elongation of TPS particles leads to particle-particle coalescence in the axial direction. The particle elongation and coalescence effects are enhanced by an increase in the dispersed phase concentration. During the re-processing of PE1/TPS blends, some glycerol was extracted resulting in a stiffening of the TPS dispersed particles. This change leads to a suppression of coalescence and deformation during the melt drawing of the blends at all volume fractions.

A new methodology for the evaluation of the size of elongated particles is also developed. It is based on the form factor and allows for the comparison of classical spherical morphologies with elongated ones. From the analysis of PE1/TPS blends prepared in a one-step extrusion process it is found that the broad particle size distribution displayed by these blends masks the effect of hot stretching on the morphology evolution. The analysis of the form factor at different intervals of particle volume give more precise information concerning the influence of HSR on the morphology. In blends prepared in a one step process, it appears that a minimum volume for the TPS particle of 20 - 30μm^3 is required for deformation to occur.

The elongational flow exerted during melt drawing is highly effective at deforming the TPS phase in blends prepared in a one-step extrusion process but not for re-processed ones. On the other hand, the elongational flow produced by changes in channel sections during die extrusion results in longitudinal deformation for both one-step processed and re-processed PE1/TPS blends.

Control of the glycerol content either at the onset of the two-step process or through controlled glycerol evaporation (use of melt seals, selective venting) can thus allow for the obtention of a dispersed phase that runs the full range from solid particle to fully thermoplastic material. The morphological versatility of such a system, in the absence of any necessary chemical reactions or interfacial modifier, is unmatched in the entire polymer blend literature.

CHAPTER 7.

SCIENTIFIC CONTRIBUTIONS

One of the most important contributions of this work is the development of an extrusion system that allows the preparation of LDPE/thermoplastic starch blends having unusually high ductility in only one processing step. Even though this is more strictly a technological contribution, which lead to a patent application, it allows for an excellent control of the different stages of the melt mixing process and the isolation of the TPS extrusion process. The role played by the glycerol content on morphology, tensile properties and biodegradation of LDPE/TPS has been established. It was observed that there is a very close relationship of TPS intrinsic properties, such as thermal, rheological and mechanical characteristics, and the influence that it has on the final properties of LDPE/TPS blends. Another interesting feature of this system was the high transparency that it shows even at high loadings of TPS. A model to explain that phenomenon was described.

The isolation of TPS extrusion process permits the obtention of water-free starch samples prepared exactly at the same conditions as those blended with LDPE. The study of the thermal and rheological properties of TPS led to a better understanding of this complex system. The influence of plasticizer content on both properties was demonstrated. It was observed that around 30% glycerol the percolation threshold of the glycerol-rich well-plasticized TPS regions occurs. Comparison of the shear and oscillation viscosity of TPS40 and PE1 show important differences in the viscosity ratio for this polymer pair. Under shear conditions, LDPE was more viscous than TPS while in the oscillation mode the trend is reversed. The lower shear viscosity displayed by TPS can be attributed to the very high deformation, out of the TPS linear viscoelastic domain, undergone by this material during the pass through the capillary die.

The influence of processing conditions and melt drawing on the morphology of LDPE/TPS blends was studied. A new methodology for the evaluation of the size of elongated particles was developed. It is based on the form factor and allows for the comparison of classical spherical morphologies with elongated ones. A volume limit at which TPS can be stretched was found. A series of parameters for the control of the morphology, including processing conditions and plasticizer content, of this particular polymer system was discussed.

High ductility is hardly found in immiscible polymer blends. For that reason, the tensile properties of LDPE/TPS blends were evaluated and compared with theoretical models. Young's modulus of these blends fit quite well with Takayanagi's model for good adhesion. Properties at break do not fit simple models because they do not consider particle-particle coalescence. The fractographic evaluation of tensile tested sample revealed the influence of particle size and particle size distribution on the fracture mechanism of these immiscible polymer blends. Fracture mechanisms consisting in three stages were proposed. The completion of those stages depends on the blend morphology. The influence of relative humidity on the energy dissipation mechanism during tensile tests was discussed.

CHAPTER 8

GENERAL DISCUSSIONS

In this chapter the whole papers and annex will be discussed in a more integral manner. Discussion will start by the description of the extrusion system. In the following sections, the thermal and rheological properties of TPS, factors influencing the morphology of PE/TPS blends, the mechanical properties of PE/TPS blends and the fracture mechanisms responsible of the high ductility of these blends will be discussed. Finally, the unusual transparency of PE/TPS blends will be discussed.

8.1 Extrusion system

An extrusion system for the preparation of PE/TPS blends has been developed. The extrusion system (Figure 4.1) was composed of a single-screw extruder (SSE) connected to a Leistritz AG 34 mm co-rotating twin-screw extruder (TSE) composed of eight zones. The starch suspension was fed in the 1st zone of the TSE. Three suspension compositions were used and are shown in Table 5.1. Native starch was gelatinized and plasticized in zones 2 to 4 of the TSE. Volatiles were extracted in the 4th zone at a temperature of 110°C by venting under vacuum. Molten LDPE (T=150°C) was fed from the SSE to the 5th zone of the TSE using an adapter designed specially for that purpose. The mixing of TPS with LDPE (T=150°C) started in the same (5th) zone and continued to the 7th zone of the TSE. The last (pumping) zone was used to increase the pressure of the extrudate (T=150°C). Main problems related to this process were the cooling of PE/TPS blends

In order to evaluate the physical properties of the TPS prepared in melt blending conditions, the TSE configuration was re-arranged to contain only the section for starch gelatinization and plasticization (zones 1-4) and the pumping section (zone 8). A mass

balance revealed that water used for gelatinization was almost entirely removed during the pass through the venting zone and that almost 100% of glycerol was maintained in TPS materials. For those reasons, TPS materials can be considered as a binary system of starch and glycerol and, consequently, the glycerol content of the materials studied is 40% (TPS40), 36% (TPS36), 33% (TPS33) and 29% (TPS29) for the suspension prepared with 32%, 27.5%, 24% and 20% glycerol (Table 5.1), respectively.

8.2 Thermal properties and structure of TPS

DSC analysis below ambient temperature shows that the Tg of TPS decreases as glycerol content increases (Figure 5.2). DSC scans of TPS above room temperature reveal no observable thermal transitions between 25° and 200°C (not shown). Disruption of the crystalline region, such as occurs during starch gelatinization (Donovan, 1979), leads to the disappearance of thermal transitions above Tg. However, X-ray diffraction showed the presence of crystalline regions (Figure 5.3). Other authors have observed the same signs of ordered regions in glycerol-plasticized wheat starch (Della Valle et al., 1998). Those peaks have been related to the presence of lipids in wheat starch granules, which have the ability to form complexes with amylose (Della Valle et al., 1998, Conde-Petit and Escher, 1995). The size of starch crystalline domains in TPS may typically be in the order of 15 to 30Å (Della Valle et al., 1998). The DSC is likely not sensitive enough to detect the presence of such small crystalline regions formed by amylose-lipid complexes.

8.3 Rheological properties of TPS

Shear viscosity (η_a) of both TPS and PE1 melts display a power-law (shear thinning) behavior at the shear rate (γ_a) interval developed over die extrusion conditions (Figure 5.1). The η_a of TPS materials depended on the plasticizer content. An increment of glycerol content from 36% to 40% resulted in a reduction of 20% of η_a of TPS36 (at $\gamma_a \sim 130\ s^{-1}$). At the same γ_a, PE1 showed a η_a 4 and 5 times higher than TPS36 and TPS40,

respectively. The Power-law index (m) and consistency (K) of TPS melts were calculated from the data in Figure 5.1 and are listed in Table 5.2. The reduction of the TPS consistency has been attributed to the plasticizing effect of glycerol (Lai and Kokini, 1990, Della Valle et al., 1992, Willett et al., 1998, Aichholzer and Fritz, 1998). Nevertheless, there are discrepancies in the changes in power-law index. There is a decrease of m as glycerol content increased, similar to that found in a study of the extrusion of waxy maize (Lai and Kokini, 1990). During the study of the shear viscosity of cornstarch, Willett *et al.* found that m varies slightly at different water contents (Willett et al., 1995). However, an important decrease of m was observed when the content of certain co-plasticizers was increased. In a further work, Willett and coworkers reported that m increases as the water content of waxy maize increases (Willett et al., 1998). It seems that the relationship between m and the plasticizer content is quite complex and depends on a number of parameters such as processing history, plasticizer type, and the presence of other additives.

As in the case of shear viscosity, the augmentation of the glycerol content in TPS results in a reduction of both G' and G". However, the trend in the modulus curves was nearly the same, regardless of the glycerol content. From the study of low-concentration starch dispersions, Conde-Petit and Escher showed that the formation of amylose-emulsifier complexes modifies the viscoelastic response of potato starch dispersions (Conde-Petit and Escher, 1995). Crystalline regions produced during the amylose-emulsifier complexation form an elastic network, which is responsible for the liquid-like to solid-like viscoelastic modification. From the similarity of the trend of the G' curves it can be inferred that glycerol modification does not affect the nature of the hypothetical crystalline elastic network, it just plasticizes the amorphous fraction of starch. This statement was corroborated by the comparison of X-ray diffraction patterns between TPS40 and TPS29 (Figure 5.3), where no change of the crystalline to amorphous fraction ratio occurs. It appears that crystalline regions created by the amylose-lipid complex are not uniquely responsible for the viscoelastic behavior shown by TPS

material, although it must be an important part of it as demonstrated by Della Valle *et al.* (1998) from the comparison of waxy maize and high amylose maize.

The reduction of G' at different glycerol contents was similar to that observed in starch gel systems (Kulicke et al., 1996). The reduction of the glycerol content from 40% to 33% results in a quasi-linear increment of G', while the reduction from 33% to 29% glycerol produces a larger variation in G'. In the case of the elastic modulus of polymer composites, percolation theory explains the non-linearity produced by the phase inversion effect at high filler content (Willett, 1994). The limit of glycerol plasticization that produces the non-linearity observed in the G' of TPS at a concentration around 30% glycerol can be explained in a similar way. TPS can be considered as a homogeneous system composed of a hard elastic network and soft amorphous regions. Amylose complex crystallites, highly entangled starch molecules, poorly plasticized starch-rich sites, or a combination of them could compose the hard elastic network. Soft amorphous regions could be composed of well-plasticized glycerol-rich starch. Even though the elastic network was present at 33% glycerol, the soft amorphous regions dominate the viscoelastic response. The increment of glycerol content produces a relatively small reduction in the rheological parameters. Around 30% glycerol, phase inversion occurs resulting in the domination of the viscoelastic response by the hard elastic network, which is in good agreement with percolation theory. That suggests a glycerol plasticization threshold at a concentration around 30%. A more in-depth study of starch microstructure is necessary to determine the actual components of the hard elastic network and the soft amorphous regions in TPS materials.

The real component of the viscosity ($\eta' = G''/\omega$) of PE1 and TPS40 was compared with the respective values of η_a (Figure 5.8). It is evident that PE1 obeys the Cox-Merz rule while TPS40 does not. The Cox-Merz rule indicates that η_a and η' should converge at high shear rate/frequencies (Dus and Kokini, 1990). The deviation of TPS rheological properties from the Cox-Merz rule has already been observed by other authors (Della Valle et al., 1998). It can also be inferred from the results published by Fritz and

coworkers (Aichholzer and Fritz, 1998, Ruch and Fritz, 2000). Another important result evidenced by Figure 5.8 is the inversion of the trend observed in Figure 5.1, where η_a of TPS < η_a of PE1. Deviation of TPS viscosity from the Cox-Merz rule may be the cause of this trend inversion. It appears that viscosity values measured in the capillary die (TSE) were out of the linear viscoelastic domain of TPS. In order to prove that, γ was gradually increased above the linear viscoelastic domain ($\gamma \sim 2\%$). At high γ, the G" drops giving place to a reduction of the η' (Figure 5.9). At 10 rad-sec^{-1}, for instance, η' drops from 14100 to 3109 Pa-s as γ increases from 1 to 50%. A crossover point between η_a and η' can be observed at a sufficiently high γ. That is extremely important considering that the rheological properties of TPS are fundamental for the theoretical prediction of the morphology of TPS-based blends.

8.4 Effect of processing conditions on the morphology

PE/TPS blends were prepared in the one-step extrusion process and compounded with 27% to 53% by weight of TPS. Blends were extruded through a 2.5 x 32mm rectangular die and quenched in water-cooled calendar rolls to form ribbons of about 2mm thickness. A hot-stretch ratio of approximately 2 was applied to these blends.

PE/TPS blends display a discrete morphology where LDPE is the matrix, especially at low TPS content. The combined effect of glycerol content and the elongational flow exerted on PE/TPS blends (TPS concentration ≈ 30 wt%) during quenching results in high level of deformation in the machine direction PE1 blends prepared with TPS40 and TPS36. Conversely, blends compounded with TPS29 show very little deformation (Figure 4.4c) and even less when prepared with PE2 (Figure 4.4d). The singular morphologies displayed by PE/TPS blends are closely related to the differences in viscosity of both TPS and PE. When the lower viscosity PE2 is used (Figure 4.4d), the dispersed particles of TPS are of a spherical nature and present a larger particle size than those observed in Figure 4.4c. It is apparent that the control of the glycerol concentration

allows one to modify the state of the starch from that of a solid particle to that of a quasi crosslinked dispersed phase to that of a highly deformable material.

PE1/TPS40 blends, containing 30% and 45% by weight of TPS, were prepared in the one-step extrusion system. A part of those bends was pelletized and mixed with additional PE1 to produce blends containing 1%, 10%, 30% and 45% TPS by weight. Both blends were melt drawn at different hot-stretch ratios (HSR).

PE1/TPS blends prepared in a one-step extrusion process showed a morphology consisting of a large population of small round particles dispersed around some large TPS particles that show an important deformation in the strain direction. As HSR increases, the concentration of large elliptical particles and fibers increases, which in the case of $\phi_{TPS} = 0.32$ form elongated structures with lengths of 300 μm or larger (Figure 6.1, bottom-right). Quantitative values of TPS deformation demonstrate the reduction of F values of at both volume fraction blends. However, a combination of particle deformation and fiber coalescence render this reduction more dramatic at $\phi_{TPS} = 0.32$. It is known that fiber formation is enhanced by the combination of particle coalescence and particle deformation (Gonzalez et al., 1996, Tsebrenko et al., 1989, Champagne et al., 1996, Favis and Therrien, 1991). The reduction of F values is less than expected probably due to the influence of a large population of small particles. This broad particle size distribution could potentially mask the effect of the hot stretch ratio applied onto those blends. In order to separate out the effect of particle size distribution on the response to elongational deformation, individual particle volume intervals were analyzed separately (Figure 6.3). As predicted by Taylor's theory, F is dependant on the particle size. The form factor of small particles, under 30 μm^3, appears to be unaffected by hot stretching, while particles above that interval of volume are clearly affected by hot stretching. Those results suggested that there was an onset of particle deformation at particle volumes somewhere between 20 – 30 μm^3. On the other hand, the analysis of the effect of HSR and ϕ_{TPS} on the evolution of TPS particle size blends reveals that at

ϕ_{TPS} =0.20 coalescence effects are not too evident. The values of $D_{n,equiv}$ at all HSR values seem to be the same, while the values of $D_{v,equiv}$ show a gradual increase as the HSR increases. In general, Dn is related to the total number of particles, whereas Dv is more influenced by the largest particles. The blends prepared at ϕ_{TPS} =0.32 show a dramatic increase in coalescence with HSR. At low hot stretch ratio, the particle diameters for both volume fraction blends are similar. As the hot stretch ratio is increased, significant differences in coalescence effects between the two different volume fraction blends becomes apparent. These results appear to indicate that a critical interparticle distance exists below which coalescence effects are dramatically increased.

The morphology of re-processed PE1/TPS blends is practically spherical even at all volume fractions and all HSR. The increase of TPS concentration and the drawing applied during calendaring do not appear to significantly influence the morphology in the case of re-processed blends. Quantitative evaluation of TPS deformation corroborates that the morphology of the reprocessed PE1/TPS blends is not altered by increasing neither ϕ_{TPS} nor HSR. Moreover, the evaluation of the evolution of TPS particle size shows that there is no increase of starch particle size with melt drawing at any of the volume fractions. The explanation for the reduced coalescence and the absence of deformation observed in the re-processed PE1/TPS40 blends is related to the intrinsic nature of TPS. In the first step, TPS is prepared from a former suspension of starch/glycerol/water. During the one-step process, most of water is extracted during the pass through the venting zone (at 110°C) resulting in a system composed only of starch and glycerol (Favis et al., 1999). During re-processing in the twin-screw extruder, PE1/TPS blends pass through the venting zone, which was under vacuum, at 150°C. It is probable that some glycerol is eliminated during re-processing leading to the stiffening of the TPS dispersed phase. It was shown that glycerol evaporation results in a marked increment of both storage and loss moduli of TPS (40% glycerol) measured at 150°C and at a frequency of 1Hz. Moreover, it has been observed that at high glycerol content (36% and 40% glycerol) TPS forms highly elongated particles, whereas TPS

compounded with 29% glycerol results in stiffer non deforming particles (Chapter 4). These results demonstrate that at high levels of glycerol, TPS behaves as a typical thermoplastic material demonstrating high levels of coalescence and deformation after melt drawing. At low levels of glycerol, the TPS phase behaves in a similar fashion to a partially crosslinked material and demonstrates low levels of deformation and virtually no coalescence during hot melt stretching.

8.5 Tensile properties of PE/TPS blends and fracture mechanisms

The relative Young's modulus (E/E_0) is clearly influenced by the glycerol content of the TPS dispersed phase (Figure AI.3). Addition of the softer TPS36 and TPS40 reduces E. As expected, the reduction increases as ϕ_{TPS} augmented. Conversely, the addition of the stiffer TPS29 leads to the increment of E despite the lack of interfacial adhesion. Even though PE and TPS are completely immiscible, experimental results show a better fit with the values predicted for good adhesion than those for poor adhesion. This unexpected result can be explained by a good interfacial contact. Leclair and Favis found that the compression exerted by a crystalline matrix (HDPE), during crystallization, on an amorphous dispersed phase (PC) results in good interfacial contact and a higher elastic modulus (Leclair and Favis, 1996). They also observed that the compression effect occurs when the glass transition temperature (Tg) of the dispersed phase is higher than the crystallization temperature (Tc) of the matrix. That was related to the smoothness of dispersed phase particles. LDPE has a Tc similar to HDPE, but all TPS materials show a Tg below room temperature (Figure 5.2). Nevertheless, TPS particles show similar smoothness to that of the PC in Leclair's work. The rheological properties of TPS materials have been compared to that of partially crosslinked rubber, in which the viscosity increases infinitely as the oscillatory frequency decreases (Chapter 5). Conversely, LDPE is characterized by a Newtonian plateau at low frequency. Considering that LDPE contraction during cooling is a low motion process (low frequency), LDPE/TPS viscosity and elasticity ratios must be high enough to avoid

interfacial deformation. It seems that the viscoelasticity of the dispersed phase plays an important role on the interfacial contact of immiscible polymer blends.

As expected, the relative elongation at break of PE/TPS blends decreases as ϕ_{TPS} increases. However, for PE1/TPS blends having high glycerol content, (TPS36 and TPS40) the elongation at break of the PE matrix is maintained even at high TPS loadings. Conversely, blends prepared with PE1 and the TPS29 result in less ductile materials that show a more marked decrease in ε_B. The addition of TPS29 to PE2 results in a dramatic reduction of ε_B. As observed in the stress-strain curves (Figure AI.2), PE2/TPS29 blends fail before yielding and, consequently, they present a fragile-like fracture. The $\varepsilon_B/\varepsilon_{B0}$ of PE/TPS blends is compared to Nielsen simple equations and no fit is observed. Deviation of experimental values from those theories can be related to particle-particle coalescence of the TPS dispersed phase and the final morphology displayed by those blends. In order to improve the understanding of the fracture mechanism of these immiscible polymer blends the *post mortem* internal structure of tested samples was evaluated.

PE1/TPS29 blends demonstrate a spherical morphology and ductile fracture at all ϕ_{TPS} values. Blends containing $\phi_{TPS} = 0.20$ have a morphology composed mainly of spherical particles smaller than 10μm and just a few particles ranging between 15-20 μm. Large particles were slightly ellipsoidal due to the elongational deformation experienced during melt drawing. In these blends, debonding starts at the poles of large particles. Gent and Park (1984) found that the stress required to debond a rigid particle from an elastomeric matrix increases as the size of the particle decreases. The homogeneous distribution of the applied stress allows for the debonding of small particles. At the beginning of the necking section the growth of elliptical voids is observed. A little farther, elliptical voids are transformed into sharp-ended voids due to stress hardening (position e). Those voids coalesce in the strain direction as a consequence of stretching.

The lateral coalescence of TPS particles, produced by the reduction of the cross section, gives rise to the formation of internal flaws which leads to sample failure

At increased ϕ_{TPS} (0.29) minor changes in the fracture development can be observed. However, important morphological changes, such as the increase of particle size and the broaden of the particle size distribution, are observed. The debonding process is similar to that of ϕ_{TPS} = 0.20 blends with debonding of large particles followed by that of the small ones. Void growth is also similar. However, a large quantity of internal flaws develops as a consequence of the larger particle size and the reduction of inter-particle distance. That results in the sample failure at a shorter strain than in the case of ϕ_{TPS} = 0.20 blends.

Major changes are observed at ϕ_{TPS} = 0.38. As observed at lower starch concentrations, debonding starts on large particles, but in this case it does not propagate to the small particles. Void growth is limited to the large particles that have already debonded. Crazes form at the equator of large particles and transfer to the neighboring particles leading to the sample failure at an even shorter strain.

The most extreme case of brittleness occurs with PE2/TPS29 blends. These blends do not demonstrate necking during tensile testing and result in a fragile fracture at all concentrations. Due to its low viscosity, PE2 transfers less masticating shear to the TPS29 dispersed phase than PE1. This leads to larger TPS particle sizes. The particle size distribution is also broader than in PE1/TPS29 blends. Particles having a diameter larger than 150μm can be observed. At the onset of strain effects, a catastrophic debonding of large particles takes place. This is observed as a generalized detachment of the matrix from the entire particle and is not just localized at the poles as in previous cases. As expected, debonding does not propagate to the small particles leading to a premature formation of cracks that rapidly propagate to the neighboring particles. Non-homogeneous stress transfer and premature crack propagation result in fragile fracture.

On the other hand, PE blends prepared with TPS36 and TPS40 possess a TPS phase in a fiber-like morphology. Although there is little difference in the elongation at break of PE1/TPS36 blends conditioned at 0% and 50% relative humidity (RH), important differences are observed in the *post-mortem* analysis

Morphological analysis of the undeformed region of PE1/TPS36 conditioned at 0% RH reveals a range of shapes from large fibers and ellipses to small spherical particles. In this case, the debonding process is more complex than that of spherical particles due to the combination of forces transferred from the matrix to the fibers, which results in a combination of debonding of the particle end and fiber breakup. The former is produced by the shear stresses exerted by the matrix to the fiber ends, whereas fiber breakup is the result of the tensile load applied by the PE matrix. This initial energy dissipation is reflected as a reduction of the yield stress as observed in the stress-strain curves. Closer to the necked section, voids at the end of TPS fibers are larger resembling those formed between fiber fragments. Void growth gives place to the formation of long tunnel-like cavities parallel to the strain direction. Many small crazes spreading perpendicular to the stress direction are also observed around the ends of fiber segments, especially around thick fiber or fiber conglomerations. The homogeneous void growth and the formation of many well-distributed crazes dissipate enough stress to allow for a smooth necking process. The elongational flow produced during the calendaring of PE/TPS blends permits not just the formation of long TPS particles, but also increases the transverse interparticle distance and the axial continuity of PE ligaments. Li and coworkers (1994a) have reported that the continuous ligaments formed by polymer matrices in polymeric multiphase systems carry the stress applied during tensile tension. Moreover, the thickness of such ligaments has been related to the transverse distance between dispersed phase particles (Mikhler et al., 1988). The presence of thick continuous PE filaments allows PE1/TPS36 blends to undergo stress hardening even at high TPS loading. During this process TPS fibers thin while the crazes observed on thick fiber segment ends continue growing. Fiber thinning and craze growth allow for the homogenous dissipation of the applied energy. Under further strain, crazes propagate

from the broken fibers to the neighboring particles leading to polyethylene matrix failure.

The failure history of PE1/TPS36 blends conditioned at 50% RH is similar to that described for blends conditioned at 0% RH. The debonding of fiber ends and fiber breakup also occur. Nevertheless, no crazing occurs at the ends of fiber segments during void growth. It seems that there was another mechanism of stress dissipation probably based on the moisture content-starch stiffness relationship. Water is a good plasticizer for starch (Shogren, 1993) and several authors have reported increased ductility of starch-based materials when those materials were exposed to high humidity (Shogren, 1993, Loomis et al., 1993, Van Soest et al., 1996). Based on this, the surface of TPS fiber fragments conditioned at 50% RH should flow under the action of the shear stress applied by the PE matrix instead of forming crazes as did TPS fragments conditioned at 0% RH. As in the previous case, blends conditioned at 50% RH also undergo stress hardening resulting in a reduction of the apparent diameter of TPS fiber fragments. Internal flaws appear and grow as a consequence of the stress concentrated in the vicinity of thick fibers or fiber conglomerations leading to the eventual failure of the PE matrix.

Another important difference between PE1/TPS36 blends conditioned at 0% and 50% RH is that the former demonstrates whitening in the necking section of the tensile sample while the latter always remains transparent. As in the work of Liu and Truss (1995), PE1/TPS36 blends conditioned at different RH were examined under the scope of Eyring's viscosity theory. In the present work both strain rate and testing temperature (T_{test}) are constant, however the glass transition temperature (Tg) of TPS36 is significantly affected by the conditioning humidity. TPS36 has Tg values of -56°C and -77°C when conditioned at 0% and 50% RH, respectively. This variation in Tg can be considered analogous to the increase of T_{test} in a system where Tg is constant. In both cases a difference between Tg and T_{test} can modify the fracture mechanism via the softening of dispersed phase particles. Hence, there is no craze formation and,

consequently, no stress whitening could be expected if the dispersed phase particles become soft enough to be deformed by the matrix. In such systems energy is dissipated by the plastic flow of the matrix and by the deformation of dispersed phase particles. As the difference between Tg and T_{test} decreases, the dispersed phase particles become stiffer and are incapable of flowing under the normal stress applied by the polymeric matrix. As a consequence, crazes can develop as a result of stress concentration. When crazing becomes the dominant mechanism of energy dissipation, stress whitening of tensile samples is observed.

8.6 Interfacial structure

In addition to the high ductility shown by the one-step processed LDPE/TPS blends in this work, these blends also demonstrated high levels of transparency even at high loadings of TPS. Opacity in immiscible polymer blends originates from two possible sources: different refractive indexes (η) between the two domains or scattering of light due to interfacial voids (Figure 4.11). The η has been related to the molecular arrangement and orientation of polymer chains (Seferis and Samuels, 1979). As the molecular packing increases, such as is found in crystalline structures, the η increases. In the case of semi-crystalline polymers, such as PE, the η is reported as the average between the crystalline (1.560) and amorphous (1.476) regions. The average η of PE1, considering its density (ρ = 0.920 g-cm^{-3}) should be around 1.514 (Brandrup and Immergut, 1989). Comparing that value with those determined for TPS40 and TPS36 (1.489 ± 0.001 and 1.491 ± 0.001, respectively), a difference of *ca.* 0.024 was obtained. This difference would be even smaller if amorphous LDPE was preferentially located at the interface with TPS. This difference in refractive index is similar in magnitude to the refractive index difference between water (η=1.333) (Budavari, 1989) and glass (η=1.356, glass standard #1, ASTM D542-90) and represents too small a value to result in opacity.

The other potential cause of opacity in immiscible polymer blends is the formation of microvoids at the interface resulting from poor surface adhesion and the different thermal expansion coefficients of matrix and dispersed phase. As previously discussed, PE/TPS blends display an excellent interfacial contact. This is likely due to the contraction of the semi-crystalline polyethylene about the amorphous TPS during cooling. Previous work has shown that such a contraction can significantly reduce interfacial voiding (Leclair and Favis, 1996). An argument could be raised that very small microvoids might be still present beyond the range of typical microscopic techniques. Even if very small microvoids existed at the interface, it is highly probable that a very thin glycerol layer coats the surface of TPS in these materials. Since TPS is a miscible starch/glycerol mixture and since the glycerol/PE and starch/PE surface energies are quite similar (23.17 and 23.95 mN m^{-1}, respectively) it is very likely that some low molecular weight glycerol migrates to the TPS/PE interface in order to reduce the overall surface free energy of the blend system as predicted by Harkin's equation rewritten by Hobbs and coworkers (Hobbs et al., 1988). This phenomenon would have the effect of even further reducing the optical effects due to interfacial voiding.

It is apparent from this work that a combination of excellent interfacial contact and very similar refractive index values are responsible for the high levels of transparency demonstrated by this immiscible polymer blend.

CHAPTER 9

CONCLUSIONS AND RECOMMENDATIONS

This study reports on a polymer blend material comprised of polyethylene and thermoplastic starch possessing highly unusual properties prepared using a novel one-step process. The PE/TPS blends demonstrate levels of ductility and modulus similar to the virgin polyethylene even at very high loadings of TPS without the addition of any interfacial modifier. The remarkable properties are a combination of both the melt blending process and a sophisticated morphology control. Furthermore, the material demonstrates very high levels of transparency even at 50:50 concentrations of PE/TPS.

The melt blending is carried out on the twin-screw extruder to produce ribbon extrudates and the first part of the process converts a starch-water-glycerol slurry into a virtually water-free thermoplastic starch. Polyethylene is added to the thermoplastic starch as a melt using a single-screw extruder connected midway on the twin-screw. The latter part of the twin-screw blends the two melts through intensive mixing zones. Using this approach it is possible to achieve blends where the thermoplastic starch morphology can be effectively controlled yielding a wide range of highly sophisticated morphological states.

Through a control of the glycerol content and thermoplastic starch volume fraction, the above process can result in morphological structures, which run the full range of those observed in classical blends of synthetic thermoplastics. Spherical, fiber-like and co-continuous morphologies are observed. Control of the glycerol content of the starch allows one to control the properties of starch from that of a solid filler through to that of a highly deformable thermoplastic material. A wide range of potential properties can be exploited for this type of material.

At 55:45 PE/TPS, and when the thermoplastic starch in the blend is highly continuous, the blend material at 36% glycerol content maintains 94% of the elongation at break and 76% of the modulus of polyethylene without the addition of any interfacial modifier. At a composition level of 71:29 PE/TPS for the same glycerol content, the blend retains 96% of the elongation at break and 100% of the modulus of polyethylene. These properties far surpass any results ever achieved through the addition of dry granular starch and is a remarkable result considering the high levels of immiscibility in the polar-nonpolar TPS-PE system. Even the properties in the cross direction demonstrate ductility at these high concentrations. At 36% glycerol contents in the TPS, the blend system demonstrates only very low levels of sensitivity to moisture. A high degree of transparency is maintained over the entire concentration range due to the similar refractive index of PE and TPS and the virtual absence of interfacial voiding.

The thermal and rheological properties of TPS materials prepared in a TSE were analyzed. The study of the thermal transition of TPS proved that granular starch was completely disrupted. The TPS showed a thermal transition below room temperature corresponding to the glass transition temperature and this Tg was dependent on glycerol content. Even though no thermal transition was observed above room temperature, a crystalline structure, which can be related to the complexation of amylose with lipids present in wheat starch granules, was detected by X-ray diffraction.

During rotational rheometry, TPS demonstrated an excellent thermal stability at 150°C but became unstable at temperatures above 180°C. The studies indicate however that TPS stability was maintained for short time periods for temperatures up to 200°C. These results are important since they indicate that the potential exists to prepare stable TPS materials at high temperature by maintaining short residence times during processing. The linear viscoelastic domain of TPS extended to $\gamma \sim 0.02$ due to the restricted motion imposed by the presence of an elastic network. The evaporation of glycerol leads to a gradual increase in the rheological properties of TPS due to the stiffening of TPS.

As was observed for the thermal properties, the rheological properties were also highly dependent on glycerol content. The apparent viscosity of TPS decreased 20% when the glycerol content was increased from 36 to 40%. In the same way, G' and G" also decreased as glycerol content increased. However, a particularly dramatic variation was observed when the glycerol content was varied from 29% to 33%. These latter results suggest a phase inversion from a hard elastic to soft amorphous regions. The glycerol plasticization threshold thus occurs at a content of approximately 30%.

Comparison of the shear and oscillation viscosity of TPS40 and PE1 show important differences in the viscosity ratio for this polymer pair. Under shear conditions, LDPE was more viscous than TPS while in the oscillation mode the trend is reversed. The lower shear viscosity displayed by TPS can be attributed to the very high deformation, out of the TPS linear viscoelastic domain, undergone by this material during the pass through the capillary die.

PE1 was blended with TPS in a one-step extrusion process at 150°C and then re-processed at the same temperature. Blends prepared in a one-step extrusion process behave as typical thermoplastic immiscible blends exposed to an elongational flow. Under such conditions, the TPS dispersed phase particles stretch producing a gradual increment in the form factor as HSR increases. The elongation of TPS particles leads to particle-particle coalescence in the axial direction. The particle elongation and coalescence effects are enhanced by an increase in the dispersed phase concentration. During the re-processing of PE1/TPS blends, some glycerol was extracted resulting in a stiffening of the TPS dispersed particles. This change leads to a suppression of coalescence and deformation during the melt drawing of the blends at all volume fractions.

A new methodology for the evaluation of the size of elongated particles is also developed. It is based on the form factor and allows for the comparison of classical spherical morphologies with elongated ones. From the analysis of PE1/TPS blends

prepared in a one-step extrusion process it is found that the broad particle size distribution displayed by these blends masks the effect of hot stretching on the morphology evolution. The analysis of the form factor at different intervals of particle volume give more precise information concerning the influence of HSR on the morphology. In blends prepared in a one step process, it appears that a minimum volume for the TPS particle of 20 - 30μm^3 is required for deformation to occur.

The elongational flow exerted during melt drawing is highly effective at deforming the TPS phase in blends prepared in a one-step extrusion process but not for re-processed ones. On the other hand, the elongational flow produced by changes in channel sections during die extrusion results in longitudinal deformation for both one-step processed and re-processed PE1/TPS blends.

Control of the glycerol content either at the onset of the two-step process or through controlled glycerol evaporation (use of melt seals, selective venting) can thus allow for the obtention of a dispersed phase that runs the full range from solid particle to fully thermoplastic material. The morphological versatility of such a system, in the absence of any necessary chemical reactions or interfacial modifier, is unmatched in the entire polymer blend literature.

PE/TPS blends (compounded with 36% and 40% glycerol) prepared in a one-step process display unusually high ductility. Blends prepared with the high viscosity PE1 and TPS29 were not only ductile but also show an important increase of E with respect to pure PE. Conversely, blends prepared with the same TPS29 and the low viscosity PE2 demonstrate significantly lower elongations at break over a range of ϕ_{TPS}.

Experimental data from tensile tests were compared with theoretical models. Takayanagi's equation for good adhesion gives a good prediction of E. This is unexpected considering the high interfacial tension that should exist between a polar (TPS) and a non-polar polymer (PE). The high modulus can be explained by the good

interfacial contact produced by the compression exerted by the PE matrix, during its crystallization, on the TPS dispersed phase. Stress and elongation at break are compared to some simple models, which only depend on ϕ_{TPS}. In those cases the experimental data do not fit the models since they do not consider the morphology changes related to particle-particle interaction during melt blending. The *post mortem* evaluation of tensile tested samples reveals how particle size and particle size distribution influence the fracture mechanisms of PE/TPS blends. The influence of humidity on the energy dissipation mechanism is also demonstrated. Blends conditioned at 0% RH have an energy dissipation mechanism based on craze formation which was characterized by stress whitening in the neck. Conversely, blends conditioned at 50% RH remain transparent after tensile testing because craze formation was replaced by the deformation of dispersed phase surface (shear yielding) as an energy dissipation mechanism.

From the evaluation of the *post mortem* microstructure, a series of fracture mechanisms dependent on blend morphology are proposed. The mechanisms are composed of three stages: debonding, void growth and failure. The completion of generalized debonding is mainly dependent on particle size and particle size distribution effects. Smooth void growth can be achieved when the stress is homogeneously distributed to all dispersed particles during debonding. This is achieved with a homogeneous distribution of small particles. The extent of void growth depends primarily on the thickness of matrix filaments which is related to the interparticle distance. Tensile failure depends on the completion of debonding or the extent of void growth.

The combination of the different structures observed in this work suggest the possibility of property tailoring via morphology control and glycerol content. Highly ductile materials can be obtained by a combination of fiber formation and unidirectional orientation during hot stretching. While a good balance of ductility and modulus can be attained with well-dispersed spherical particles.

Considering the significantly lower cost of starch as compared to polyethylene, this material represents a serious potential route towards polyethylene replacement. Furthermore the material has the added benefit of containing large quantities of a renewable resource. Since the starch can be fully interconnected through morphology control, it is also completely accessible for biodegradation.

REFERENCES

ABURTO, J., THIEBAUD, S., ALRIC, I., BORREDON, E., BIKIARIS, D., PRINOS, J. and PANAYIOTOU, C. (1997). Properties of Octanoated Starch and its Blends with Polyethylene. *Carbohyd. Polym.*, 34, 101-112.

AICHHOLZER, W. and FRITZ,H.-G. (1998). Rheological Characterization of Thermoplastic Starch Materials. *Starch/Stärke*, 50, 77-83.

ALLEN, G. (1985). *Polymer*, 26, 1248

ARENDS, C.B. (1992). Percolation in Injection molding Polymer Blends. *Polym. Engng. Sci.*, 32 (13), 841-844.

AVEROUS, L., MORO, L., DOLE, P. and FRINGANT, C. (2000a). Properties of Thermoplastic Blends: Starch-Polycaprolactone. *Polymer*, 41, 4157-4167.

AVEROUS, L., FAUCONNIER, N., MORO, L. and FRINGANT, C. (2000b). Blends of Thermoplastic Starch and Polyesteramide: Processing and Properties. *J. Appl. Polym. Sci.*, 76, 1117-1128.

AVEROUS, L. FRINGANT, C. and MORO, L. (2001a). Plasticized starch-cellulose interactions in polysaccharide composites. *Polymer*, 42, 6565-6572.

AVEROUS, L. and FRINGANT, C. (2001b). Association between Plasticized Starch and Polyesters: Processing and Performance of Injected Biodegradable Systems. *Polym. Engng. Sci.*, 45 (5), 727-734.

AVEROUS, L., DOLE, P., MARTIN, O., SCHWACH, E. and COUTURIER, Y. (2001c). Étude de mélanges: polyesters biodégradables-amidon plastifié, *Symposium de la société Polymérique du Québec*, Nancy, France, (Poster).

AVGEROPOULOS, G. N., WEISSERT, F. C., BIDDISON, P. H. and BÖHM, G. C. A. (1975). *Rubber Chemistry and Technology*, 49, 93.

BAINS, M., RESHADAT, R., LEW, R., CLUETT, W.R., BALKE, S.T. and HALL, J.W. (1994). Quantitative near-infrared monitoring of polyethylene-polypropylene melt blending. *Proceedings of the 52nd Annual Technical Conference ANTEC 94*, part 2 (of 3), 2227-2229.

BAIRD D.G. and LABROPOULOS A.E. (1982). Invited Review: Food Dough Rheology. *Chem. Eng. Commun.*, 15, 1-25.

BALKE, S.T., HU, J., JOSEPH, S., KARAMI, A., SALERNI, R., PLANETA, M., SUHAY, J. and TAMBER, H. (1998). Polymer and particle separation during extrusion. *Proceedings of the 56th Annual Technical Conference ANTEC 98*, part 1 (of 3), 205-209.

BAZHENOV, S., LI, J.X., HILTNER, A. and Baer, E. (1994). Ductility OF Filled Polymers, *J. Appl. Polym. Sci.*, 52, 243-254.

BIKIARIS, D., PRINOS, J. and PANAYIOTOU, C. (1997a). Effect of EAA and Starch on the Thermooxidative Degradation of LDPE. *Polym. Degrad. Stab.*, 56, 1-9.

BIKIARIS, D., PRINOS, J. and PANAYIOTOU, C. (1997b). Effect of Methyl Methacrylate-Butadiene Styrene Copolymer on the Thermooxidation and Biodegradation of LDPE/Plasticized Starch Blends. *Polym. Degrad. Stab.*, 58, 215-228.

BIKIARIS, D., PRINOS, J., KOUTSOPOULOS, K., VOUROUTZIS, N., PAVLIDOU, E., FRANGIS, N. et PANAYIOTOU, C. (1998). LDPE/Plasticized Starch Blends Containing PE-g-MA Copolymer as Compatibilizer. *Polym. Degrad. Stab.*, 59, 287-291.

BOURRY, D., and FAVIS, B. D. (1997). Morphology development in a polyethylene/polystyrene binary blend during twin-screw extrusion. *Polymer*, 39 (10), 1851-1856.

BOURRY, D., and FAVIS, B. D. (1998). Cocontinuity and phase inversion in HDPE/PS blends: influence of interfacial modification and elasticity. *J. Polym. Sci. Polym. Phys.*, 36, 1889-1899.

BRANDRUP J. and IMMERGUT E.H. (1989). *Polymer Handbook*, 3rd ed.: John Wiley.

BUDAVARI S. (1989). *The Merck Index*, Eleventh ed. New Jersey: Merck & Co., Inc.

CHAMPAGNE, M.F., DUMOULIN, M.M. and UTRACKI, L.A. (1996). Generation of Fibrillar Morphology in Blends of Block Copolyetheresteramide and Liquid Crystal Polyester. *Polym. Engng. Sci.*, 36 (12), 1636-1646.

CHANDRA, R. and RUSTGI, R. (1997). Biodegradation of Maleated Linear Low-Density Polyethylene and Starch Blends. *Polym. Degrad. Stabil.*, 56, 185-202.

CHAPLEAU, N. and FAVIS, B.D. (1995). Droplet/fiber transition in immiscible polymer blends generated during melt processing. *J. Mater. Sci.*, 30, 142-150.

CHEN, J., HAHN, P.S. and SLATTERY, J.C. (1984). *AICHE J.*, 30, 622.

CHEUNG, P.C. and BALKE, S.T. (1997). Reactive Extrusion of Polypropylene/Polyethylene Blends: Kinetic Model Development. *Ind. Eng. Chem. Res.*, 36, 1191-1201.

CONDE-PETIT, B. and ESCHER, F. (1995). Complexation Induced Changes of Rheological Properties of Starch Systems at Different Moisture Levels. *J. Rheol.*, 39 (6), 1497-1518.

COULALOGLOU, C.A. and TAVLARIDES, L.L. (1977). Description of the interaction processes in agitated liquid-liquid dispersions. *Chem. Eng. Sci.*, 32 (11), 1289-1297.

COX, R.G. (1969). The deformation of a drop in a general time-dependent fluid flow. *J. Fluid Mech.*, 37, 601-623.

DAVID, B., KOZLOWISKI, M. and. TADMOR, Z. (1993). *Polym. Eng. Sci.*, 33, 227.

DEHENNAU, C. et DEPIREUX, T. (1993). Composition à base d'amidon. *European Patent* EP 0 554 939 A2

DELLA VALLE, G., VERGNES, B. and TAYEB, J. (1992). Mesure de la viscosité d'amidons fondus faiblement hydratés dans un nouveau rhéomètre en ligne. *Entropie*, 169, 59-63.

DELLA VALLE, G., BULEON, A., CARREAU, P.J., LAVOIE, P.-A. and VERGNES, B. (1998). Relationship Between Structure and Viscoelastic Behavior of Plasticized Starch. *J. Rheol.*, 42 (3), 507-525.

DESA, S., CLUETT, W.R., BALKE, S.T. and HORN, J.T. (1995). Quality monitoring of recycled plastic waste during extrusion: II. In-line particle detection. *Proceedings of the 53rd Annual Technical Conference ANTEC 95*, part 2 (of 3), 2062-2065.

DOANE, W.M., SWANSON, C.L. and FANTA, G.F. (1992). Emerging Polymeric Materials Based on Starch. *Emerging Technologies for Materials and Chemicals from Biomass*, R.M. Rowell, T.P. Schultz, and R. Narayan, American Chemical Society, 197-230.

DONOVAN, J.W. (1979). Phase Transitions of the Starch-Water System. *Biopolymers*, 18, 263-275.

DUS, S.J. and KOKINI, J.L. (1990). Prediction of the Nonlinear Viscoelastic Properties of a Hard Wheat Flour Dough Using the Bird-Carreau Constitutive Model. *J. Rheol.*, 34 (7), 1069-1084.

ELMENDORP, J.J. (1986). A study on polymer blending microrheology. *Polym. Engng. Sci.*, 26 (6), 418-426.

ELMENDORP, J.J. and VAN DER VEGT, A.K. (1986). *Polym. Engng. Sci.*, 26 (19), 1322-1328.

ELMENDORP, J.J. (1991). Dispersive Mixing in Liquid Systems. *Mixing in Polymer Processing*, C. Rauwendaal, Marcel Dekker, Inc. Chapter 2.

EVANGELISTA, R.L. et al., *Ind. Eng. Chem. Res.*, 30, 1841, 1991.

EVERAERT, V., AERTS, L. and GROENINCKX, G. (1999). Phase morphology development in immiscible PP/(PS/PPE) blends influence of the melt-viscosity ratio and blend composition. *Polymer*, 40 (24), 6627-6644.

FANTA, G.F., SWANSON, C.L. and DOANE, W.M. (1990). Composites of Starch and Poly(ethylene-co-acrylic acid). Complexing between Polymeric Components. *J. Appl. Polym. Sci.*, 40 (5-6), 811-821.

FANTA, G.F., SWANSON, C.L. and SHOGREN, R.L. (1992). Starch Poly(ethylene-co-Acrilic Acid) Composite Films. Effect of Processing Conditions on Morphology and Properties. *J. Appl. Polym. Sci.*, 44, 2037-2042.

FAVIS, B.D. and CHALIFOUX, J.P. (1987). The Effect of the Viscosity Ratio on the Morphology of Polypropylene/Polycarbonate Blends During Processing. *Polym. Engng. Sci.*, 27 (20), 1591-1600.

FAVIS, B.D. and CHALIFOUX, J.P. (1988). Influence of Composition on the Morphology of Polypropylene/Polycarbonate Blends. *Polymer*, 29, 1761-1767.

FAVIS, B.D. and THERRIEN, D. (1991). Factors influence structure formation and phase size in an immiscible polymer blend of polycarbonate and polypropylene prepared by twin-screw extrusion. *Polymer*, 32 (8), 1474-1483.

FAVIS, B.D. (1991). Polymer Alloys and Blends: Recent Advances. *Can. J. Chem. Eng.*, 69, 619-625.

FAVIS, B .D. (1992). *Makromol. chem. Macromol. symp.*, 56, 143.

FAVIS, B.D., RODRIGUEZ, F. and RAMSAY, B.A. (1999). Polymer Compositions Containing Thermoplastic Starch and Process of Making. *US Patent Appl.* No. 09/472,242.

FAVIS, B.D. (2000). Factors Influencing the Morphology of Immiscible Polymer Blends in Melt Processing. *Polymer Blends*, D. Paul and C. Bucknall, Wiley-Interscience, Chapter 16.

FLETCHER, S.I., MCMASTER, T.J., RICHMOND, P. and SMITH, A.C. (1985). Rheology and Extrusion Of Maize Grits. *Chem. Eng. Commun.*, 32, 239-262.

FLUMERFELT, R.W. (1980). Effect of dynamic interfacial properties on drop deformation and orientation in shear and extensional flow fields. *J. Colloid Interfac. Sci.*, 76, 330-.

FORTELNY, I. and KOVAR, J. (1989). *Eur. Polym. J.*, 25, 317.

FORTELNY, I. and KOVAR, J. (1992). Effect of the composition and properties of components on the phase structure of polymer blends. *Eur. Polym. J.*, 28, 85-90.

FORTELNY, I., CERNA, Z., BINKO, J., KOVAR, J. (1993). *J. Appl. Polym. Sci.*, 48, 1731.

FRENCH, D. (1984). *Starch Chemistry and Technology*, Academic Science, New York.

FRITZ, H.G., AICHHOLZER, W., SEIDENSTÜCKER, T. und WIDMANN, B. (1995). Abbaubare polymerwerkstoffe auf der basis nachwachsender rohstoffe- mölichkeiten und grenzen. *Starch/Stärke*, 47, 475-491.

GENT, A.N. and PARK, B. (1984). *J. Mater. Sci.*, 19, 1947.

GHODGAONKAR, P. G. and SUNDARARAJ, U. (1996). *Polym. Eng. Sci.*, 36, 1656.

GOMEZ, M.H. and AGUILERA, J.M. (1983). Changes in the Starch Fraction during Extrusion-Cooking of Corn. *J. Food Sci.*, 48, 378-381.

GOMEZ, M.H. and AGUILERA, J.M. (1984). A Physicochemical Model for Extrusion of Corn Starch. *J. Food Sci.*, 49, 40-43.

GONZALEZ-NUNEZ, R., FAVIS, B.D., CARREAU, P.J. and LAVALLÉE, C. (1993). Factors Influencing the Formation of Elongated Morphologies in Immiscible Polymer Blends During Melt Processing. *Polym. Engng. Sci.*, 33 (13), 851-859.

GONZALEZ-NUNEZ, R., DE KEE, D. and FAVIS, B.D. (1996). The influence of coalescence on the morphology of the minor phase in melt drawn polyamide-6/HDPE blends. *Polymer*, 37 (21), 4689-4693.

GRACE, H.P. (1982). Dispersion phenomena in high viscosity immiscible fluid systems and application of static mixers as dispersion devices in such systems. *Chem. Eng. Commun.*, 14 (3-6), 225-277.

GRIFFITH, G.J.L. (1977). Synthetic Resin Sheet Material. *US Patent* 4 021 388.

HOBBS, S.Y., DEKKERS, M.E.J. and WATKINS W.H. (1988). *J. Mater. Sci.*, 23, 1219.

HSU, W. Y. and WU, S. (1993). Percolation behaviour in morphology and modulus of polymer blends. *Polym. Eng. Sci.*, 33, 293-302.

JEELANI, S.A.K. and HEARTLAND, S. (1991). *Chem. Eng. Sci.*, 46, 1807.

JORDHAMO, G. M., MANSON, J. A. and SPERLING, L. H. (1986). Phase continuity and inversion in polymer blends and simultaneous interpenetrating networks. *Polym. Eng. Sci.*, 26, 517-524

JORGENSEN, J.L. and UTRACKI, L.A. (1991). Dual phase continuity in polymer blends. *Makromol. Chem., Macromol. Symp.*, 48/49, 189.

KALICHEVSKY, M.T., JEROSZKIEWICZ, E.M. and BLANSHARD, J.M.V. (1993). A study of the glass transition of amylopectin-sugar mixtures. *Polymer*, 34 (2), 346-358.

KARAMI, A. and BALKE, S. (2000). Polymer Blend De-mixing and Morphology Development of Immiscible Polymer Blends During Tube Flow. *Polym. Engng. Sci.*, 40 (11), 2342-2355.

KELNAR, I., STEPHAN, M., JAKISCH, L., JANATA, M. and FORTELNY, I. (2001). Compatibilization of PA6/PPO Blends with Carboxylated Poly(styrene) Compounds. *J. Appl. Polym. Sci.*, 80, 2273-2280.

KIM, Y.J., LEE, H.M. and PARK, O.O. (1995). Processability and Mechanical Properties of Surlyn-Treated Starch/LDPE Blends. *Polym. Engng. Sci.*, 35 (20), 1652-1657.

KULICKE, W.M., EIDAM, D., KATH, F., KIX, M. and KULL, A.H. (1996). Hydrocolloids and Rheology: Regulation of Vico-elastic Characteristics of Waxy Rice Starch in Mixtures with Galactomannans. *Starch/Stärke*, 48 (3), 105-114.

KUNORI, T. and GEIL, P.H. (1980a). Morphology-Property Relationship in Polycarbonate-Based Blends. I. Modulus. *J. Macromol. Sci.-Phys.*, B18 (1), 93-134.

KUNORI, T. and GEIL, P.H. (1980b). Morphology-Property Relationship in Polycarbonate-Based Blends. II. Tensile and Impact Strength. *J. Macromol. Sci.-Phys.*, B18 (1), 135-175.

LAI, L.S. and KOKINI, J.L. (1990). The Effect of Extrusion Operating Conditions on the On-Line Apparent Viscosity of 98% Amylopectin (Amioca) and 70% Amylose (Hylon 7) Corn Starches during Extrusion. *J. Rheol.*, 34 (8), 1245-1266.

LAI, L.S. and KOKINI, J.L. (1991). Physicochemical Changes and Rheological Properties of Starch during Extrusion (A Review). *Biotechnol. Prog.*, 7, 251-266.

LAWTON, J.W. and FANTA, G.F. (1994). Glycerol-plasticized films from starch-poly(vinyl alcohol) mixtures: effect of poly(ethylene-co-acrylic acid). *Carbohydr. Polym.*, 23, 275-280.

LEIDNER, J. and WOODHAMS, R.T. (1974). Strength of Polymer Composites Containing Spherical Fillers. *J. Appl. Polym. Sci.*, 18 (6): 1639.

LEVITT, L. and MACOSKO, C. W. (1996). *Polym. Eng. Sci.*, 36, 1647.

LECLAIR, A. and FAVIS, B.D. (1996). The role of interfacial contact in immiscible binary polymer blends and its influence on mechanical properties. *Polymer*, 37 (21), 4723-4728.

LI J., MA P.L. and FAVIS B.D. (2002). The role of the blend interface type on morphology in co-continuous polymer blends. *Macromolecules*, 35 (6), 2005-2016.

LI, J.X., HILTNER, A. and BAER, E. (1994a). Fractography and Failure Mechanisms of Particulate-Filled Thermoplastic Polyester. *J. Appl. Polym. Sci.*, 52, 269-283.

LI, J.X., TWIGG, M.V., HILTNER, A. and BAER, E. (1994b). PVC/MBS Blends with Small Concentrations of PET: Failure Process in Thin Films During Uniaxial Tension. *J. Appl. Polym. Sci.*, 52, 285-299.

LIEM, A.J.S. and WOODS, D.R. (1974). *A.I.C.H.E. Symp. Ser.*, 144, 70.

LIU, Y. and TRUSS, R.W. (1995). Tensile Yielding and Microstructures of Blends of Isotactic Polypropilene and Linear Low-Density Polyethylene. *J. Polym. Sci. Polym. Phys.*, 33, 813-822.

LOOMIS, G.L., HOPKINS, A.R. and GEORGE, E.R. (1993). Starch-Based Materials. *Biodegradable Polymers and Packaging.* C.T.K. Ching, D.L. Kaplan and E.L. Thomas; Lancaster PA: Technomic Publishing Co., 43-51.

LOURDIN, D., BIZOT, H. and COLONNA P. (1997). "Antiplasticization" in Starch-Glycerol Films? *J. Appl. Polym. Sci.*, 63, 1047-1053.

LOVINGER, A.J. and WILLIAMS, M.L. (1980). Tensile Properties and Morphology of Blends of Polyethylene and Polypropylene. *J. Appl. Polym. Sci.*, 25, 1703-1713.

LUCIANI, A. and JARRIN, J. (1996). Morphology Development in Immiscible Polymer Blends. *Polym. Engng. Sci.* 36 (12), 1619-1626.

MAITI, S.N. and MAHAPATRO, P.K. (1991). Mechanical Properties of I-PP/$CaCO_3$ Composites. *J. Appl. Polym. Sci.*, 42, 3101-3110.

MARGOLINA, A. and WU, S. (1988). Percolation model for brittle-tough transition in nylon/rubber blends. *Polymer*, 29, 2170-2173.

MARGOLINA, A. (1990). *Polym. Commun.*, 31, 95.

MARTIN, O. and AVEROUS, L. (2001). Poly(Lactic Acid): Plasticization and Properties of Biodegradable Multiphase Systems. *Polymer*, 42, 6209-6219.

METELKIN, V.I. and BLEKHT, V.S. (1984). *Colloid J. USSR*, 46, 425.

MIKHLER, G., TOVMASYAN, Yu-M., TOPOLKARAEV, V.A., DUBNIKOVA, I.L. and SHMIDT, V. (1988). Deformation structure of the crazing type in a dispersion-filled polyethylene. *Mech. Compos. Mater.*, 24 (2), 167-175.

MILES, I. S. and ZUREK, A. (1988). Preparation, structure, and properties of two phase co-continuous polymer blends. *Polym. Eng. Sci.*, 28, 796-805.

MIROSHNIKOV, Y.P., GOL'MAN, A.M. and KULEZNEV, V.N. (1979). *Kolloid Zh.*, 41, 1120.

NIELSEN, L.E. (1966). Simple Theory of Stress-Strain Properties of Filled Polymers. *J. Appl. Polym. Sci.*, 10, 97-103.

NIELSEN, L.E. (1974) *Mechanical Properties Of Polymers And Composites*, New York: Marcel Dekker, (chapters 7, 8).

OTEY, F.H. WESTHOFF, R.P. and DOANE, W.M. (1980). Starch-Based Blown Films. *Ind. Eng. Chem. Prod. Res. Dev.*, 19, 592-595.

OTEY, F.H. and WESTHOFF, R.P. (1982). Biodegradable Starch-Based Blown Films, *US Patent* 4,337,181.

OTEY, F.H. WESTHOFF, R.P. and DOANE, W.M. (1987). Starch-based Blown Films. 2, *Ind. Eng. Chem. Res.*, 26, 1659-1663.

PABEDINSKAS, A., CHEUNG, P. and BALKE, S.T. (1994). Modeling of Polypropylene degradation during Reactive Extrusion with Implications for Process Control. *Polym. Engng. Sci.*, 34, 598.

PAKULA, T., GREBOWICZ, M. and KRYZEWSKI, M. (1980). *Polym. Bull.*, 2, 799-.

PAUL, D. P. and BARLOW, J. W. (1980). *J. Makromol. Sci. Rev. Macromol. Chem.*, C18, 109.

PEANASKY, J.S., LONG, J.M. and WOOL, R.P. (1991). Percolation Effects in Degradable Polyethylene-Starch Blends. *J. Polym. Sci.: Part B: Polym. Phys.*, 29, 565-579.

PIGGOTT, M.R. and LEIDNER, J. (1974). Misconceptions About Filled Polymers. *J. Appl. Polym. Sci.*, 18 (6), 1619-1623.

PRINOS, J., BIKIARIS, D., THEOLOGIDIS, S. and PANAYIOTOU, C. (1998). Preparation and Characterization of LDPE/Starch Blends Containing Ethylene/Vinyl Acetate Copolymer as Compatibilizer. *Polym. Engng. Sci.*, 38 (6), 954-964.

PSOMIADOU, E., ARVANITOYANNIS, I., BILIADERIS, C.G., OGAWA, H. and KAWASAKI, N. (1997). Biodegradable Films Made from Low Density Polyethylene (LDPE), Wheat Starch and Soluble Starch for Food Packaging Applications. Part 2. *Carbohydr. Polym.*, 33, 227-242.

RAMSAY, B.A., LANGLADE, V., CARREAU, P.J. AND RAMSAY, J.A. (1993). Biodegradability and Mechanical Properties of Poly-(β-Hydroxybutyrate-Co-β-Hydroxyvalerate)-Starch Blends. *Appl. Environ. Microbiol.*, 59 (4), 1242-1246.

RATTO, J.A., STENHOUSE, P.J., AUERBACH, M., MITCHELL, J. and FARRELL, R. (1999). Processing, Performance and Biodegradability of a Thermoplastic Aliphatic Polyester/Starch System. *Polymer*, 40, 6777-6788.

RAYLEIGH, J. W. S. (1879). *Proc. London Math. Soc.*, 10, 4.

REDL, A., MOREL, M.H., BONICEL, J., GUILBERT, S. and VERGNES, B. (1999). Rheological Properties of Gluten Plasticized with Glycerol: Dependence on Temperature, Glycerol Content and Mixing Conditions. *Rheol. Acta*, 38, 311-320.

RESHADAT, R., CLUETT, W.R., BALKE, S.T. and HALL, J.W. (1995). Quality monitoring of recycled plastic waste during extrusion: I. In-line near infrared spectroscopy. *Proceedings of the 53rd Annual Technical Conference ANTEC 95*, part 2 (of 3), 2057-2061.

RIZZO, G. and SPADARO, G. (1984). Necking Behavior of Low-Density Polyethylene-Isotactic Polypropylene Blends: A Morphological Investigation. *Polym. Engng. Sci.*, 24 (4), 264-267.

RODRIGUEZ-GONZALEZ, F.J., RAMSAY B.A. and FAVIS B.D. (1999). Low Density Polyethylene/Thermoplastic Starch Blends: Effect of Glycerol Content and LDPE Concentration on Morphology and Tensile Properties in the Dual Phase Continuity Region. *Proceedings of the Annual Technical Conference ANTEC'99*, vol.57, no.2, 2770-2774.

RODRIGUEZ-GONZALEZ, F.J., RAMSAY B.A. and FAVIS B.D. (2001a). *Proceedings of Seventeenth Annual Meeting of Polymer Processing Society*, Montreal (Canada). 312-319.

RODRIGUEZ-GONZALEZ, F.J., VIRGILIO, N., RAMSAY B.A. and FAVIS B.D. (2001b). Melt Drawing of LDPE/Thermoplastic Starch Blends. *Proceedings of the Annual Technical Conference ANTEC'01*, vol.59, 2354-2358.

RODRIGUEZ-GONZALEZ, F.J., RAMSAY, B.A. and FAVIS, B.D. (2002a). High Performance LDPE/Thermoplastic Starch Blends: A Sustainable Alternative to Pure Polyethylene. *Submitted to Polymer.*

RODRIGUEZ-GONZALEZ, F.J., RAMSAY, B.A. and FAVIS, B.D. (2002b). Study of the Rheological and Thermal Properties of Thermoplastic Starch. *Submitted to Polymer.*

RODRIGUEZ-GONZALEZ, F.J., VIRGILIO, N., RAMSAY, B.A. and FAVIS, B.D. (2002c). The Influence of Melt Drawing on the Morphology of One and Two-Step Processed LDPE/Thermoplastic Starch Blends. *Submitted to Adv. Polym. Technol.*

ROLAND, C.M. and BÖHM, G.G.A. (1984). *J. Polym. Sci., Polym. Phys. Ed.*, 22, 79.

ROSS-MURPHY, S.B. (1995). Structure-Property Relationship in Food Biopolymer Gels and Solutions. *J. Rheol.*, 39 (6), 1451-1463.

RUCH, J. and FRITZ, H.G. (2000). Phase Morphology and Material Properties of Polymer Blends Including Thermoplastic Starch. *Proceedings of Sixteenth Annual Meeting of Polymer Processing Society*, Shanghai, China, pg. 350-351.

RUMSCHEIDT, F.D. and MASON, S.G. (1961). *J. Colloid Sci.*, 16, 238.

SATO, Y. and FURUKAWA, J. (1963). *Rubber Chem. Technol.*, 36, 1081.

SEFERIS J.C. and SAMUELS R.J. (1979). Coupling of Optical and Mechanical Properties in Crystalline Polymers. *Polym. Engng. Sci.*, 19 (14), 975-994.

SENOUCI, A. and SMITH, A.C. (1988). An Experimental Study of Food Melt Rheology. I. Shear Viscosity Using a Slit Die Viscometer and a Capillary Rheometer. *Rheol. Acta*, 27, 546-554.

SERPE, G., JARRIN, J. and DAWANS, F. (1990). *Polym. Engng. Sci.*, **30**, 553.

SHI, B. and SEIB, P.A. (1995). Effects of Poly(Ethylene Glycol) and Relative Humidity on the Physical Properties of Commingled Molecules of Starch and Poly(Ethylene-Co-Acrylic Acid), *Proc. ACS Div. Polym. Mater. Sci. and Engng.*, Proceeding of the 1995 Spring ACS meeting, v 72, 188-189.

SHOGREN, R.L., THOMPSON, A.R., GREENE, R.V., GORDON, S.H. and COTE, G. (1991a). Complexes of Starch Polysaccharides and Poly(ethylene-co-acrylic acid). Structural Characterization in the Solid State. *J. Appl. Polym. Sci.*, 42 (8), 2279-2286.

SHOGREN, R.L., GREENE, R.V. and WU, Y.V. (1991b). Complexes of Starch Polysaccharides and Poly(ethylene-co-acrlylic acid). Structure and Stability in Solution, *J. Appl. Polym. Sci.*, 42 (6), 1701-1709.

SHOGREN, R.L., THOMPSON, A.R., FELKER, F.C., HARRY-O'KURU, R.E., GORDON, S.H., GREENE, R.V. and GOULD, J.M. (1992). Polymer Compatibility and Biodegradation of Starch-Poly(ethylene-co-acrylic acid)-Polyethylene Blends. *J. Appl. Polym. Sci.*, 44, 1971-1978.

SHOGREN, R.L. (1993). Effect of Moisture and Various Plasticizers on the Mechanical Properties of Extruded Starch. *Biodegradable Polymers and Packaging*. C.T.K. Ching, D.L. Kaplan and E.L. Thomas; Lancaster PA: Technomic Publishing Co., 141-150.

SLADE, L. and LEVINE, H. (1987). Collagen as a Food. *Advances in Meat Research*. Pearson AM, Dutson TR and Bailey A, New York: Van Nostrand Reinhold. vol 4.

SLADE, L., LEVINE, H. and FINLEY, J.W. (1988). *Protein Quality and the Effect of Processing*. Phillips, D. and Finley J.W. New York, Marcel Dekker.

SMITH T.L. (1959). *Trans. Soc. Rheol.*, 3, 113.

SMOLUCHOWSKI, M. (1916). *Physik. Z.*, **17**, 557.

SMOLUCHOWSKI, M. (1917). *Z. Phys. Chem.*, 92, 129-.

ST-PIERRE, N., FAVIS, B.D., RAMSAY, B.A., RAMSAY, J.A. and VERHOOGT, H. (1997). Processing and Characterization of Thermoplastic Starch/Polyethylene Blends. *Polymer*, 38 (3), 647-655.

STAUFFER, D. (1979). Scaling theory of percolation clusters. *Physics Report*, 54, 1. (1980)

STENHOUSE, P.J., MAYER, J.M., HEPFINGER, M.J., COSTA, E.A., DELL, P.A. and KAPLAN, D.L. (1993), Starch-Based Blown Films. *Biodegradable Polymers and Packaging*. C.T.K. Ching, D.L. Kaplan and E.L. Thomas; Lancaster PA: Technomic Publishing Co., 151-158.

STONE, H.A., BENTLEY, B.J. and LEAL, L.G. (1986). An experimental study of transient effects in the breakup of viscous drops. *J. Fluid Mech.*, 173, 131-158.

SUNDARARAJ, U. and MACOSKO, C.W. (1995). Drop breakup and coalescence in polymer blends: the effects of concentration and compatibilization. *Macromolecules*, 28 (8), 2647-2657.

SUWANDA, D., LEW, R. And BALKE, S.T. (1988a). Reactive Extrusion of Polypropylene I: Controlled Degradation. *J. Appl. Polym. Sci.*, 35, 1019.

SUWANDA, D., LEW, R. And BALKE, S.T. (1988b). Reactive Extrusion of Polypropylene II: Degradation Kinetic Modeling. *J. Appl. Polym. Sci.*, 35, 1033.

SUWANDA, D. and BALKE, S.T. (1993). The Reactive Modification of Polyethylene. II: Mathematical Modeling. *Polym. Engng. Sci.*, 33, 1592.

TANNA, S.T., GROSS, R. and MCCARTHY, S.P. (1992). Biodegradation of Bacterial Polyester and Starch in a Compost Environment. *Proc. ACS Div. Polym. Mater. Sci. and Engng.*, Aug 23-27 Washington, DC, USA, 294-295.

TAYLOR, G.I. (1932). The viscosity of a fluid containing small drops of another fluid *Proc. Roy. Soc.*, A138, 41-48.

TAYLOR, G.I. (1934). The formation of emulsions in definable fields of flow. *Proc. Roy. Soc.*, A146, 501-523.

TOKITA, N. (1977). Analysis of Morphology Formation in Elastomer Blends. *Rubber Chem. Tech.*, 50, 292-300.

TOMOTIKA, S. (1935). On the stability of cylindrical thread of a viscous liquid surrounded by another viscous fluid. *Proc. Roy. Soc. London*, A150, 322-337.

TSEBRENKO, M.V., DANILOVA, G.P. and MALKIN, A.Y. (1989). *J. Non-Newtonian Fluid Mech.*, 31, 1.

UEMURA, S. and TAKAYANAGI, M.J. (1966). Application of the Theory of Elasticity and Viscosity of Two-Phase Systems to Polymer Blends. *J. Appl. Polym. Sci.*, 10, 113-125.

UTRACKI, L.A. (1989). *Polymer Alloys and Blends: thermodynamics and rheology*, Hanser.

UTRACKI, L.A. (1991). On the viscosity-concentration dependence of immiscible polymer blends. *J. Rheol.*, 35 (8), 1615-1637.

VAN GISBERGEN, J. (1991). PhD Thesis, Eindhoven University of Technology, Eindhoven, The Netherlands.

VAN OENE, H. (1972). Modes of dispersion of viscoelastic fluids in flow. *J. Colloid Interface Sci.*, 40, 448-467.

VAN SOEST, J.J., WIT, D. DE and VLIEGENTHART, J.F.G. (1996). Mechanical Properties of Thermoplastic Waxy Maize Starch. *J. Appl. Polym. Sci.*, 61, 1927-1937.

VAN SOEST, J.J.G. and BORGER, D.B. (1997). Structure and Properties of Compression-Molded Thermoplastic Starch Materials from Normal and High-Amylose Maize Starches. *J. Appl. Polym. Sci.*, 64, 631-644.

VERHOOGT, H., TRUCHON F.S., FAVIS B.D., ST-PIERRE N., and RAMSAY B.A. (1995). Morphology and mechanical properties of blends containing thermoplastic starch and P(HB-co-12%-HV). *Proceedings of the Annual Technical Conference ANTEC'95.* 2028-2032 1995.

VIYARAN, S. and PONTER, P.B. (1974). *Tenside*, 11, 241-.

VIYARAN, S. and PONTER, P.B. (1975). *Chem.-Ing.-Tech.*, 47, 748-.

WILLEMS, R. C., POSTHUMS DE BOER, A., VAN DAM, J. and GOTSIS, A. D. (1999). *Polymer*, 39, 5879.

WILLETT, J.L. (1994). Mechanical Properties of LDPE/Granular Starch Composites. *J. Appl. Polym. Sci.*, 54, 1685-1695.

WILLETT, J.L., JASBERG, B.K. and SWANSON, C.L. (1995). Rheology of Thermoplastic Starch: Effects of Temperature, Moisture Content, and Additives on Melt Viscosity. *Polym. Engng, Sci.*, 35 (2), 202-210.

WILLETT, J.L., MILLARD, M.M and JASBERG, B.K. (1998). Extrusion of Waxy Maize Starch: Melt Rheology and Molecular Weight Degradation of Amylopectin. *Eur. Polym. J.*, 34 (10), 1477-1487.

WILLIS, J.M., CALDAS, V. and FAVIS, B.D. (1991). Processing-morphology relationship of compatibilized polyolefin/polyamide blends. Part II. The emulsifying effect of an ionomer compatibilizer as a function of blend composition and viscosity. *J. Mater. Sci.*, 26, 4742-4750.

WOOL, R.P., OELSCHLAEGER, P. , and WILLETT, J. (1990). Injection Molded Biodegradable Starch Polymer Composite. *PCT Patent* WO 90/14388.

WU, S. (1987). Formation of dispersed phase in incompatible polymer blends: interfacial and rheological effects. *Polym. Eng. Sci.*, **27**, 335-343.

ZOBEL, H.F. (1988). Molecules to Granules: A Comprenhesive Starch Review. *Starch/Stärke*, 40 (2), 44-50.

ANNEX I DUCTILITY OF LDPE/THERMOPLASTIC STARCH BLENDS.

AI.1 Abstract

In this paper, the tensile properties of LDPE/thermoplastic starch (TPS) blends prepared in a one-step process are studied as a function of TPS composition, glycerol content, morphology and relative humidity. Blends with TPS containing 36% and 40% glycerol, show an unusually high ductility. Blends prepared with TPS containing 29% glycerol and a high viscosity PE are also ductile and possess an improved modulus. Blends of a low viscosity PE and the same TPS result in a material with significantly reduced elongation at break. Data from the tensile testing of PE/TPS blends are compared with theoretical models. The Young's modulus fits the Takayanagi model for good interfacial adhesion. Conversely, properties at break did not fit simple models well because such models do not consider morphologies produced by particle coalescence during melt blending. The relationship between the morphology and fracture mechanisms of PE/TPS blends was evaluated by observation of the evolution of the microstructure of tensile tested samples. Those observations reveal not just the influence of particle size and particle size distribution on the fracture mechanism but also the effect of humidity on the energy dissipation mechanism. Fracture mechanisms composed of three stages (debonding, void growth and failure) are proposed. The completion and extent of those stages are dependent on the morphology.

AI.2 Introduction

Starch is a natural carbohydrate storage polymer accumulated in the form of intracellular granules by plants. It is composed of linear polysaccharides called amylose and branched polysaccharides called amylopectin. In order to destabilize the granular structure, moisture, heat and/or shear must be applied. Once starch molecules are separated, a suitable plasticizer can be used to produce a thermoplastic material. This

thermoplastic starch (TPS) can be processed using similar processing equipment as that used with synthetic polymers.

Native granular starch has been studied as an organic filler for polymer composites and as a thermoplastic component of polymer blends. In composite materials, granular starch behaves as typical filler, increasing the elastic modulus while decreasing the stress and elongation at break. Willett (1994) studied the influence of starch volume fraction, granule size and the presence of compatibilizer on the mechanical properties of LDPE/granular starch composites. He found that his experimental results fit quite well with theoretical predictions. Humidity and interfacial modifiers affect neither the stress nor the elongation at break, while an increase of interfacial adhesion improves the elastic modulus.

Hiltner and co-workers presented a series of papers devoted to the study of tensile properties of PETG filled with organic and inorganic fillers (Bazhenov et al., 1994, Li et al., 1994a). PETG is an amorphous polymer that exhibits yielding and stress hardening in stress-strain curves. They proposed five fracture modes based on the macroscopic stress-strain behavior and the surface fracture characteristics of specimens cryogenically fractured in the longitudinal direction (Li et al., 1994a). Only spherical particles of regular size were considered for the fracture mode schemes and particle coalescence (or agglomeration) was not considered. It is known that cohesive dispersed particles, such as thermoplastic polymers (Kunori and Geil, 1980a, 1980b, Favis and Chalifoux, 1988) and uncoated mineral fillers (Maiti and Mahapatro, 1991), tend to coalesce as dispersed phase volume fraction (ϕ_d) increases. Due to their underestimation of particle coalescence, those models are not useful for the evaluation of the fracture mechanism of immiscible polymer blends and composite materials filled with cohesive particles.

Fracture mechanisms of multiphase polymeric systems have been related to macroscopic changes in the material structure, such as stress whitening. Stress whitening of immiscible polymer blends (Kunori and Geil, 1980a, Li et al., 1994b, Liu and Truss,

1995) and composites (Bazhenov et al., 1994, Li et al., 1994b) has been related to cavitation and debonding of dispersed phase particles. Liu and Truss (1995) studied the tensile yielding and microstructure of isotactic PP/LLDPE blends. Tensile yielding of those blends was evaluated at different strain rates and different testing temperatures and compared to Eyring's viscosity theory. The yielding mechanism was found to be related to both strain rate and temperature by means of Eyring's processes I and II. When process I dominates (low strain rate and high temperature) no stress whitening is observed, whereas stress whitening is present when process II (high strain rate and low temperature) is predominant. SEM observations revealed that the surfaces of cryo-fractured unwhitened samples were smoother than that of whitened samples. It was also found that in both cases the originally spherical LLDPE particles elongate under the action of shear stress transferred from the isotactic PP matrix. However, in the case of whitened samples an extensive debonding of LLDPE particles from the isotactic PP matrix was observed. LLDPE debonding is found to be accompanied by craze-like microstructures. They relate the stress whitening to the presence of those micro voids.

In a previous work from this laboratory, St.-Pierre *et al.* (1997) showed that TPS materials blended in low concentrations with LDPE and LLDPE in the absence of compatibilizer possess a good balance of mechanical properties. In more recent work (Favis et al., 1999, Rodriguez et al., 1999, 2002a), it was demonstrated that LDPE/TPS blends could maintain excellent mechanical properties, especially ductility, at high starch loading. The purpose of the present work is the detailed study of the tensile properties of LDPE/TPS blends. A special emphasis will be made to elucidate the mechanism responsible for the high ductility demonstrated by those blends.

AI.3 Theoretical Considerations

The tensile properties of ductile polymeric composites can be divided into low and high strain properties accordingly. Tensile properties measured at low strains are, for example, Young's or elastic modulus (E) and stress and elongation at yield. These

properties are highly influenced by the amount of interfacial adhesion between the particulate filler and the polymeric matrix.

Various models have been proposed to relate the filler content to the modulus of composite materials. The most frequently used is Kerner's equation. It can be used to describe the bulk, shear and elastic (Young's) modulus of filled composites. Kerner's theory was applied to the prediction of the modulus of polymer blends by Uemura and Takayanagi (1966). Takayanagi's equation for blends that present good interfacial adhesion is:

$$\frac{E}{E_0} = \frac{E_0(7 - 5\nu) + E_F(8 - 10\nu) - \phi_F(7 - 5\nu)(E_0 - E_F)}{E_0(7 - 5\nu) + E_F(8 - 10\nu) + \phi_F(8 - 10\nu)(E_0 - E_F)} \quad (1)$$

where E and E_0 are the Young's modulus of composite and unfilled polymer, E_F is the Young's modulus of filler, and ν is the Poisson's ratio for the polymer. For a system that demonstrates poor interfacial adhesion equation (1) is reduced by extrapolation of E_F to zero to:

$$\frac{E}{E_0} = \frac{E_0(7 - 5\nu) - (7 - 5\nu)E_0\phi_F}{E_0(7 - 5\nu) + (8 - 10\nu)E_0\phi_F} \quad (2)$$

In the case of ductile polymeric systems, it is also interesting to study the properties at high strain, such as stress and elongation at break. The theory devoted to the prediction of such properties is not as well-developed as those for modulus. The most noticeable theories for tensile strength prediction are those proposed by Nielsen (1966) and Leidner (Piggott and Leidner, 1974, Leidner and Woodhams, 1974). In both theories, strength is dependent on filler composition in terms of a function of the cross sectional area. These theories differs in the exponent of the area function with respect to the filler composition, 2/3 and 1 for Nielsen's and Leidner's theory, respectively:

$$\sigma_B/\sigma_{B0} = (1 - \phi_F^{2/3})S \quad (3)$$

$$\sigma_B/\sigma_{B0} = (1 - \phi_F)S \quad (4)$$

where σ_{B0} is the stress at break of unfilled polymer and S is the stress concentration fraction. S generally has a value of 0.5, with 1 being the maximum when there is no stress concentration. Both expressions were developed for poor adhesion systems.

Several theories have been proposed to predict the elongation at break of polymer blends and composites. Smith (1959) developed an expression to evaluate the debonding strain of filled rubbers. This expression was extended by Nielsen (1966) to predict the elongation at break of filled polymers (ε_B), assuming perfect adhesion:

$$\varepsilon_B/\varepsilon_{B0} = 1-\phi_F^{1/3} \tag{5}$$

where ε_{B0} is the elongation at break of the unfilled polymer and ϕ_F is the filler volume fraction.

Nielsen (1966) also considered the case of no adhesion between filler and polymer (equation 2). In this case, filler particles do not contribute to carrying the applied load. That is manifested in a reduction of the effective cross sectional area. Moreover, filler particles distort the stress field promoting a fracture transfer from one particle to another. Equation 2 was incorporated into the theory of Sato and Furukawa (1963) for the modulus of filled systems with no adhesion to estimate the elongation at break for the case of no adhesion. This new expression is as follows:

$$\varepsilon_B/\varepsilon_{B0} = (1 - \phi_F^{2/3})S/\{[1 + (y^2/2(1 - y))](1 - \psi\zeta) - [y^2\psi\zeta/(1 - y)y^3]\} \tag{6}$$

where $\phi_F = y^3$

and

$$\psi = (y^3/3)(1 + y - y^2)/(1 - y + y^2)$$

and ζ is the adhesion parameter; $\zeta = 0$ for perfect adhesion, and $\zeta = 1$ for no adhesion. The surface effect in the theory of Sato and Furukawa has been omitted from the above equation for moduli.

AI.4 Experimental

AI.4.1 Materials

Two types of polyethylene, LDPE2040 (PE1) and LDPE2049 (PE2) from Rexene Chemical Co., showing different melt flow indexes (MFI 12 and 20 g/10min, respectively) were used. Wheat starch, Supergell 1203-C, was supplied by ADM/Oglivie. Glycerol, from SIMCO Chemical Products Inc., and distilled water were used to plasticize and gelatinize starch. Wheat starch was mixed in different proportions with water and glycerol as shown in Table AI.1.

Table AI.1 Composition of starch suspensions.

Code	Starch (%)	Glycerol (%)	Water (%)
TPS40	48	32	20
TPS36	48.5	27.5	24
TPS29	50	20	30

AI.4.2 One-step extrusion process

Blending was carried out in a one-step process. A single-screw extruder (SSE); C.W. Brabender Instruments (L/D = 26, length = 495 mm, and compression ratio = 2; was connected to an intermediate zone of a co-rotating twin-screw extruder (TSE); Leistritz AG (LM 30.34), L/D = 28, and length = 960 mm; using an adapter especially designed for this purpose. The screw speed was maintained at 150 rpm. The processing temperature in the TSE ranged from 25° to 110°C in the section for starch gelatinization and plasticization, and was 150°C for the melt mixing of TPS and PE. The extrusion

temperature in the SSE was also 150°C. More details of the PE/TPS blends processing is reported elsewhere (Favis et al., 1999). Blends were extruded through a rectangular die (3.5 height × 32 width mm) then quenched using calendar rolls. The gap between the rolls was *ca.* 2 mm and the hot stretch ratio was around 2. The hot stretch ratio is the relation between the velocity of the extrudate and the velocity of the ribbon at the exit of the calendar (Gonzalez et al., 1993). Blend compositions ranged from around 27% to 53.3% TPS by weight. Volume fractions of TPS (ϕ_{TPS}) were calculated based on the densities of LDPE (0.920 g-cm^{-3}) and TPS (1.410 g-cm^{-3}).

It has been reported in previous work from this laboratory that the passage of TPS through the venting zone allows for the full extraction of water (Favis et al., 1999). On this basis, TPS can be considered as a binary mixture of starch and glycerol. As a consequence, the glycerol content for the different TPS was calculated to be 40%, 36% and 29 wt% for TPS40, TPS36 and TPS29, respectively.

AI.4.3 Characterization of LDPE/TPS blends

AI.4.3.1 Morphology

PE/TPS blends were cryogenically cut in the longitudinal direction. Samples were coated with a gold/palladium alloy and observed in a JEOL JSM-820 scanning electron microscope (SEM).

AI.4.3.2 Tensile properties

Blends were tested according to the ASTM D-638 standard method. Tensile specimens of type V were cut longitudinally from PE/TPS ribbons. Before testing PE, TPS and PE/TPS blends were conditioned, at room temperature and ambient humidity, for at least 48 hr. PE1/TPS36 blends were also conditioned at 0% and 50% relative humidity (RH). Samples were strained at 10 mm/min on a M30K machine (JJ Instruments) equipped with a 5kN cell and a data acquisition system. The average values of the Young's

modulus, tensile strength and elongation at break were calculated from at least 12 measurements.

AI.4.3.3 Fractography

The post-mortem evaluation of tensile specimens of PE/TPS blends was observed using an optical microscope. To improve the contrast of this transparent material, tensile specimens were exposed to iodide vapors for 30 minutes. Before observation with the optical microscope, iodide-stained samples were left for 24 hours to allow the evaporation of the excess iodide. Iodide-stained samples were supported between two glass slides to achieve a flat surface.

AI.5 Results and Discussion

AI.5.1 Morphology

The morphology of the different PE/TPS blends can be observed in Figure AI.1. TPS particle size drops as glycerol content increases due to a reduction in TPS viscosity (Rodriguez et al., 2001a). In the case of PE2/TPS29 blends, a combination of the low viscosity (high MFI) PE2 and the high viscosity of TPS29 results in a strong effect of viscosity ratio on the blend morphology. It appears as though PE2 does not transfer enough shear stress to TPS29 to reduce and homogenize TPS particles. It is important to mention that all blends were subjected to an elongational flow at the exit of the extruder. The presence of elongated particles and fibers in blends prepared with TPS compounded with 36 and 40% glycerol is a consequence of that elongational flow. In contrast, blends prepared with the more viscous TPS29 demonstrate a strong resistance to hot stretching. Morphological differences exhibited by both TPS36 and TPS40, and TPS29 were in good agreement with the difference in rheological properties exhibited by TPS materials prepared in the one-step process (Rodriguez et al., 2001a).

AI.5.2 Stress-strain curves

Typical stress-strain curves of PE/TPS blends prepared in a one-step process conditioned at ambient humidity and temperature are depicted in Figure AI.2. Both PE1 and PE2 present an almost indistinguishable yield point due to the stress increment during neck formation. The increment in stress is more significant at the onset of neck propagation. Neck propagation is followed by a region of stress hardening where the applied stress augments more gradually because of the more uniform straining of the necked material.

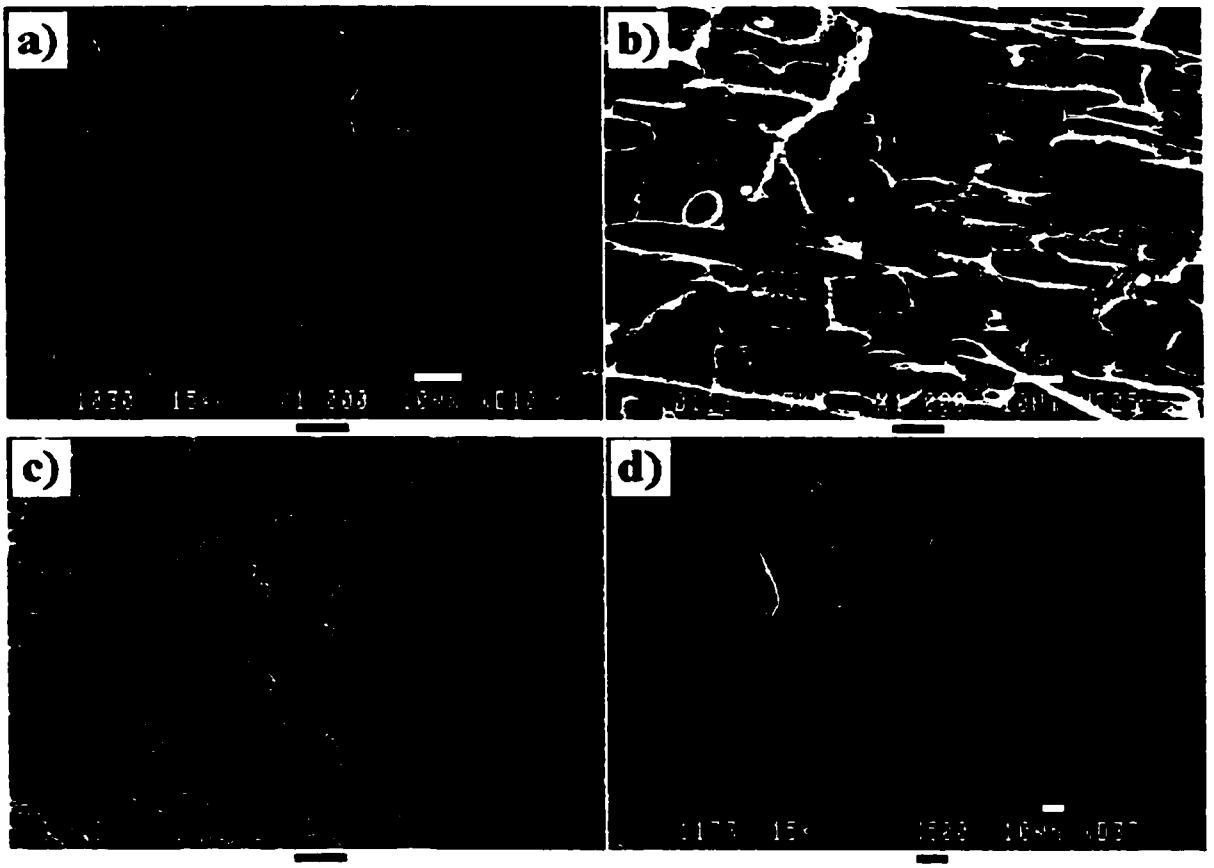

Figure AI.1 Morphology of PE/TPS blends (70:30) cryogenically fractured in the longitudinal direction. PE1/TPS blends: a) TPS40, b) TPS36, and c) TPS29. d) PE2/TPS29. The black bar below the micrographs represents 10 μm.

The stress-strain behavior is influenced by both blend morphology and the glycerol content in TPS. Blends prepared with TPS36 and TPS40 show a very similar stress-strain behavior, which was identical to that displayed by neat PE. In both PE1/TPS40 and PE1/TPS36 blends, the fracture stress and strain decrease as ϕ_{TPS} increases. Tensile fracture took place into the stress hardening region, even at the highest ϕ_{TPS} (ϕ_{TPS} = 0.41). This was amazing considering that at this composition TPS has been reported to be 100% accessible for hydrolytic degradation (Favis et al., 1999, Rodriguez et al., 1999, 2002a). It seems that the uniaxial orientation and elongated shape of TPS particles play an important role in controlling the stress-strain behavior and tensile strength of this polymer pair. It is important to mention that, as observed with neat LDPE, no stress whitening was perceived in these blends.

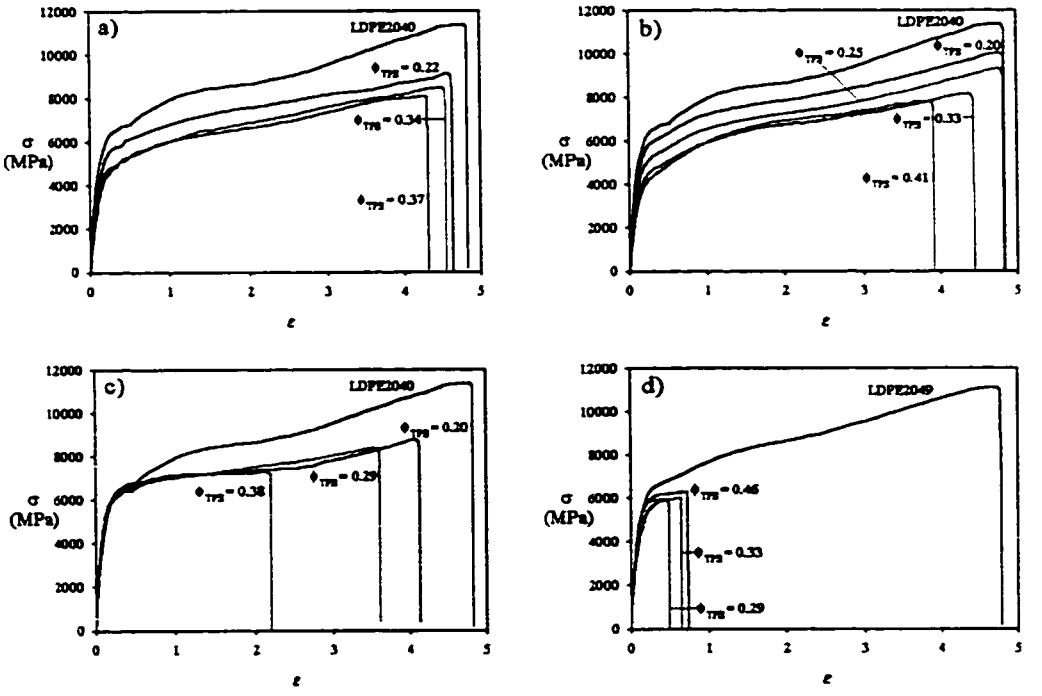

Figure AI.2 Stress-strain curves of PE/TPS blends evaluated at 10 cm-min^{-1} and conditioned at ambient humidity. Curves of PE1 blended with TPS40, TPS36 and TPS29 are represented in a), b) and c), respectively. PE2/TPS29 blends are represented in d).

As mentioned in the morphological evaluation, PE1/TPS29 blends show an almost spherical morphology. In this case, yield stress remains practically constant. The stress and strain at break decreases as the TPS concentration increases. This reduction is more dramatic than that observed in the PE1/TPS36 and PE1/TPS40 blends. At $\phi_{TPS} \leq 0.29$, samples fail during stress hardening, whereas at higher ϕ_{TPS} they fail during necking but always in a ductile manner. No stress whitening is observed for these blends.

PE2/TPS29 blends also show an almost spherical morphology although a few extremely large ellipsoidal particles can be observed. All these blends fail during yielding independently of ϕ_{TPS}. Isolated white regions are observed around large particles. Both large particles and white regions are easily observable with the naked eye.

AI.5.3 Tensile properties

The relative tensile properties are determined from stress-strain curves and are plotted against ϕ_{TPS} (Figures AI.3 to AI.5). The relative Young's modulus (E/E_0) is clearly influenced by the glycerol content of the TPS dispersed phase, as shown in Figure AI.3. E denotes the Young's modulus of all PE/TPS blends and PE2, and E_0 is that of neat PE1.

Addition of the less viscous TPS materials, TPS36 and TPS40, reduces E. As expected, the reduction increases as ϕ_{TPS} augmented. Conversely, the addition of the more viscous TPS29 leads to the increment of E despite the lack of interfacial adhesion. Evaluation of the rheological properties of TPS suggests the presence of a limit for glycerol as a plasticizer of gelatinized starch at concentrations of around 30wt% (Rodriguez et al., 2001a, 2002b). This is related to the percolation of well-plasticized glycerol-rich regions (Rodriguez et al., 2002b). It appears that the percolation of such soft regions also exert an important influence on the mechanical properties of TPS at room temperature.

The experimental Relative Young's modulus of PE/TPS blends can be compared with values calculated from equations (1) and (2). The Poisson ratio in both cases is 0.5 and

the Young's modulus of PE1 is 55.9 MPa. The values of Young's modulus of TPS, determined at ambient humidity, used for the calculations with equation (1) were 13.5, 33.2 and 95 for TPS40, TPS36 and TPS36, respectively. In the case of good adhesion, the elastic modulus of the three different TPS materials, conditioned at ambient humidity is used. Even though PE and TPS are completely immiscible, experimental results show a better fit with the values predicted for good adhesion than those for poor adhesion. This unexpected result can be explained by a good interfacial contact. Leclair and Favis found that the compression exerted by a crystalline matrix (HDPE), during crystallization, on an amorphous dispersed phase (PC) results in good interfacial contact and a higher elastic modulus (Leclair and Favis, 1996). They also observed that the compression effect occurs when the glass transition temperature (Tg) of the dispersed phase is higher than the crystallization temperature (Tc) of the matrix. That was related to the smoothness of dispersed phase particles. LDPE has a Tc similar to HDPE, but all TPS materials show a Tg below room temperature (Rodriguez et al., 2002b). Nevertheless, TPS particles show similar smoothness to that of the PC in Leclair's work. The rheological properties of TPS materials have been compared to that of partially crosslinked rubber, in which the viscosity increases infinitely as the oscillatory frequency decreases (Rodriguez et al., 2002b). Conversely, LDPE is characterized by a Newtonian plateau at low frequency. Considering that LDPE contraction during cooling is a low motion process (low frequency), LDPE/TPS viscosity and elasticity ratios must be high enough to avoid interfacial deformation. It seems that the viscoelasticity of the dispersed phase plays an important role on the interfacial contact of immiscible polymer blends.

The relative stress at break (σ_B/σ_{B0}), where σ_{B0} is the stress at break of neat PE1, is plotted against ϕ_{TPS} (Figure AI.4). In PE1/TPS blends, the glycerol content appears to have little influence on σ_B. The σ_B values of these blends decrease proportionally with ϕ_{TPS}. However, the use of the less viscous PE2 results in a more severe reduction of σ_B.

The σ_B of PE2 was about 10% lower than σ_{B0} and the σ_B of PE2/TPS blends dropped to a plateau value which was independent of ϕ_{TPS}.

The σ_B/σ_{B0} experimental values of PE/TPS blends were compared to Nielsen's (Eq. 3) and Leidner's theories (Eq. 4) for poor interfacial adhesion. No stress concentration was considered (S=1). PE1/TPS blends fit the predictions of Liedner's equation. In the case of σ_B of PE2/TPS29 blends, the lack of fit seems to be related to the brittle nature of these polymer blends, which was practically independent of ϕ_{TPS} at the interval measured.

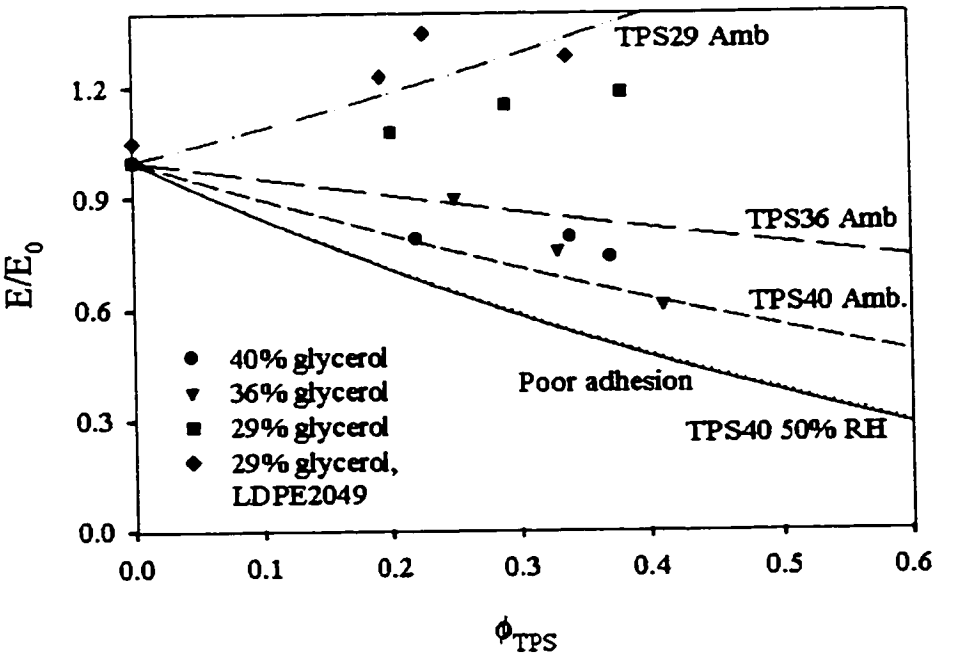

Figure AI.3 Comparison of the relative Young's modulus (E/E_0) of PE1/TPS and PE2/TPS29 blends with theoretical predictions.

The relative elongation at break ($\varepsilon_B/\varepsilon_{B0}$) of PE/TPS blends *versus* the volume fraction of TPS (ϕ_{TPS}) is shown in Figure AI.5. ε_B and ε_{B0} denote the elongation at break of PE/TPS blends and neat PE1, respectively. As expected, the relative elongation at break of

PE/TPS blends decreases as ϕ_{TPS} increases. However, for PE1/TPS blends having high glycerol content, (TPS36 and TPS40) the elongation at break of the PE matrix is maintained even at high TPS loadings. Conversely, blends prepared with PE1 and the TPS29 result in less ductile materials that show a more marked decrease in ε_B. The addition of TPS29 to PE2 results in a dramatic reduction of ε_B. As observed in the stress-strain curves, PE2/TPS29 blends fail before yielding and, consequently, they present a fragile-like fracture.

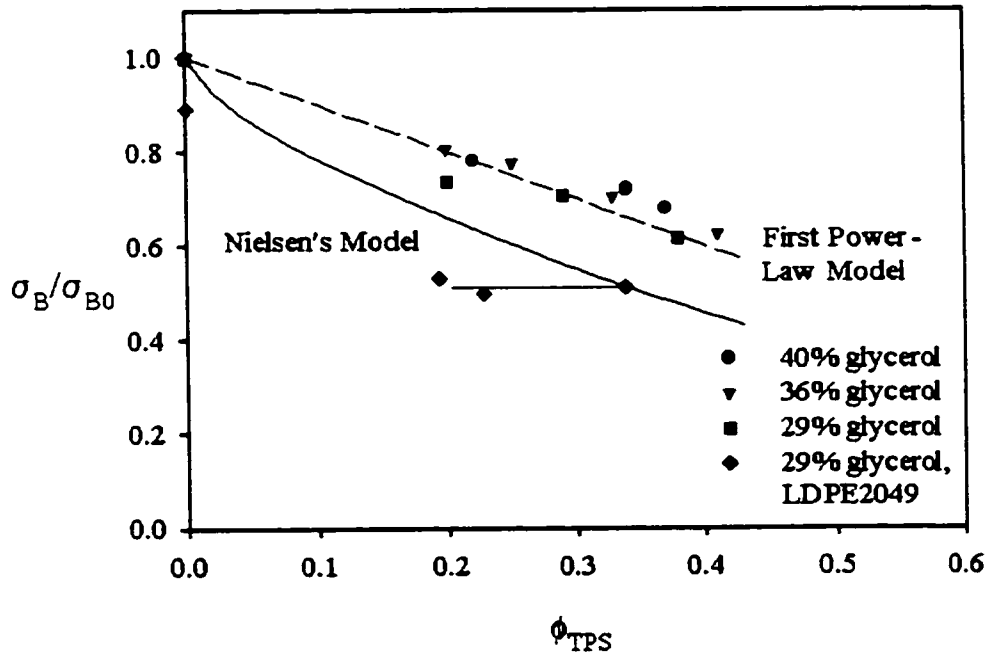

Figure AI.4 Comparison of the relative maximum stress (σ_B/σ_{B0}) of PE1/TPS and PE2/TPS29 blends with theoretical models.

The $\varepsilon_B/\varepsilon_{B0}$ of PE/TPS blends was compared to Equations (5) and (6) which are not applicable to these blends. Deviation of experimental values from those theories can be related to particle-particle coalescence of the TPS dispersed phase and the final morphology displayed by those blends. In order to improve the understanding of the

fracture mechanism of these immiscible polymer blends the *post mortem* internal structure of tested samples was evaluated.

AI.5.4 Post-mortem evaluation of tensile tested samples

In order to avoid modifications induced by cryogenic fracture, tensile tested samples of PE/TPS blends were observed by optical microscopy. Samples were chosen to evaluate the different fracture modes: ductile and fragile fractures of spherical morphology, and ductile fracture of fiber-like morphology.

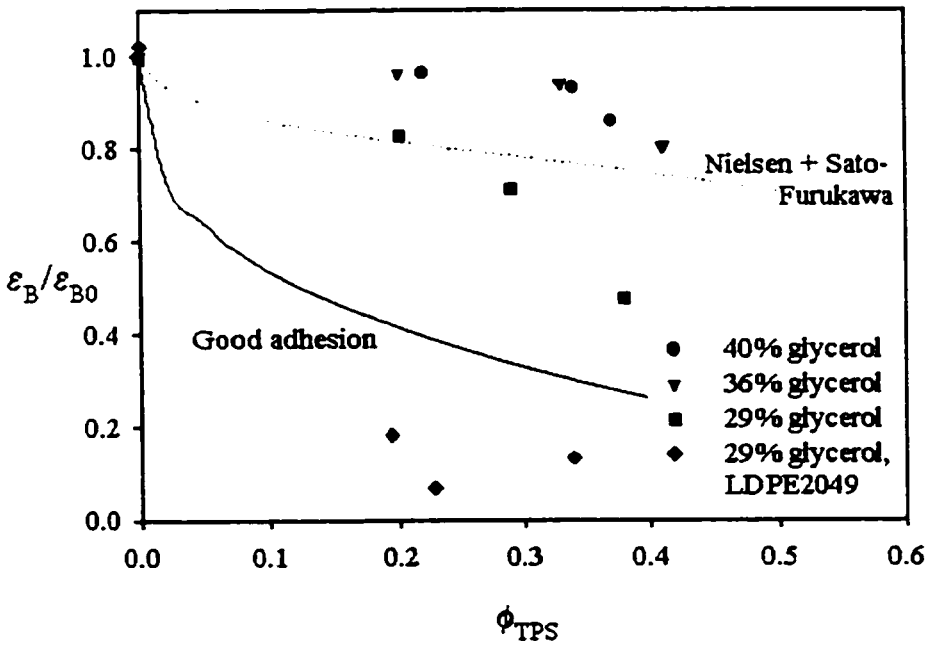

Figure AI.5 Comparison of the relative elongation at break ($\varepsilon_B/\varepsilon_{B0}$) of PE1/TPS and PE2/TPS29 blends with theoretical measurements.

AI.5.4.1 PE1/TPS blends

PE1/TPS29 blends demonstrate a spherical morphology and ductile fracture at all ϕ_{TPS} values. Optical micrographs of the blend containing ϕ_{TPS} = 0.20 and its position in the

tensile sample are presented in Figure AI.6. Beyond the tensile deformation zone (position a), the morphology of this blend is composed mainly of spherical particles smaller than 10μm and just a few particles ranging between 15-20 μm. Large particles were slightly ellipsoidal due to the elongational deformation experienced during melt drawing. Large TPS particles have been found to be more susceptible to elongational deformation than small ones (Rodriguez et al., 2001b).

The influence of tensile deformation began at the position b. This point represents the onset of debonding. Debonding starts at the poles of large particles. Gent and Park (1984) found that the stress required to debond a rigid particle from an elastomeric matrix increases as the size of the particle decreases. The homogeneous distribution of the applied stress allows for the debonding of small particles (position c). At the beginning of the necking section (position d) the smooth growth of elliptical voids can be observed. Elliptical voids are transformed into sharp-ended voids due to stress hardening (position e). These voids coalesce in the strain direction as a consequence of stretching. Some small crazes growing perpendicular to the strain direction are observed close to the failure region (position f). The lateral coalescence of TPS particles, produced by the reduction of the cross section, gives rise to the formation of internal flaws. Highly drawn fiber bundles can be observed in the area adjacent to the internal flaws such as those in the fracture zone (position g).

At increased ϕ_{TPS} (0.29) minor changes in the fracture development can be observed (Figure AI.7). As expected, not only the particle size increases but the particle size distribution also broadens (Figure AI.7a). The debonding process is similar to that of ϕ_{TPS} = 0.20 blends with debonding of large particles (Figure AI.7b) followed by that of the small ones (Position c). Void growth is also similar (position d). However, a larger quantity of internal flaws develop as a consequence of the larger particle size and the reduction of inter-particle distance.

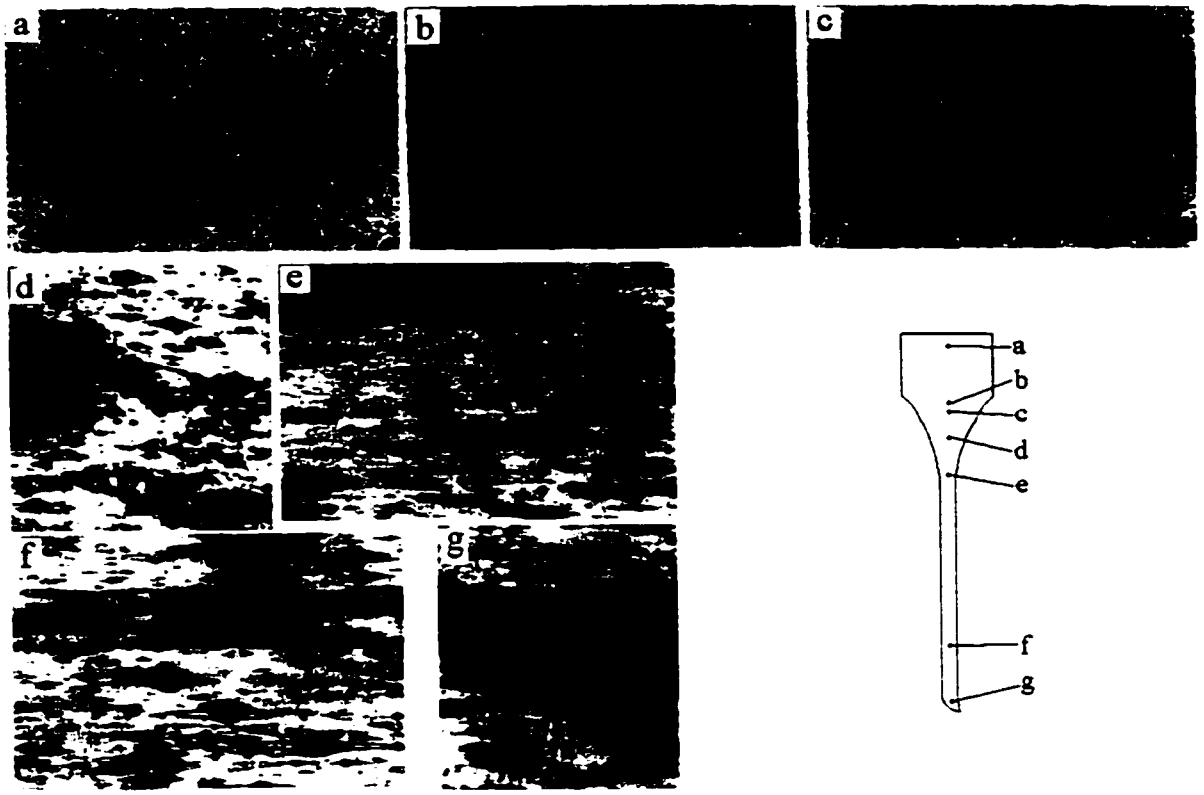

Figure AI.6 Optical micrographs of PE1/TPS29 blends (ϕ_{TPS} = 0.20) conditioned at ambient humidity. The schematic representation of the fractured sample represents the position where the micrograph was taken.

Major changes are observed at ϕ_{TPS} = 0.38. As observed for lower starch concentrations, debonding starts on large particles, but in this case it does not propagate to the small particles (Figure AI.8a). Void growth is limited to the large particles that have already debonded (Figure AI.8b). Crazes form at the equator of large particles and transfer to the neighboring particles, as observed near the failure region (Figure AI.8c).

AI.5.4.2 PE2/TPS29 blends

The most extreme case of brittleness occurs with PE2/TPS29 blends. These blends do not demonstrate necking during tensile testing and result in a fragile fracture at all concentrations. Due to its low viscosity, PE2 transfers less masticating shear to the

TPS29 dispersed phase than PE1. This leads to larger TPS particle sizes. The particle size distribution is also broader than in PE1/TPS29 blends, as observed in Figure AI.9a. Particles having a diameter larger than 150μm could be observed. At the onset of strain effects (position b), a catastrophic debonding of large particles takes place. This is observed as a generalized detachment of the matrix from the entire particle and is not just localized at the poles as in previous cases. As expected, debonding does not propagate to the small particles. Micrographs from position c show that the complete debonding of large particles leads to a premature formation of cracks that rapidly propagate to the neighboring particles. Non-homogeneous stress transfer and premature crack propagation leaded to fragile fracture.

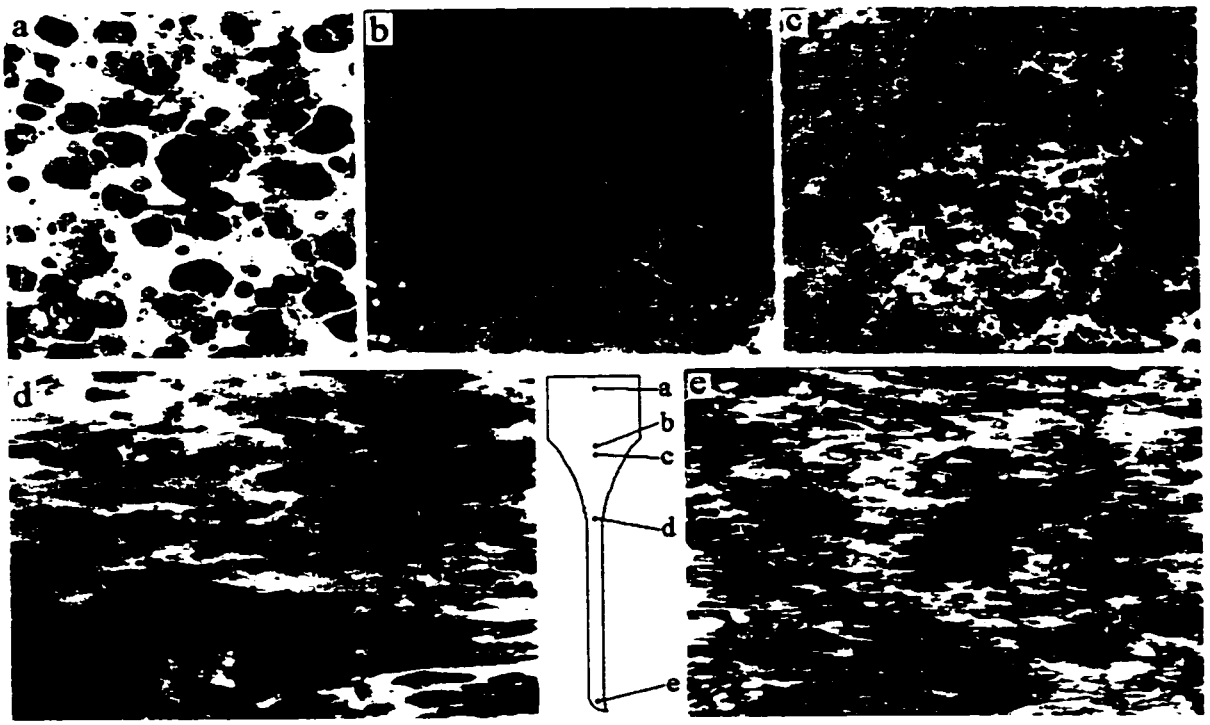

Figure AI.7 Optical micrographs of PE1/TPS29 blends (ϕ_{TPS} = 0.29) conditioned at ambient humidity. The schematic representation of the fractured sample represents the position where the micrograph was taken.

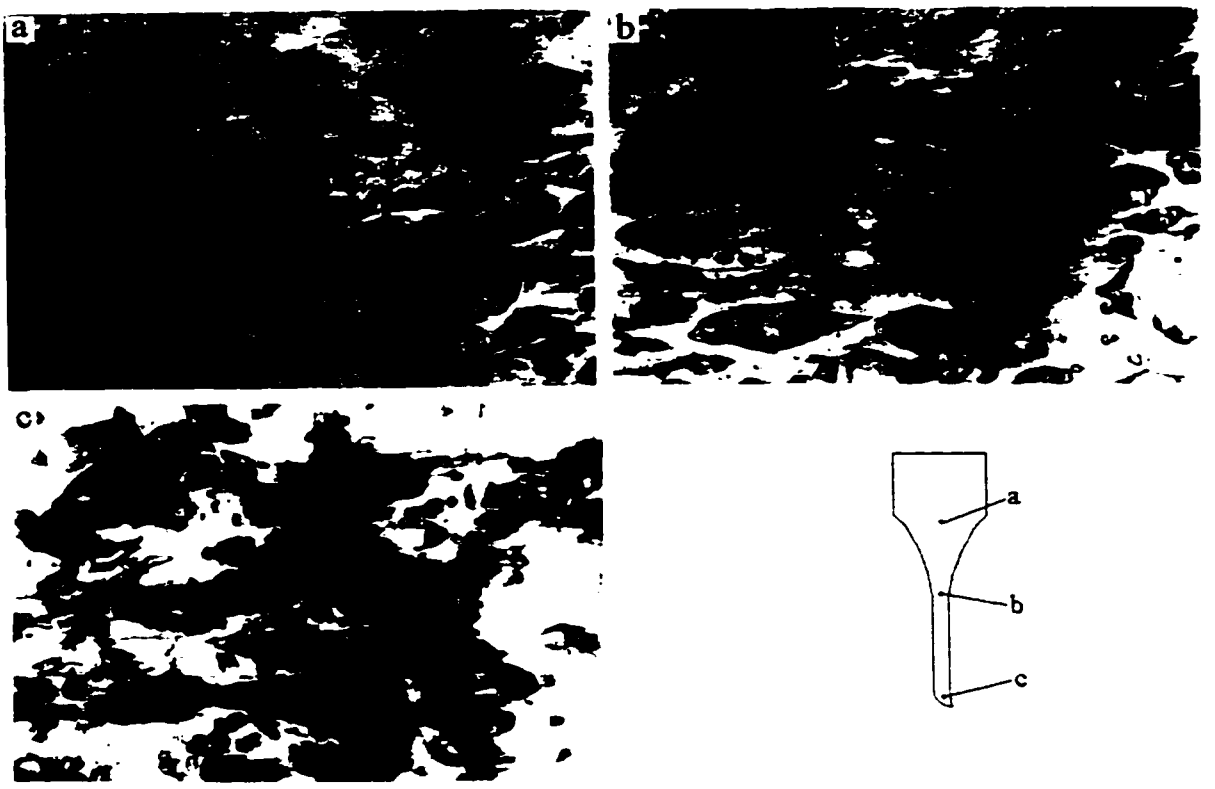

Figure AI.8 Optical micrographs of PE1/TPS29 blends (ϕ_{TPS} = 0.38) conditioned at ambient humidity. The schematic representation of the fractured sample represents the position where the micrograph was taken.

AI.5.4.3 PE1/TPS36 and PE1/TPS40 blends

PE blends prepared with TPS36 and TPS40 possess a TPS phase in a fiber-like morphology. This results from the application of elongational flow during calendaring (Favis et al., 1999, Rodriguez et al., 2001b). Due to the similarity of the mechanical properties and morphological characteristics of PE1/TPS36 and PE1/TPS40 blends only the former was analyzed in detail. Although there is little difference in the elongation at break of PE1/TPS36 blends conditioned at 0% and 50% relative humidity (RH), important differences are observed in the *post-mortem* analysis (Figures AI.10 and AI.11).

Figure AI.9 Optical micrographs of PE2/TPS29 blends (ϕ_{TPS} = 0.29) conditioned at ambient humidity. The schematic representation of the fractured sample represents the position where the micrograph was taken.

Morphological analysis of the undeformed region of PE1/TPS36 reveals a range of shapes from large fibers and ellipses to small spherical particles (position a). The first signs of debonding of TPS particles in the blends conditioned at 0% RH can be observed in Figure AI.10b. The debonding process is more complex than that of spherical particles due to the combination of forces transferred from the matrix to the fibers. It is well-known that shear stress in the matrix is at a maximum near the fiber ends and zero at the center, while tensile loads on the fiber are zero at the ends and gradually increase to a maximum plateau at the fiber center (Nielsen, 1974). In this case, a combination of debonding of the particle end and fiber breakup are observed. The former is produced by the shear stresses exerted by the matrix to the fiber ends, whereas fiber breakup is the result of the tensile load applied by the PE matrix. This initial energy dissipation is reflected as a reduction of the yield stress as observed in the stress-strain curves (Figures AI.2a and AI.2b). Closer to the necked section (Figure AI.10c) voids at the end of TPS fibers are larger, resembling those formed between fiber fragments. Void growth gives place to the formation of long tunnel-like cavities parallel to the strain direction. Many small crazes spreading perpendicular to the stress direction are also observed around the ends of fiber segments, especially around thick fiber or fiber conglomerations. The homogeneous void growth and the formation of many well-distributed crazes dissipate enough stress to allow for a smooth necking process.

The elongational flow produced during the calendaring of PE/TPS blends permits not just the formation of long TPS particles, but also increases the transverse interparticle distance and the axial continuity of PE ligaments (Figures AI.10 and AI.11). Li and coworkers (1994a) have reported that the continuous ligaments formed by polymer matrices in polymeric multiphase systems carry the stress applied during tensile tension. Moreover, the thickness of such ligaments has been related to the transverse distance between dispersed phase particles (Mikhler et al., 1988). The presence of thick continuous PE filaments allows PE1/TPS36 blends to undergo stress hardening even at high TPS loading. During this process TPS fibers thin while the crazes observed on thick fiber segment ends continue growing (Figures AI.10d and AI.10e). Fiber thinning and craze growth allow for the homogenous dissipation of the applied energy. Under further strain, crazes propagate from the broken fibers to the neighboring particles leading to polyethylene matrix failure.

The failure history of PE1/TPS36 blends conditioned at 50% RH (Figure AI.11) is similar to that described for blends conditioned at 0% RH. The debonding of fiber ends and fiber breakup also occur (position b). Nevertheless, no crazing occurs at the ends of fiber segments during void growth (position c). It seems that there was another mechanism of stress dissipation probably based on the moisture content-starch stiffness relationship. Water is a good plasticizer for starch (Shogren, 1993) and several authors have reported increased ductility of starch-based materials when those materials were exposed to high humidity (Shogren, 1993, Loomis et al., 1993, Van Soest et al., 1996). Based on this, the surface of TPS fiber fragments conditioned at 50% RH should flow under the action of the shear stress applied by the PE matrix instead of forming crazes as did TPS fragments conditioned at 0% RH. As in the previous case, blends conditioned at 50% RH also undergo stress hardening resulting in a reduction of the apparent diameter of TPS fiber fragments. Internal flaws appear and grow as a consequence of the stress concentrated in the vicinity of thick fibers or fiber conglomerations leading to the eventual failure of the PE matrix.

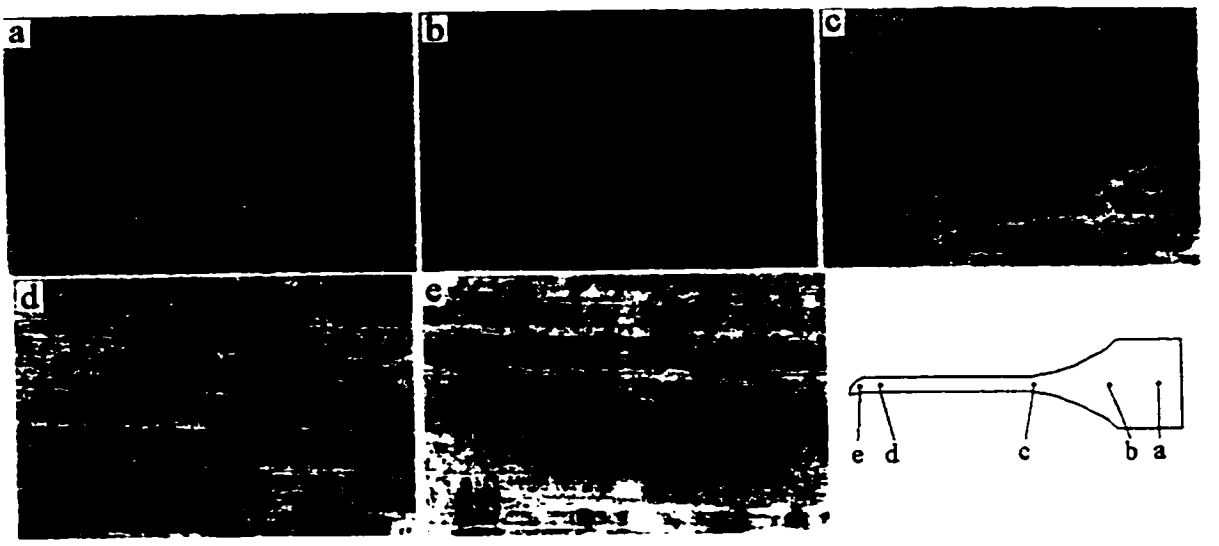

Figure AI.10 Optical micrographs of PE1/TPS36 blends (ϕ_{TPS} = 0.42) conditioned at 0% relative humidity. The schematic representation of the fractured sample represents the position where the micrograph was taken.

Another important difference between PE1/TPS36 blends conditioned at 0% and 50% RH is that the former demonstrates whitening in the necking section of the tensile sample while the latter always remains transparent. As in the work of Liu and Truss (1995), PE1/TPS36 blends conditioned at different RH were examined under the scope of Eyring's viscosity theory. In the present work both strain rate and testing temperature (T_{test}) are constant, however the glass transition temperature (Tg) of TPS36 is significantly affected by the conditioning humidity. TPS36 has Tg values of -56°C and -77°C when conditioned at 0% and 50% RH, respectively. This variation in Tg can be considered analogous to the increase of T_{test} in a system where Tg is constant. In both cases a difference between Tg and T_{test} can modify the fracture mechanism via the softening of dispersed phase particles. Hence, there is no craze formation and, consequently, no stress whitening could be expected if the dispersed phase particles become soft enough to be deformed by the matrix. In such systems energy is dissipated by the plastic flow of the matrix and by the deformation of dispersed phase particles. As the difference between Tg and T_{test} decreases, the dispersed phase particles become

stiffer and are incapable of flowing under the normal stress applied by the polymeric matrix. As a consequence, crazes can develop as a result of stress concentration. When crazing becomes the dominant mechanism of energy dissipation, stress whitening of tensile samples is observed.

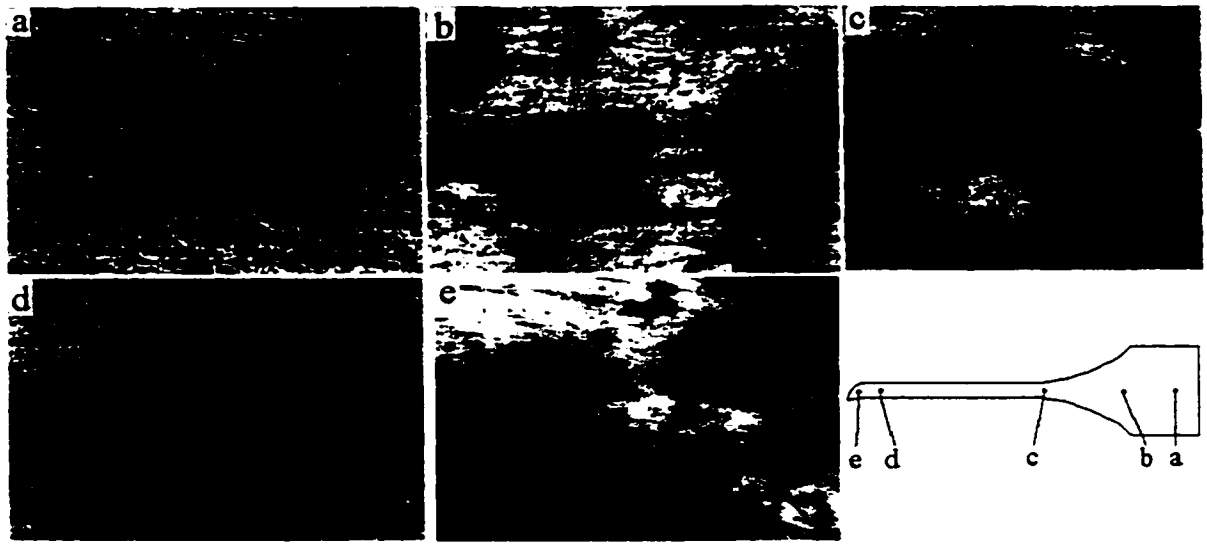

Figure AI.11 Optical micrographs of PE1/TPS36 blends (ϕ_{TPS} = 0.42) conditioned at 50% relative humidity. The schematic representation of the fractured sample represents the position where the micrograph was taken.

AI.5.5 Fracture mechanisms

In this section, some fracture mechanisms that consider the morphology changes produced by the change of the ϕ_d of the immiscible polymer blends will be discussed.

AI.5.5.1 Ductile fracture, spherical morphology

A schematic representation of the mechanism of ductile fracture, as observed in PE1/TPS29 blends (ϕ_{TPS} = 0.20) is depicted in Figure AI.12. The mechanism of ductile fracture can be divided into three main steps: debonding, void growth and fracture. Considering that the energy stored per unit volume increases proportionally to the

particle volume, debonding begins in large particles, and then it propagates to the small ones. Debonding is localized at the poles of dispersed phase particles. Generalized debonding results in a homogeneous stress distribution and a more effective stress dissipation. The completion of the debonding process allows a stable neck formation and, consequently, the smooth void growth. If the interparticle distance is large enough, ligaments formed between dispersed phase particles can resists thinning during necking. Stress hardening and fracture will occur when local strain reaches the fracture strain of the pure matrix. The augmentation of ϕ_d results in a reduction of the interparticle distance, which can lead to a premature coalescence of dispersed phase particles during straining. Large particle agglomerates are points of stress concentration, which promotes microscopic tearing of the matrix (Mikhler et al., 1988). Sample failure via tear propagation, during either necking or stress hardening, will depend on the interparticle distance (see ϕ_d). At even higher ϕ_d, particle size increases as a result of particle-particle coalescence during melt blending. In that case, the fracture mechanism differs from the one previously discussed since in that case there is no completion of the debonding step (Figure AI.13). As in the previous case, debonding starts with the large particles, but in this case it does not propagate to the small ones. The stress applied is not homogeneously distributed, it is localized at the numerous large particles. If the interparticle distance is high enough to allow polymer ligaments to release the applied energy, neck formation can take place. Neck formation leads to the thinning of polymer ligaments during straining and, consequently, the transverse coalescence of dispersed phase particles. Fracture occurs at the cracks formed around large particles and particle clusters.

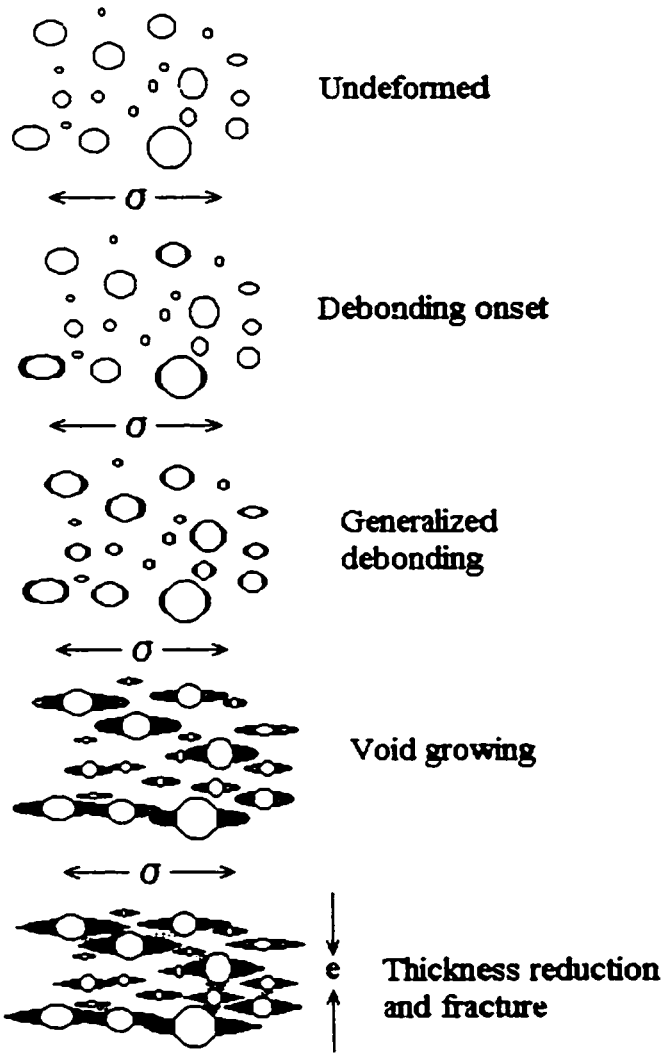

Figure AI.12 Schematic representation of the ductile fracture mechanism of polymer blends having spherical morphology. Low ϕ_d.

AI.5.5.2 Brittle fracture

Poor dispersion and distribution of particles in multiphase polymeric systems can be produced by insufficient shear during mixing, or when the interfacial tension or viscosity (elasticity) ratio of the system is extremely high. Such morphologies are characterized by the presence of very large particles (or agglomerates) and a broad particle size

distribution. These systems can result in brittle materials even though the matrix is ductile as observed in PE2/TPS29 blends. Figure AI.14 shows a schematic representation of the brittle fracture mechanism. In this case, the debonding step is characterized by the catastrophic debonding of dispersed phase particles due to the high stress concentrated around a reduced number of large particles (or particle clusters). The entire applied stress is localized around a few of the fully debonded particles producing a severe cracking that propagates rapidly to the neighboring particles leading to the fragile fracture of the polymer matrix.

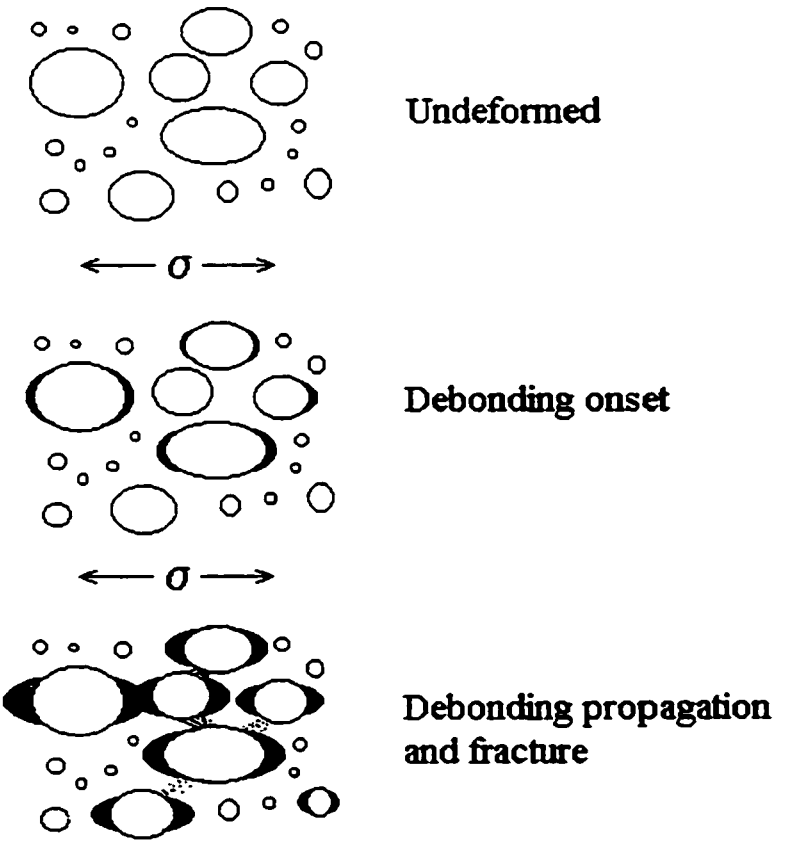

Figure AI.13 Schematic representation of the ductile fracture mechanism of polymer blends having spherical morphology. High ϕ_d.

The above fracture mechanisms, where the morphology-ϕ_d relationship is important, are a more realistic representation of how fracture occurs in immiscible polymer blends or polymer composites compounded with cohesive filler than the mechanisms where only ϕ_d variation is considered.

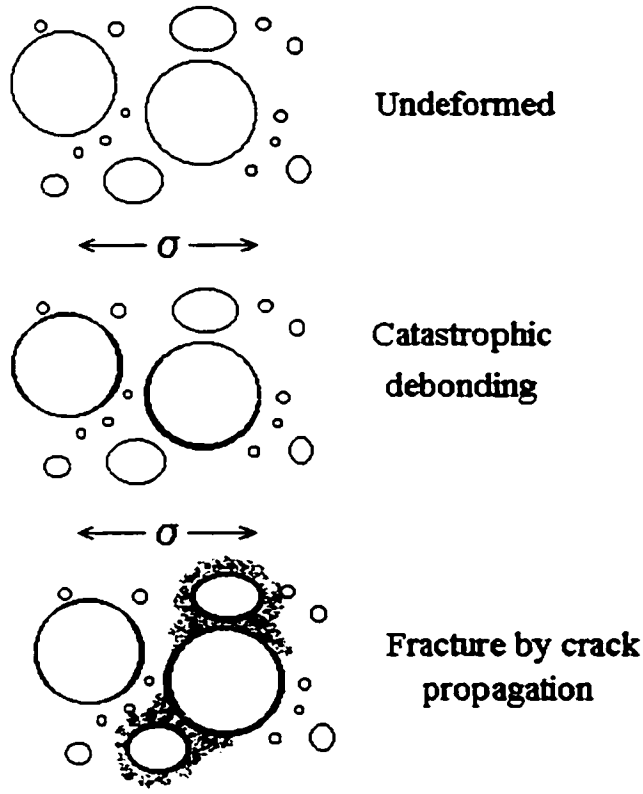

Figure AI.14 Schematic representation of the fragile fracture mechanism of polymer blends with spherical morphology.

AI.5.5.3 Ductile Fracture, elongated particles

Spherical particles can be transformed into ellipsoids or even long fibers under the influence of an elongational flow such as that exerted during the pass through capillary dies (Chapleau and Favis, 1995, Rodriguez et al., 2002c) or calendaring rolls (Gonzalez, et al., 1993, 1996, Rodriguez et al., 2001b, 2002c). Schematic representations of the

fracture mechanism of immiscible polymer blends having elongated morphology are depicted in Figure AI.15. This figure shows the special case of elongated particles oriented in the strain direction and where the dispersed phase has a different stiffness.

As in the case of spherical particles, the fracture mechanisms can be divided in the same three steps: debonding, void growth and fracture. However, the breakup of dispersed fiber further complicates the fracture mechanism. At low strain, the debonding of dispersed particles starts. The breakup of thin fiber occurs at the same time interval as debonding. A combination of these two processes, debonding and fiber breakup, allows for the homogeneous transfer of the applied stress. During the void growth step, the influence of the elastic modulus of the dispersed phase can be observed. In the case of a low modulus dispersed phases (Figure AI.15, left), void growth proceeds by the separation and thinning of the segments of the broken fibers. In the case of high modulus dispersed fibers (Figure AI.15, right), void growth also proceeds by the separation of the segments of broken fibers, but the formation and growth of small crazes at the end of the segments replace the yielding of the dispersed phase observed in the previous case. The good distribution and large number of the fiber segments are essential for the excellent energy dissipation in both the yielding and craze formation processes. Failure of the strained sample takes place when the matrix filaments reach a critical elongation or when internal flaws are produced as a consequence of stress concentration around thick fibers or fiber agglomerations.

AI.6 Conclusions

PE/TPS blends (compounded with 36% and 40% glycerol) prepared in a one-step process display unusually high ductility. Blends prepared with the high viscosity PE1 and TPS29 were not only ductile but also show an important increase of E with respect to pure PE. Conversely, blends prepared with the same TPS29 and the low viscosity PE2 demonstrate significantly lower elongations at break over a range of ϕ_{TPS}.

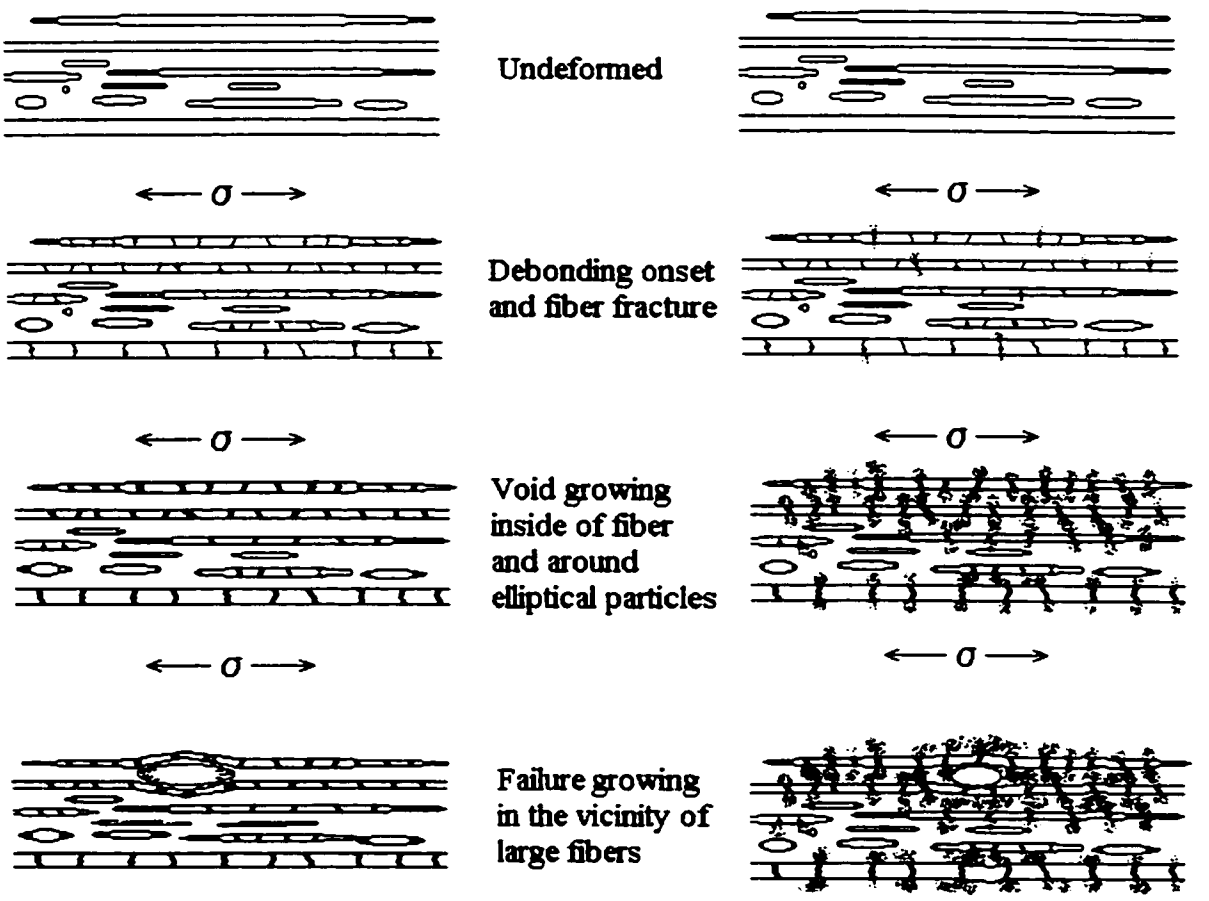

Figure AI.15 Schematic representation of the ductile fracture mechanism of polymer blends with elongated morphology. The fracture mechanisms of two types of dispersed phase particles having low (left) and high (right) modulus are compared.

Experimental data from tensile tests were compared with theoretical models. Takayanagi's equation for good adhesion gives a good prediction of E. This is unexpected considering the high interfacial tension that should exist between a polar (TPS) and a non-polar polymer (PE). The high modulus can be explained by the good interfacial contact produced by the compression exerted by the PE matrix, during its crystallization, on the TPS dispersed phase. Stress and elongation at break are compared to some simple models, which only depend on ϕ_{TPS}. In those cases the experimental data

do not fit the models since they do not consider the morphology changes related to particle-particle interaction during melt blending. The *post mortem* evaluation of tensile tested samples reveals how particle size and particle size distribution influence the fracture mechanisms of PE/TPS blends. The influence of humidity on the energy dissipation mechanism is also demonstrated. Blends conditioned at 0% RH have an energy dissipation mechanism based on craze formation which was characterized by stress whitening in the neck. Conversely, blends conditioned at 50% RH remain transparent after tensile testing because craze formation was replaced by the deformation of dispersed phase surface (shear yielding) as an energy dissipation mechanism.

From the evaluation of the *post mortem* microstructure, a series of fracture mechanisms dependent on blend morphology are proposed. The mechanisms are composed of three stages: debonding, void growth and failure. The completion of generalized debonding is mainly dependent on particle size and particle size distribution effects. Smooth void growth can be achieved when the stress is homogeneously distributed to all dispersed particles during debonding. This is achieved with a homogeneous distribution of small particles. The extent of void growth depends primarily on the thickness of matrix filaments which is related to the interparticle distance. Tensile failure depends on the completion of debonding or the extent of void growth.

The combination of the different structures observed in this work suggest the possibility of property tailoring via morphology control and glycerol content. Highly ductile materials can be obtained by a combination of fiber formation and unidirectional orientation during hot stretching. While a good balance of ductility and modulus can be attained with well-dispersed spherical particles.

ANNEX II BIODEGRADATION OF THERMOPLASTIC STARCH IN LDPE/TPS BLENDS. EFFECT OF THE HOT-STRETCH RATIO.

AII.1 Introduction

Polyethylene (PE) cannot be degraded by microorganisms due to its high molecular weight. The melt blending of LDPE with thermoplastic starch (TPS) has been extensively studied by this research group (Favis, 1999, Rodriguez, 2001, Rodriguez, 2002a, Rodriguez, 2002b). The continuity of the partially biodegradable LDPE/TPS blends has been studied by hydrolytic extraction with a HCl 6N aqueous solution at 60°C (Favis, 1999, Rodriguez, 2002a). In those papers, the percent of continuity was related to the morphology, which was dependent of glycerol content in TPS dispersed phase. In this work, the biodegradation extent of partially biodegradable LDPE/TPS blends is evaluated as a function of the extrusion conditions.

AII.2 Procedure

AII.2.1 Sample preparation

A PE1/TPS blend containing 30% TPS were prepared in a one step process and drawn at different hot-stretch ratios (HSR). A part of these blends was pelletized and re-extruded (two-step process). The re-extruded blend was also drawn through the calendar rolls. More detail about materials and processing conditions were reported elsewhere (Favis, 1999; Rodriguez, 2001b, 2002c).

Samples for biodegradation studies were prepared by cutting specimens at different lengths from the axial direction (Figure AII.1). PE1/TPS ribbons were cut in 1 mm, 5 mm and 10 mm to evaluate the effect of the biodegradation extent in the axial direction. Samples of 10 mm were cut in a half and two quarters to evaluate the connectivity of TPS particles in the transverse direction.

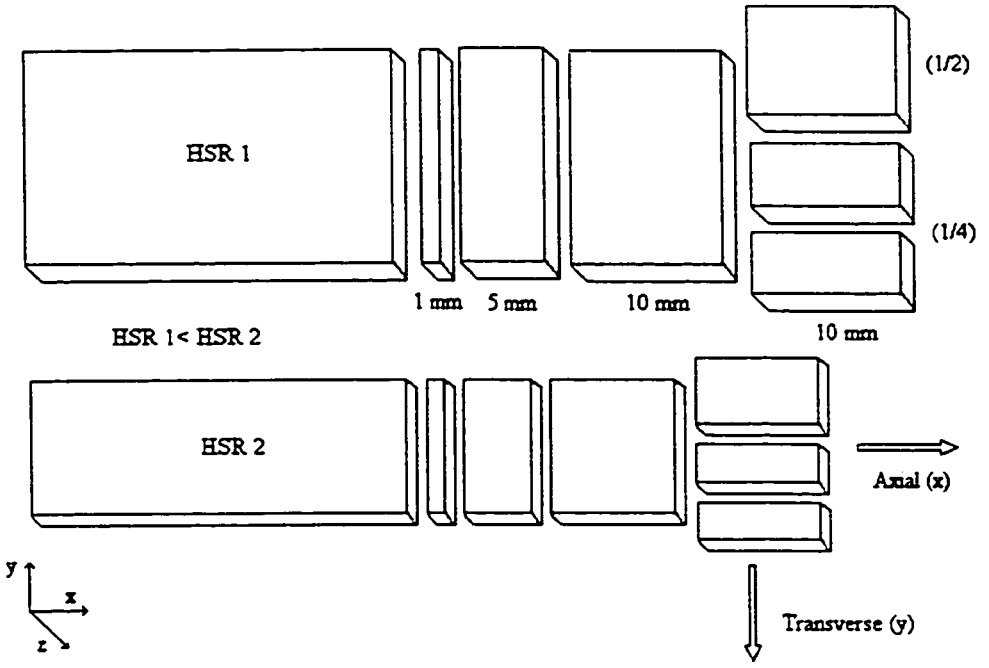

Figure AII.1 Schematic representation of the specimens used in biodegradation studies.

AII.2.2 Hydrolytic extraction

TPS was extracted from PE1 matrix using hydrolytic degradation and bacterial biodegradation. Hydrolytic degradation was carried out in a HCl 6N aqueous solution at 60°C.

AII.2.3 Biodegradation conditions

Biodegradation was performed using an activated sludge source of bacteria. Bacteria were maintained in a carbon-limited medium with soluble starch the sole carbon source. Table AII.1 shows the composition of the culture medium. A 20 Liter reactor was used for biodegradation studies (Figure AII.2). Nutrients were continuously added at a dilution rate of 0.05 h^{-1}.

Table AII.1 Composition of the culture medium.

Element	Element	Concentration (g/L)
Carbon Source	Soluble starch	4
Nitrogen Source	$(NH_4)_2SO_4$	2
	Ferric ammonium citrate	0.06
Phosphates	Na_2HPO_4	1.96
	KH_2PO_4	0.83
Other mineral salts	$MgSO_4$, $7H_2O$	0.20
	CaCl, $2H_2O$	0.01
Microelements	$ZnSO_4$, $7H_2O$	0.10
	$MnCl_2$, $4H_2O$	0.03
	H_3BO_3	0.30
	$CoCl_2$	0.20
	$CuSO_4$, $5H_2O$	0.02
	$NiCl_2$, $6H_2O$	0.02
	$NaMoO_4$	0.03

Samples exposed to activated sludge were taken out from the medium, washed several times with distilled water and dried for 48 h at 60°C under vacuum. The extent of biodegradation was calculated from the difference between the initial weight of the sample and the weight after drying. It was reported as the weight loss of sample and related to the TPS content in the blend. It is important to remark that the extent of biodegradation includes partially degraded starch molecules that were dissolved by the medium.

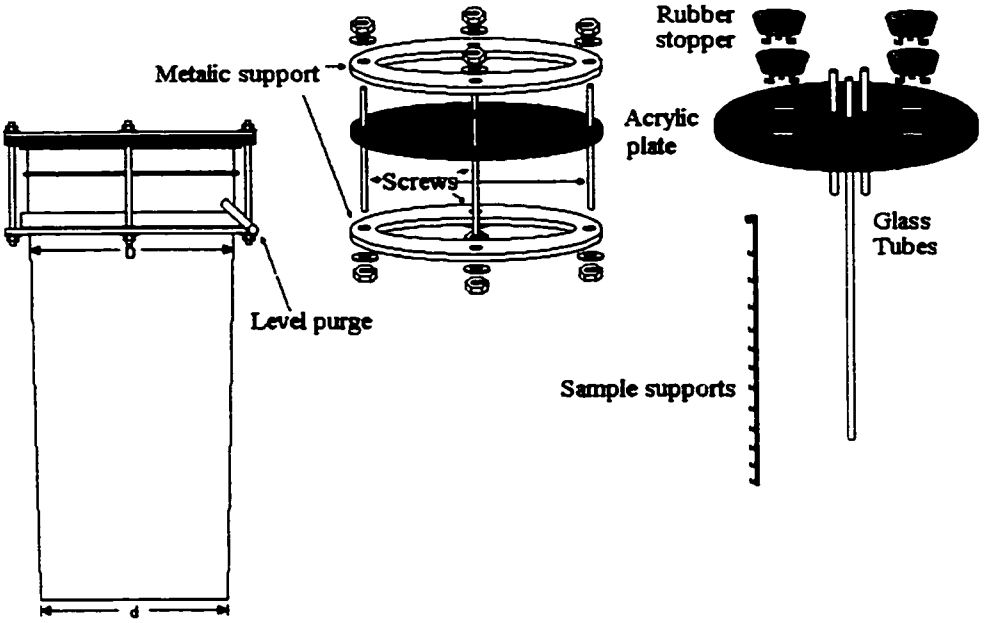

Figure AII.2 Schematic representation of the biodegradation reactor.

AII.3 Results

AII.3.1 Microbial degradation

These blends displayed a fiber-like morphology as previously reported (Rodriguez, 2001; Rodriguez, 2002a). Another interesting characteristic of the morphology was observed when the surface of a PE1/TPS blend (70:30), prepared in a one-step process, was exposed to water and microorganisms for 5 days in the bioreactor (Figure AII.3).

Micrographs clearly show the low amount of TPS on the ribbon surface. Moreover, the TPS particles seem to be isolated, indicating that a PE1-rich skin covers the ribbon surface rendering the accessibility in the z direction practically impossible.

Into the bulk of PE1/TPS blends, particle-particle coalescence has been observed in blends compounded with high glycerol content (40%) while a suppressed coalescence was displayed by re-processed blends (Rodriguez, 2001). In order to compare the

influence of the different morphologies displayed by these blends, the samples with different dimensions were tested in the bioreactor (Figure AII.4).

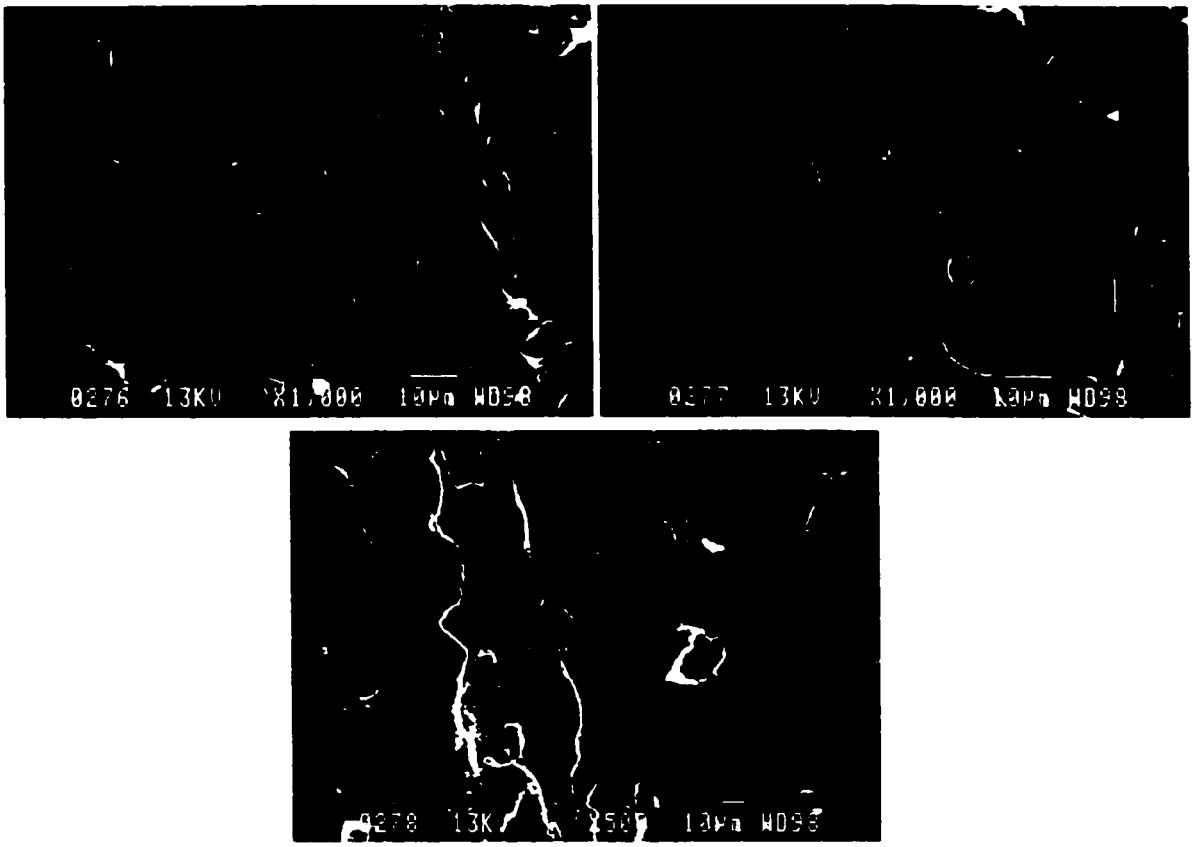

Figure AII.3 SEM micrographs of the surface of a PE1/TPS ribbon prepared in a one-step process (HSR=0.51) after five days of biodegradation.

Blends prepared in one-step process seem to reach a maximum extraction value at 48% (Figure AII.4a). As expected, samples of 1 mm reached the maximum extraction extent in the shortest period of time (about 5 days). Samples of 5 and 10 mm gradually increase the percent of TPS lost to reach values close to that of 1 mm samples. Conversely, re-extruded LDPE/TPS blends reached maximum values at 32%, 14% and 8% for the samples of 1 mm, 5 mm and 10 mm, respectively (Figure AII.4b). The larger biodegradation extent obtained with PE1/TPS blends processed in a one-step process could be related to the high continuity displayed by these blends (Rodriguez, 2001).

Those results highlight the importance of morphology control on the biodegradation extent of PE1/TPS blends.

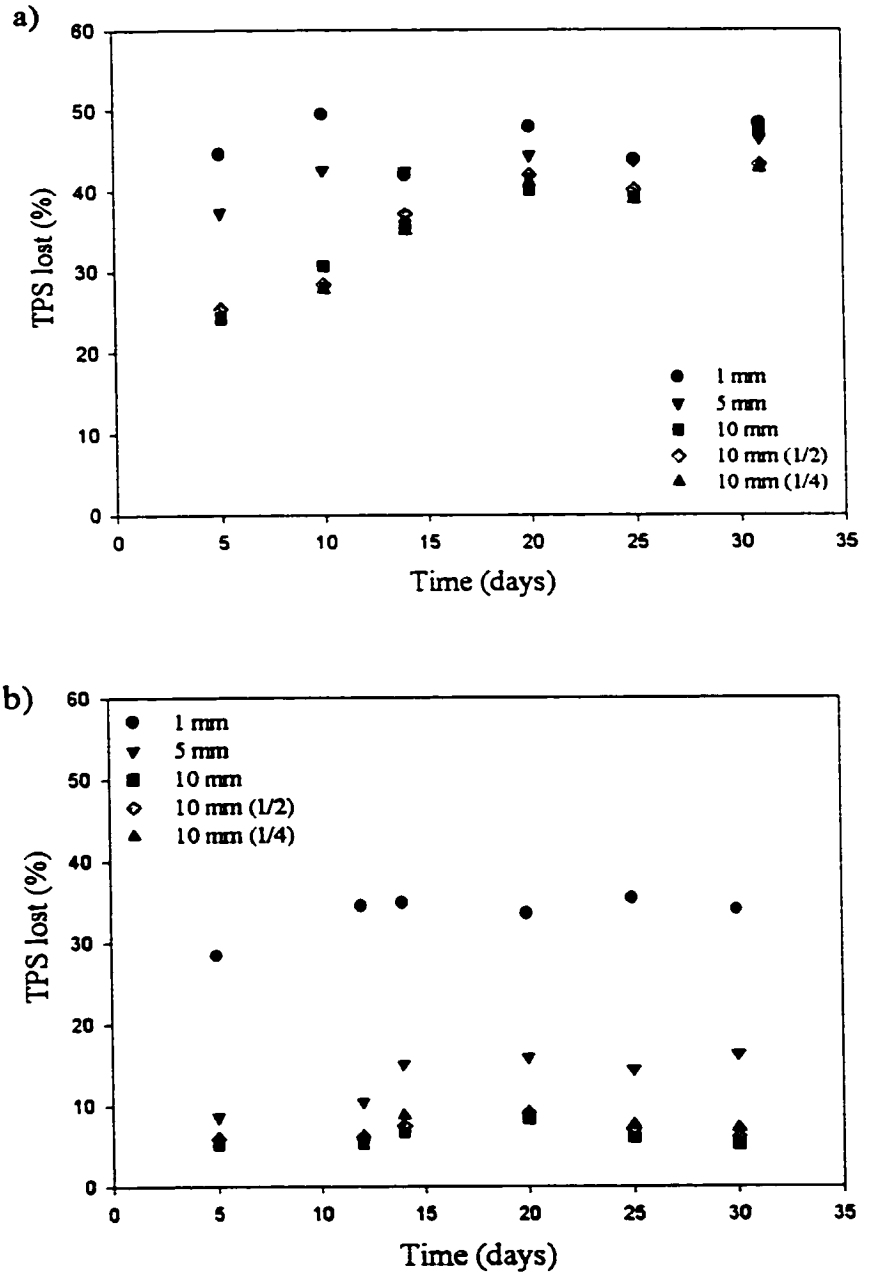

Figure AII.4 Effect of sample dimensions on the percent of TPS lost at different times of PE1/TPS blends, 30 wt% TPS. a) 2-step, HSR=0.59; b) 1-step, HSR=0.73

Another important observation is that the biodegradation extent of all 10 mm samples is practically the same. This suggests that coalescence of TPS in the dispersed phase in the transverse direction (y) was almost negligible. It can be assumed that the TPS particles were only extractable in the machine direction (x).

AII.3.2 Hydrolytic degradation

The continuity of PE1/TPS blends was also evaluated by hydrolytic degradation of the starch domains. Hydrolytic degradation was more effective than bacterial attack since 100% extraction was obtained (Figure AII.5). There was no sign of coalescence in the transverse direction, as was the case of bacterial degradation. It can be concluded that PE1/TPS blends prepared in one-step process were composed by long fibrillar domains of starch which are highly continuous in the machine direction. Even though particle coalescence in the transverse direction has been observed (Rodriguez, 1999), it was not enough to improve the degradation of starch domains in hot-stretched PE1/TPS blends.

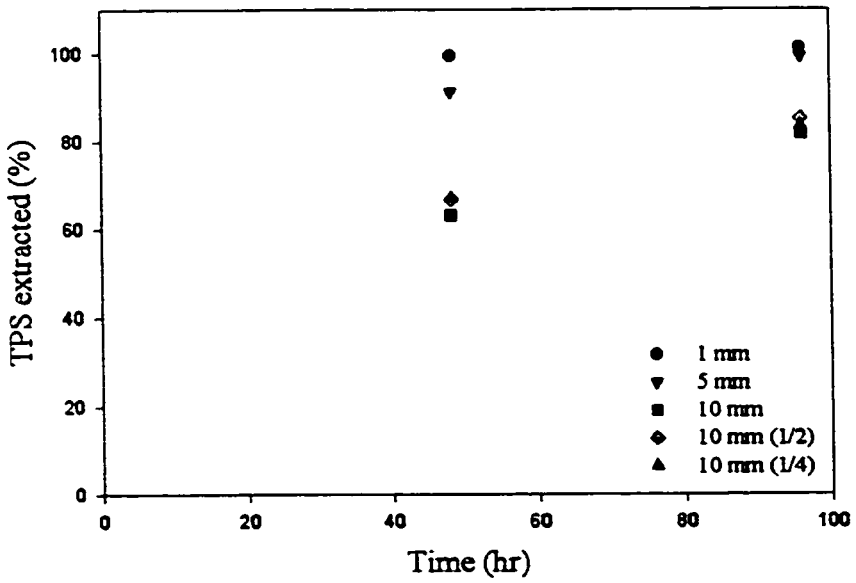

Figure AII.5 Effect of acid hydrolysis on loss of starch from LDPE/TPS blends (30% TPS, 1-step, HSR=0.73) as a function of time.

From the comparison of the results of both degradation techniques it can be inferred that some phenomenon is taking place during the bacterial degradation of TPS. As mentioned in the previous section, the maximum extent of biodegradation in the case of the one-step processed blends was around 48% regardless the sample dimensions. At first sight it suggests a lack of continuity even in 1mm samples. However, hydrolytic degradation demonstrated the complete continuity of starch domains. Considering the unidirectional orientation of starch domains, a schematic representation of the bacterial degradation of PE1/TPS blends is presented in Figure AII.6

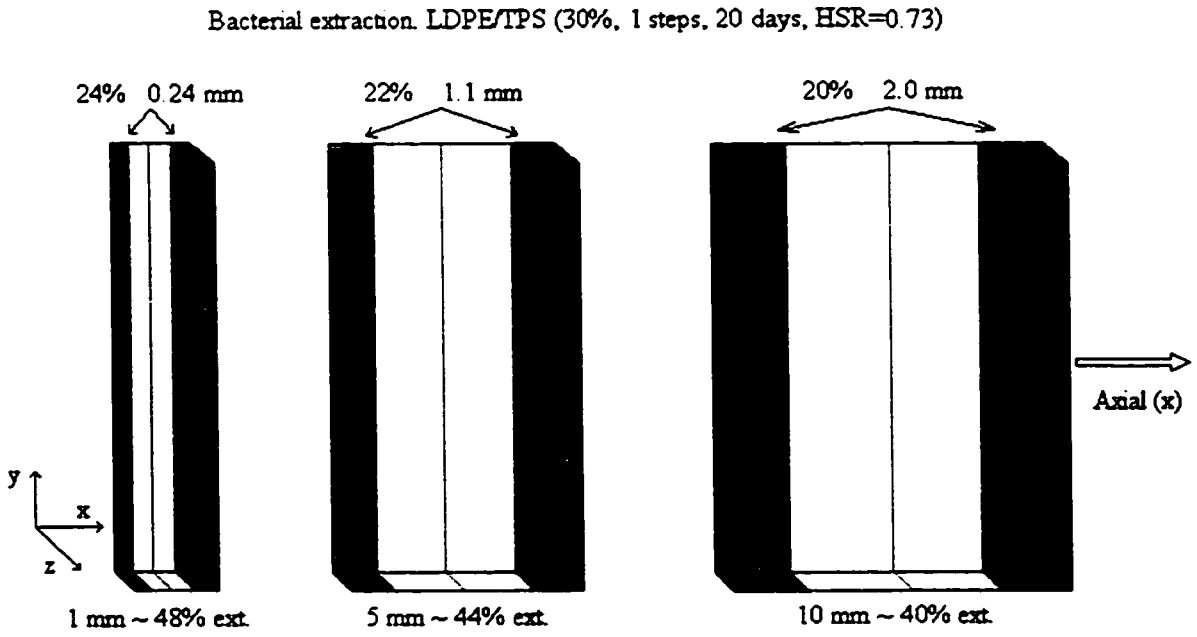

Figure AII.6. Bacterial extraction of LDPE/TPS blends (30% TPS, 1-step, 20 days, HSR=0.73).

The percentage of TPS loss from samples of 1, 5 and 10 mm was 48%, 44% and 40%, respectively. Some assumptions are made to evaluate the extent of biodegradation:

1. TPS particles are homogeneously distributed through extruded ribbons.

2. The percent of TPS lost is proportional to the percent volume removed from the sample.

3. The exposed area occupied by TPS particles in y-z surface is identical to the area occupied by TPS particles in any other y-z surface of the sample.

In this way, the percent of TPS lost is proportional to the half of a linear distance in the machine direction (x) on each side of the sample. Thus, the transformation of the percent of TPS lost gives an extraction length of 0.24 mm, 1.1 mm and 2.0mm for the samples of 1 mm, 5 mm and 10 mm, respectively. The fact that more than 1 mm of the samples of 5 mm and 10 mm has been lost means that in the same time the sample of 1 mm should be completely lost as in the case of hydrolytic degradation. The lower percent of TPS lost can be attributed to the deposit of bacteria or bacterial secretions through the empty channel left by TPS lost. Another possible explanation is the presence of TPS crystalline regions composed of amylose-lipid complex which are more resistance for bacterial attack (Shogren, 1991). Such crystalline regions should remain at the interior of the sample due to the difficulty of transport through PE1 channels.

AII.4 Conclusion

The continuity of PE1/TPS (70:30 w/w) blends prepared in one and two-step processes was evaluated by means of the bacterial and hydrolytic degradation of starch domains. Both blends possessed a PE1-rich skin which avoided access from ribbon surfaces. Blends prepared in a one-step process were highly continuous due to the axial coalescence of TPS fibers. The absence of TPS coalescence in the machine direction of blends prepared in the two-step process restricted the biological extraction of starch domains. Both blends displayed almost no coalescence in the transverse direction. Bacterial extraction reached a maximum at around 48% while hydrolytic degradation allowed 100% starch removal to be obtained. Probable causes of the lower biological extraction could be related to bacterial residues and the presence of amylose-lipid complexed crystalline regions.

ANNEX III. DETERMINATION OF THE DIMENSIONS OF ELONGATED TPS PARTICLES.

Classical morphologies of immiscible polymer blends are characterized by spherical particles of one component dispersed in a continuous matrix of the second component. Under the influence of elongational flow fields such spherical particles can be deformed into ellipsoid or even long fibers depending on a number of parameters including the viscosity and elasticity ratios, the interfacial tension and the extent of the applied stress. In order to quantify the dimensions of elongated dispersed particle a new methodology is proposed. The calculated dimension is related to the deformation index known as form factor ($F = 4\pi A/P^2$) where A and P are the surface area and perimeter of the dispersed particle, repectively. F varies from 1 (perfect sphere) to 0 (thin fiber of infinite length). This quantification is based on the following assumptions:

- Particle shapes vary from spherical to ellipsoidal. Even long fibers are considered as ellipsoids
- Particles are considered to be cut through the equator.

The volume of an ellipsoid can be calculated from $V_{ellipsoid} = 4/3\ \pi$ abc where a and b are the minor axes and c is the major axe (Figure AIII.1). The evaluation of the cross section of PE/TPS blends revealed that TPS dispersed particles are mainly round in this direction. From this result, it can be assumed that the minor axes are equal (a=b) and, therefore, the formulae for an ellipse in revolution can be used instead ($V = 4/3\ \pi\ a^2c$). One extreme case is the sphere (F=1) where all the axes are equal, a=b=c=r, where r is the radium of a sphere.

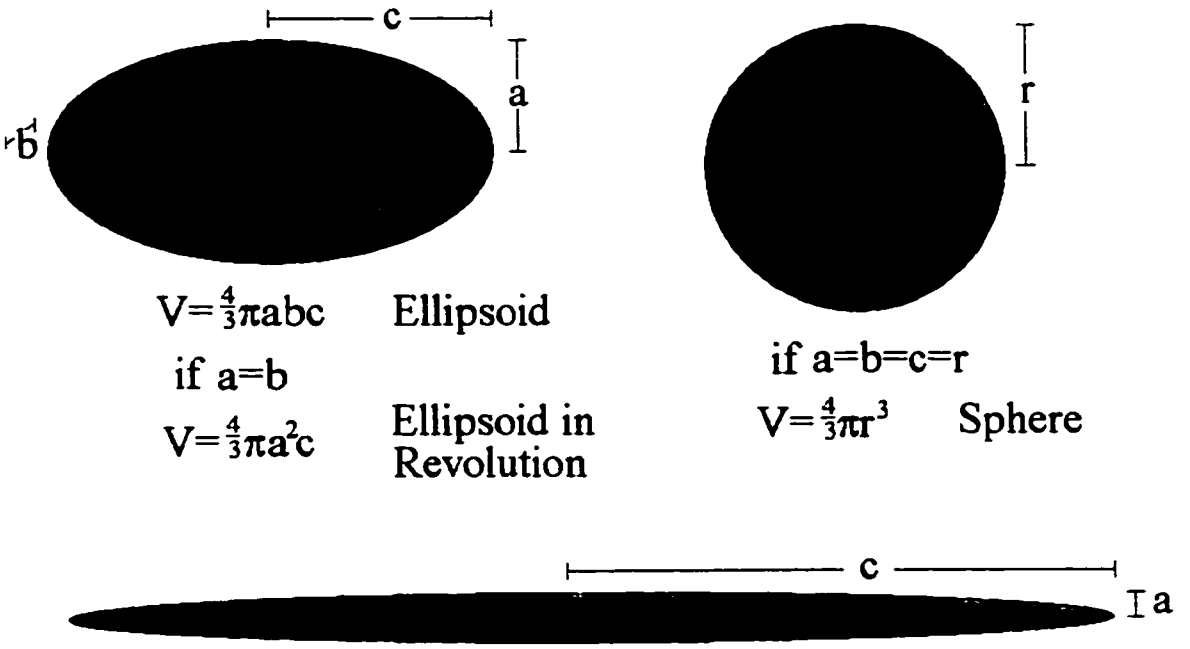

Figure AIII.1 Schematic representation of the different particles shapes that can be evaluated using the 1/F-c/a relationship.

The calculation of the particle dimensions is based on the relationship between the form factor F and the axes of the longitudinal section (a and c):

$$F = \frac{4\pi A}{P^2}$$

The area of an ellipse:

$$A = \pi ac$$

The perimeter of an ellipse:

$$P = \pi\sqrt{2(a^2 + c^2)}$$

In the case of an elliptical particle, F=f(a, c). F=f(r) in the case of a circular particle, where r=a=c. Values from 1 to 100 were assigned to c/a and the respective values of 1/F were calculated and plotted using a log-log scale (Figure AIII.2). The nonlinear regression of a hyperbola (double rectangular of 5 parameters) fits perfectly using a log-log scale. That expression is:

$$y = \frac{b_1 x}{b_2 + x} + \frac{b_3 x}{b_4 + x} + b_5 x$$

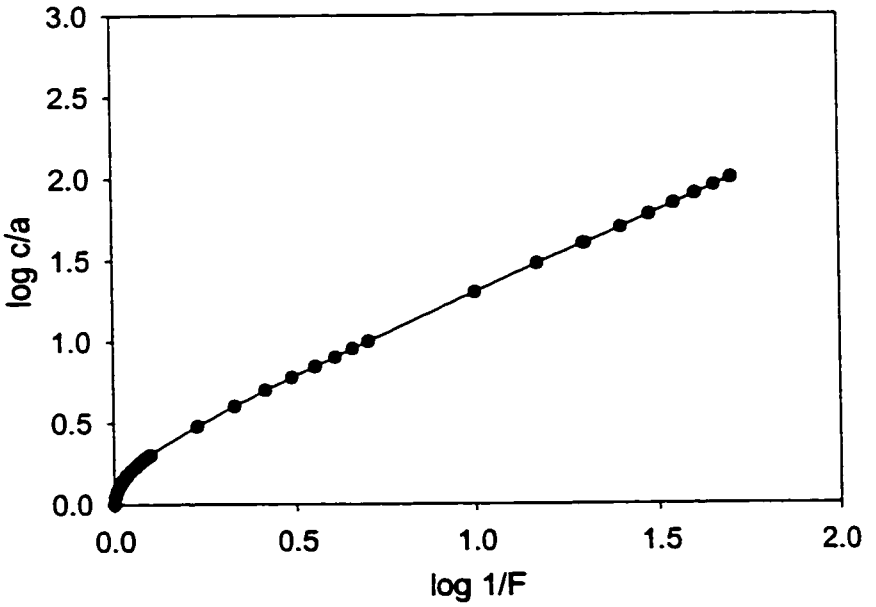

Figure AIII.2 The values of c/a are plotted against the inverse of F to determine a relationship for the calculation of the volume of an ellipsoid as a function of its shape. The equation that showed the best fit was a hyperbola double rectangular of 5 parameters.

where b_1, b_2, b_3, b_4, and b_5 are constants. Their values were determined to be 0.0736, 0.0024, 0.2643, 0.0931, and 0.9858, respectively, using Sigma Plot software.

Using a digitalizing table, the values of P and A of each particle were determined. F was calculated from the previously determined values and the c/a ratio can be calculated using the hyperbolic equation:

$$\log\left(\frac{c}{a}\right) = \frac{b_1 \log(1/F)}{b_2 + \log(1/F)} + \frac{b_3 \log(1/F)}{b_4 + \log(1/F)} + b_5 \log(1/F)$$

Once c/a ratio has been calculated, the respective dimensions of a and c can be determined using the following equation which was obtained from the surface area of the ellipse:

$$a = \sqrt{\frac{A}{\pi(c/a)}}$$

$$c = \frac{A}{\pi a}$$

The volume of the ellipsoid is determined using the values of the axes, a and c, calculated from F:

$$V = \frac{4\pi a^2 c}{3}$$

In order to handle the results in a more robust fashion, independent of the degree of deformation, the volume of the different ellipsoids are considered as the volume of an equivalent sphere. Using that assumption an equivalent diameter is calculated (Table AIII.1).

The different average form factors (F and Fv) and equivalent diameters ($D_{n,equiv}$ and $D_{v,equiv}$) were calculated using the following formulas:

$$D_{n,equiv} = \frac{\Sigma n_i D_{equiv}}{\Sigma n_i}$$

$$D_{v.equiv} = \frac{\Sigma n_i D_{equiv}^3}{\Sigma n_i D_{equiv}^2}$$

$$F = \frac{\Sigma n_i F}{\Sigma n_i}$$

$$Fv = \frac{\Sigma n_i F^3}{\Sigma n_i F^2}$$

Table AIII.1 Calculation of the dimensions of elongated particles as a function of F

Area	Perimeter	$F=4\pi A/P^2$	log(c/a)	c/a	a	c	V (μm^3)	D_{equiv} (μm)
2.385212	7.494497	0.534	0.54	3.46	0.47	1.62	1.5	1.42
1.311866	4.212365	0.929	0.17	1.47	0.53	0.78	0.9	1.21
4.05486	7.41009	0.928	0.17	1.48	0.94	1.38	5.1	2.13
8.348241	12.65817	0.655	0.43	2.69	0.99	2.67	11.1	2.76
2.02743	5.464909	0.853	0.25	1.79	0.60	1.07	1.6	1.46
14.3709	19.04293	0.498	0.57	3.75	1.10	4.14	21.2	3.43
5.963029	9.820079	0.777	0.32	2.10	0.95	2.00	7.6	2.43
4.412642	8.065407	0.852	0.25	1.79	0.89	1.58	5.2	2.15
0.477042	2.732609	0.803	0.30	1.99	0.28	0.55	0.2	0.69
3.756708	7.420783	0.857	0.25	1.77	0.82	1.45	4.1	1.99
3.398927	6.89727	0.898	0.20	1.60	0.82	1.32	3.7	1.92
1.013715	4.260069	0.702	0.39	2.45	0.36	0.89	0.5	0.98
9.600477	15.52258	0.501	0.57	3.72	0.91	3.37	11.6	2.81
5.664878	11.26313	0.561	0.51	3.26	0.74	2.42	5.6	2.21
9.361956	13.73121	0.624	0.46	2.86	1.02	2.92	12.7	2.90
0.655933	3.054921	0.883	0.22	1.66	0.35	0.59	0.3	0.84
231.1866	97.50836	0.306	0.80	6.38	3.40	21.66	1047.0	12.60
1.192606	6.670366	0.337	0.76	5.75	0.26	1.48	0.4	0.92
185.2713	125.738	0.147	1.13	13.53	2.09	28.24	515.8	9.95
3.339296	7.50519	0.745	0.35	2.25	0.69	1.54	3.1	1.80
0.477042	2.684905	0.832	0.27	1.87	0.28	0.53	0.2	0.70
5.068575	9.307258	0.735	0.36	2.29	0.84	1.92	5.7	2.21
0.417412	2.684905	0.728	0.37	2.32	0.24	0.56	0.1	0.63
2.444842	7.695391	0.519	0.55	3.57	0.47	1.67	1.5	1.43
2.385212	6.670058	0.674	0.41	2.59	0.54	1.40	1.7	1.49
1.311866	4.212365	0.929	0.17	1.47	0.53	0.78	0.9	1.21
3.875969	7.827502	0.795	0.31	2.03	0.78	1.58	4.0	1.97
2.683363	6.574958	0.780	0.32	2.09	0.64	1.34	2.3	1.63
3.518187	7.409782	0.805	0.30	1.98	0.75	1.49	3.5	1.89
5.068575	8.995639	0.787	0.31	2.06	0.88	1.82	6.0	2.25